Waterborne vessels as mobile hubs

A design for shared courier micro-delivery resources management for an instant delivery platform

Master Thesis

Chenghua Yang

Delft University of Technology

TU Delft

Waterborne vessels as mobile hubs

A design for shared courier micro-delivery resources management for an instant delivery platform

by

Chenghua Yang

to obtain the degree of Master of Science

at the Delft University of Technology,

to be defended publicly on Friday August 23, 2024 at 13:00.

Student number:	5722780	
Project duration:	January 25, 2024 – August 23, 2024	
Thesis committee:	Prof. dr. Shadi Sharif Azadeh,	TU Delft, Chair
	Prof. dr. Yousef Maknoon,	TU Delft, Daily supervisor
	Dr. Kuldeep Kavta,	TU Delft, Third examiner

Cover: Created by the author using OpenArt

An electronic version of this thesis is available at `http://repository.tudelft.nl/`.

TU Delft

Preface

Finally, I am approaching the end of my master's study at TU Delft. At this moment, I am very excited to look back on the countless efforts, challenges, excitements, and joys that I have experienced over the past two years in the Netherlands.

First of all, I would like to thank my graduation committee sincerely. Thank you, Yousef, my daily supervisor and mentor, for your patient guidance over these eight intense months. From helping me define a clear problem description, to guiding me through developing elegant OR-style mathematical models, to refining meaningful results, and improving my academic writing, your detailed and thoughtful comments, feedback, and advice have always been invaluable and helpful. As a naive researcher, I am also very grateful for the essential research skills you've taught me. Your belief in my potential has made all the difference, and I really appreciate everything you've done to help me grow as a researcher. I am also very grateful to my chairperson, Shadi, for offering the opportunity to explore such an innovative topic. Your oversight and advice during those milestone meetings, as well as our many email exchanges, were crucial to the success of this project. Thank you also for the opportunity to talk with industry partners, which provided me with new perspectives to reflect on my research. To Kuldeep, my third examiner, thank you for all your insights, and I am truly thankful for every feedback you've provided on my thesis. I would also like to thank Dongyang and Sara, whose suggestions helped me refine my research. Also, thanks to every kind and supportive person I met at TU Delft during this two-year master's study.

I also want to thank my family for your support during my two years in the Netherlands. The warm words in the two-hour WeChat call every Saturday are always a great comfort for me. Life is full of challenges, especially when trying to achieve ambitious goals, but your support always gives me the strength to keep going, even when the journey feels hard.

Finally, I want to especially thank myself, for embracing challenges as opportunities to grow, for persevering and working hard, and for striving to be a better person. After some break, I will continue to pursue a PhD under Professor Bilge Atasoy's supervision at TU Delft. I truly hope, my future self, continues to find joy in the academic journey ahead, and realizes all the bold dreams.

Chenghua Yang

Delft, August 2024

Summary

This study addresses the operation limitations of the current practice in managing shared micro-delivery resources (MDRs) for on-demand meal delivery platforms. The current static hub approach requires long courier non-service riding time for MDR pickups and returns, and the multi-static-hub configuration needs hiring a truck to rebalance the hub inventories, which is pollutant and can cause extra burden to the road traffic.

In this research, by making use of the well-developed infrastructures in canal-rich cities and the latest advancements in electric vessel technology, we propose an innovative Mobile-Hub strategy that utilizes electric vessels as mobile hubs (MHs) for MDRs. We formulate the problem as mixed-integer linear programming and name it the Capacitated Mobile Facility Location Problem with Multiple Demands (CMFLP-MDs). The objective of our model is to minimize the total system cost including capital investment and operational cost, while satisfying the demands for MDR pickups and returns of the couriers.

Our results show that the Mobile-Hub strategy significantly outperforms the current static central hub approach. The proposed system helps maintain lower and more stable MH inventory levels while providing superior service, which demonstrates the benefits of the Mobile-Hub strategy.

Keywords: Meal delivery problem; Mobile hub, Capacitated facility location, Urban waterway logistics.

Contents

List of Figures

List of Tables

1

Introduction

As one of the most important technology innovations in the logistics sector, on-demand delivery services are rapidly reshaping urban lifestyles. These platforms provide instant delivery services by digitally and seamlessly connecting senders, couriers, and recipients[27]. In the Netherlands, a considerable proportion of couriers are directly employed by the platforms. They are paid hourly wages and use the shared micro-delivery resources (MDRs), such as scooters and bikes, provided by the platforms to conduct deliveries. Efficient management of these MDRs is crucial for the platforms to ensure timely MDR availability for couriers to start their services. Platforms often manage MDRs using a centrally located static hub within the service area.

The employed couriers operate under a shift-based business model. They begin their shifts by collecting an MDR from the hub, then travel to pick up the meal at the restaurant of the first assigned order. The time between the MDR collection and the first pickup is called the pre-service time. The courier service starts there. The service time spans from the first pickup to the last delivery. After delivering at the last household, the couriers ride back to the hub to return the MDR, with this time being the post-service time. Thus, a typical courier shift comprises pre-service, service, and post-service periods, with the pre- and post-service periods named non-service time.

While straightforward, the current static hub strategy has many limitations. The courier non-service riding times are paid by the platforms, so the platforms naturally seek to shorten this time

to increase courier productivity. Some platforms operate multiple hubs to distribute the MDR availability more sparsely in the service area to reduce the non-service times. This approach operates similarly to public bike-sharing systems, which require more capital investment for the hubs and additional effort to rebalance the inventories compared to the single-hub approach. Additionally, rebalancing trucks may worsen traffic congestion in cities with narrow streets like Amsterdam and generate heavy emissions, thus reducing the quality of life for residents.

On the other hand, electric vessels are emerging as an efficient and sustainable solution for logistics in cities with canals, helping to alleviate traffic in densely populated areas [22][26]. This technology is already widely applied to various services, from parcel delivery to waste transportation [8]. The Central Commission for the Navigation of the Rhine [9] has documented several successful or ongoing innovative projects using electric vessels in inland waterway transportation across European cities, demonstrating the technology's potential to meet diverse urban transportation needs.

In this research, we explore the use of electric vessels as a means of MDR parking and relocation for on-demand delivery services, expanding the usage portfolio of this new technology. We propose an integrated Mobile-Hub system, which features deploying electric vessels as mobile hubs (MHs) for MDRs. In our design, the operation of the MHs is complemented by some discretionary docking points (DDPs) strategically positioned along the city canals. The MHs follow fixed daily routes and schedules to store, transport, and deliver MDRs to synchronize with courier services. The proposed Mobile-Hub strategy offers three key advantages: reduced land use for MDR storage, environmentally friendly operation, and no extra burden to road traffic.

The Mobile-Hub system helps satisfy two types of demand from couriers: MDR pickups and returns. We develop a Capacitated Mobile Facility Location Problem with Multiple Demands (CMFLP-MDs) model. For the Mobile-Hub system to be effective, it requires an efficient operation scheme to synchronize the courier services. The objective of the CMFLP-MDs model is to minimize the total system cost, including the capital investment for MHs, DDPs, and MDRs, as well as the opportunity cost of courier non-service times. This is achieved by simultaneously considering the following decisions: the size of the MH fleet, the number and location of DDPs, the number of required MDRs, and the operation of the MDRs.

The contributions of this research are summarized as follows: (1) an investigation into the feasibility of the Mobile-Hub strategy for managing shared courier MDRs; (2) consideration of hybrid operations involving MHs, DDPs, and courier demand self-fulfillment; and (3) the

development of Mixed-Integer Programming (MIP) models, in both arc-based and route-based formulations, to study this problem.

1.1. Research question

To realize our research goal, we develop our research question as follows:

Is "waterborne vessels as mobile hubs" a viable and even better alternative for the management of shared micro-delivery resources (e.g. bikes, scooters) for on-demand delivery platforms? If yes, to what extent?

To answer this research question, the following sub-questions are asked:

- How to consider the courier service dynamics to optimize the operation of the Mobile-Hub system while synchronizing the courier services?
- How to consider the trade-off between the infrastructure investment, and operational costs in optimizing the system?
- What are the factors that impact the design and operation of the Mobile-Hub system?
- How does the proposed mobile hub strategy compare to the current static hub approaches in terms of cost efficiency, resource utilization, and courier service levels?

1.2. Report structure

The remainder of this report is structured as follows: In Chapter 2, we discuss the relevant literature. In Chapter 3, we formalize the problem. In Chapter 4, we present the mathematical formulations of the proposed model. In Chapter 5, we show the experimental results, and we conclude our findings in Chapter 6.

2

Literature Review

In this section, we discuss the literature relevant to our research. We situate our study within two streams of the literature, namely the Mobile Facility Location Problem (MFLP) and fleet sizing for shared vehicle systems.

2.1. Mobile facility location problem

The facility location problem (FLP) addresses the strategic and tactical decisions of placing facilities among several candidates to serve customers or clients through an established transportation network[12]. Facilities can include a variety of strategically located entities, such as transportation hubs, factories, warehouses, and fuel stations. The locations of these facilities are crucial because capital costs for infrastructure investments are often substantial, and facility locations can significantly impact the tactical and operational decisions of an organization[29].

In recent years, advances in modularization and miniaturization have led to an increase in the use of modularized mobile facilities. [25] define the concept of mobility as the ability to move between geographical locations with little effort. Problems studying relocatable units are referred to as mobile facility location problems (MFLPs), introduced by [10]. This problem considers the relocation of facilities and customer allocation with the aim of, for example, minimizing total transport time for both movable units and the assigned customers. [21] further extend this problem by considering facility capacities for a more practical approach. For facilities serving as parking or storage places, like the MHs in our study, locating them close to where the goods

or services are demanded helps reduce transportation distance and delivery time. This improves customer service levels and helps organizations maintain low and stable inventory levels[5].

MFLPs have been extensively studied in various applications, including healthcare, emergency services, humanitarian relief, manufacturing, and so on. Readers are referred to [2] for a systematic review of the various topics on MFLPs. [20] examine the relocation and scheduling of mobile humanitarian facilities to deliver aid service bundles to migrating refugees, with an objective to minimize total mobile facility costs. [24] consider the stochastic MFLP and model the optimal sizing, routing, and scheduling of a fleet of mobile facilities over a planning horizon. They propose two distributionally robust optimization models to study the problem and assume random demand levels in each period with unknown probability distributions. What sets our research apart from theirs is that we consider the fleet sizing of both the MHs and shared courier vehicles in the on-demand delivery setting. [7] consider the problem of relocating emergency vehicles to minimize the largest service time between customers assigned to vehicles during a multi-period planning horizon.

[23] address the routing of mobile clinics to deliver healthcare to refugees, modeling the problem with hierarchical objectives to minimize the number of clinics and their travel distance while maximizing refugee coverage. [30] investigate the problem of stop selection and routing for mobile medical vehicles, considering partial coverage of scored customer locations to maximize the total score collected. [1] examine the relocation of capacitated recycling units for waste collection to minimize total transport time. [16] study the stochastic scheduling of emergency vehicle relocation in response to traffic accidents, considering uncertainties in both service demand and vehicle unavailability times. [13] study an MFLP in railway construction management, synchronizing the decisions on the number, type, and schedule of capacitated mobile facilities, as well as production allocation.

2.2. Fleet sizing for shared vehicle systems

Although there is extensive literature on shared vehicle systems and fleet sizing ([15], [19], [4]), they only consider the static vehicle stations. Limited research considers the fleet sizing of the shared vehicles under the mobile hub situation, as in our study. However, some research is still relevant to our research. [11] study the fleet sizing and management of shared autonomous vehicle service, considering optimal fleet sizing and service level decisions from a strategic perspective, as well as vehicle parking and relocation from an operational perspective. [28] study an electric autonomous on-demand service and use Bayesian optimization to optimize fleet size and charging facility locations, considering the congestion caused by the fleet.

[6] study the dimensioning of a shared vehicle system using a closed queueing network, considering the randomness of both rental duration and vehicle availability at each location. [14] model the minimum size of a hybrid fleet of autonomous and human-driven vehicles for an on-demand ride service system, considering uncertain demands. [17] optimize the fleet size of a car-sharing system with the objective of serving as many clients as possible. They consider two service types: round-trip (pickup and dropoff locations are the same) and one-way (different locations), similar to our research, where we consider the different service ranges of couriers. Their results show that round-trip service is better for scaling up. [18] study the dimensioning of a hybrid fleet of private and pooled services, modeling the problem from the perspectives of two different stakeholders (authority and service provider). Their results show that the authority requires a larger fleet size.

2.3. Our contributions

Existing research offers extensive literature on the applications of MFLPs and fleet sizing for shared vehicle systems. However, to the best knowledge of the authors, no studies have explored the use of electric vessels as mobile hubs for shared courier vehicles in the on-demand delivery sector, nor the simultaneous decision-making of MHs and shared courier vehicle fleet sizes. Investigating the feasibility of the concept of Mobile-Hub for highly time-sensitive on-demand delivery services, and understanding their interaction with courier services remains a gap in the literature. This research aims to address this gap by systematically examining this strategy from an operations research perspective.

3

Problem Statement

We consider an operator for an on-demand delivery platform operating in an urban area connected by canals, such as those in Amsterdam, Venice, or Bangkok. The platform utilizes two types of resources: MDRs, including bikes, scooters, and similar modes of transport that start their operations from specific zones within the system, and electric vessels that act as MHs of these MDRs. We discretize the service area into a set of equal-sized, regular hexagon-shaped zones (Figure 3.1), classifying them into two groups: zones with a DDP where the MHs can dock temporarily and zones without one. The itinerary of an MH includes only the zones where it can dock, and we assume these zones are connected by canals, defining the operating area of the MHs.

We assume that the on-demand delivery service operates within a company-owned business model, with MDRs owned by the company. The delivery service of a typical day operates in several courier shifts, varying in starting time, starting zone, ending time, and ending zone. Each shift begins when a courier picks up an MDR from a DDP. After picking up his/her MDR, the courier rides to collect the meal from the first restaurant, and this riding time is defined as the pre-service time. The duration between the first meal collection and the last meal delivery is defined as the service time. After delivering the last order at the last household, the courier rides to a DDP to return the bike; this duration is defined as the post-service time.

MHs initiate their routes from a central depot with charging facilities. During their operation, the MHs selectively visit a series of DDPs to load and unload MDRs. Each DDP has a small

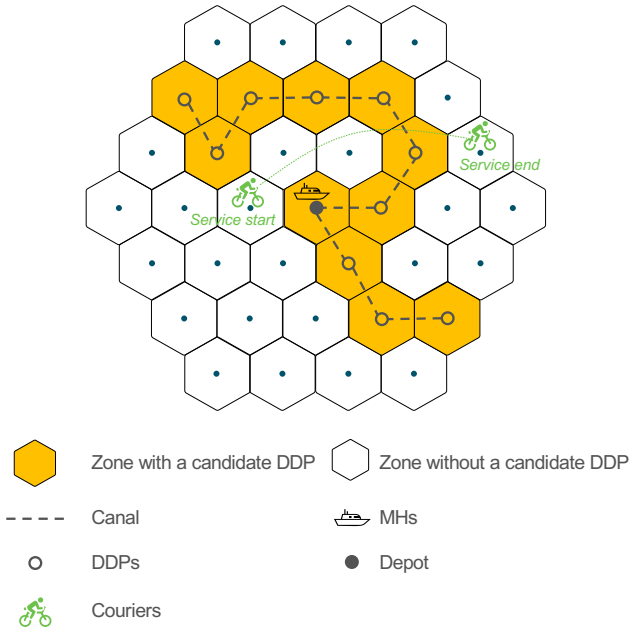

Figure 3.1: Infrastructure settings

staging area with limited capacity to facilitate the synchronization of MH movements and courier activities. MHs periodically return to the central depot for recharging with this time defined as a vessel interval. The routes and schedules of the vessels must be synchronized with the shifts and operations of the couriers. The objective is to minimize the total system cost, including capital investment and MDR operations, while satisfying all courier demands for MDR pickups and returns. The objective is realized by synchronizing the following decisions: (1) the number of MHs, DDPs, and MDRs; (2) the operations of the MDRs.

3.1. Courier dynamics

Given the highly dynamic nature of the on-demand environment, we use historical data to model courier dynamics. In this problem, we assume that the Mobile-Hub system is established in an existing operating area where the operator has historical information about the couriers. This historical data includes the couriers' itineraries, allowing us to identify courier dynamics through their service times. Specifically, we consider the starting location and time of the service, as well as the ending location and time.

Observation 1. We assume that in each zone z and each discredited period t, there is a probability distribution for the number of services starting there and when. By introducing a courier service level α, we can calculate the expected value d_{zt}, representing the number of couriers starting in

zone z and period t, such that α of cases are covered. Let X_{zt} be the random variable representing the number of couriers starting in zone z and period t:

$$P(d_{zt} \geq X_{zt}) \geq \alpha$$

Furthermore, we determine the transition probability $n_{zt}^{z't'}$, which indicates the likelihood that a courier starting in zone z at period t will end their service in zone z' at period t'. Using this transition probability, we can calculate the expected number of services ending at a given zone z' at period t'. The calculated $r_{z't'}$ is a fractional number, which we round down to get the integer value. This is represented as:

$$r_{z't'} = \sum_{z} \sum_{t} n_{zt}^{z't'} d_{zt}$$

3.2. Courier demand fulfillment

We consider three methods to fulfill courier pickup and return demands: by MHs, by established DDPs, and by courier self-fulfillment. These correspond to five MDR operation modes: O = {**DM**: dropped off from MHs; **RM**: returned to MHs; **DD**: dropped off from DDPs; **RD**: returned to DDPs; **SF**: self-fulfillment}.

(1) "Satisfied by MHs" refers to the process where couriers pick up and return MDRs from and to docked mobile hubs. We use a set of homogeneous electric vessels $v \in \mathcal{V}$ serving as mobile hubs with a fixed capacity of Q^{MH}. An MH tour is defined as the sequence of DDP visits, including the duration of the stay at each DDP. An MH can either stay at a DDP to load and unload MDRs or bypass it without stopping. An MH tour is composed of equal-length intervals, with each interval comprising several periods. The MHs start and end the tours at a central depot z_o and must return to the depot at the end of each interval to recharge. We further consider a pre-lag for which time the start of the first courier service is later than the start of the planning horizon, to ensure that the pickup demand in the outermost zones can be satisfied. A post-leg is also considered to ensure the MDR return in the outermost zones can be served. In Figure 3.2 we use an example to explain the relationship between the planning horizon, intervals, service shifts (composed of per-service time, service time, and post-service time).

MHs operate in two modes: **DM**, indicating MDRs are dropped off from MHs, and **RM**, indicating MDRs are returned to MHs. After docking, MHs will wait for at least one period to load and unload MDRs. Couriers needing an MDR will be at a DDP before their shift starts. When the MH arrives, they board to pick up the MDR and ride to the restaurant of

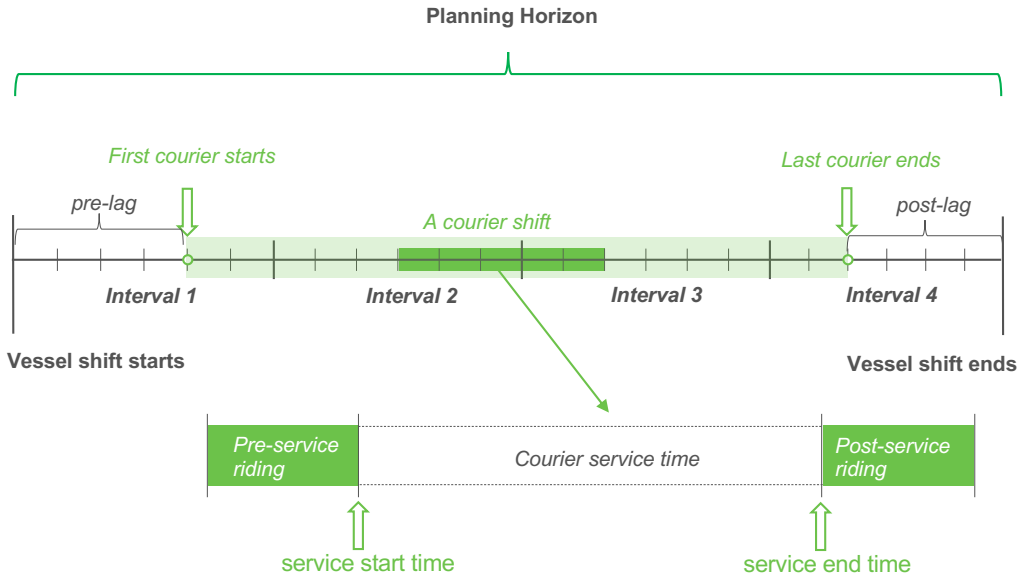

Figure 3.2: An example of the planning horizon, intervals, and the courier shifts

the first order to start the service. The monetary value of this pre-service riding is included in the operation cost. For MDR returns, after delivering their last order, couriers ride to a DDP designated by the platform, ensuring they arrive at the DDP in the same period as the MH. Their shift ends once the MDR is returned. The value of the post-service time for MDR returns is also considered, along with fixed costs associated with vessel leasing, driver salaries, and energy.

(2) "Satisfied by DDPs" is the process where couriers use established DDPs as mini static stations for MDRs, regardless of the presence of a docking vessel. The candidate locations for the homogeneous DDPs of capacity $Q^D DP$ are assumed known, and the establishment of a DDP depends on whether it will be visited and docked by MHs. Operation modes **DD** and **RD** are associated with this method, namely MDRs dropped off at DDPs and returned to DDPs. The platform can assign couriers to a specific DDP for their pickup and return demands. Costs associated with this service include the capital investment for establishing DDPs and the value of couriers' riding time for pre- and post-service.

(3) We consider that in each zone there is a small free-floating location where couriers can meet to hand over MDRs at no charge. Operation mode "Self-fulfillment (SF)" refers to the process where the platform directs courier A, who finishes the last order, to ride to the free-floating location in a zone where another courier B is asked by the platform to wait there to take over A's MDR so that B can directly start service in that zone and the MDR of A is returned. We consider the

free-floating location as a hand-over location with no capacity. The riding time of couriers of type A is included in the operational cost.

4

CMFLP-MDs Models

In this chapter, we describe the proposed mathematical model based on the problem description in Chapter 3. In Section 4.1, we introduce the graphs and sets. In Section 4.2 we explain how the courier demand for MDR pickups and returns are satisfied with an example. In Section 4.3 and Section 4.4 we describe the model in its arc-based and route-based formulations.

4.1. Network representation

We define the CMFLP-MBs on a directed physical graph $\mathcal{G} = (\mathcal{Z}, \mathcal{E})$, which is composed of two subgraphs: $\mathcal{G}^C = (\mathcal{Z}^C, \mathcal{E}^C)$ associated with the couriers, and $\mathcal{G}^M = (\mathcal{Z}^M, \mathcal{E}^M)$ associated with the MHs. $\mathcal{Z} = \{1, 2, 3, \ldots, |\mathcal{Z}|\}$ is the set of zones representing the service area, each represented by its center. The set $\mathcal{Z}^C$ comprises the zones where courier services can start and end, while $\mathcal{Z}^M$ denotes the zones with candidate DDPs where the MHs can be located. Specifically, an MH located in zone $z \in \mathcal{Z}^M$ can relocate to its adjacent zones that are connected by canals, denoted by $Z^M(z)$.

Each edge in the set $\mathcal{E}^C = \{(z, z'') | z, z'' \in \mathcal{Z}\}$ represents the bike lanes between zone z and zone z''. We assume the courier travel distance is zero within the same zone. In the set $\mathcal{E}^M$ we define two types of arcs: $\mathcal{E}^D = \{\mathcal{E}^{D1}, \mathcal{E}^{D2}\}$. The arcs in $\mathcal{E}^{D1} = \{(z, z') | z \in \mathcal{Z}^M, z' \in Z^M(z)\}$ represent the relocation of MHs from z to z', while the arcs in $\mathcal{E}^{D2} = \{(z, z) | z \in \mathcal{Z}^M\}$ represent the MHs docking at the DDP in zone z to load and unload MDRs.

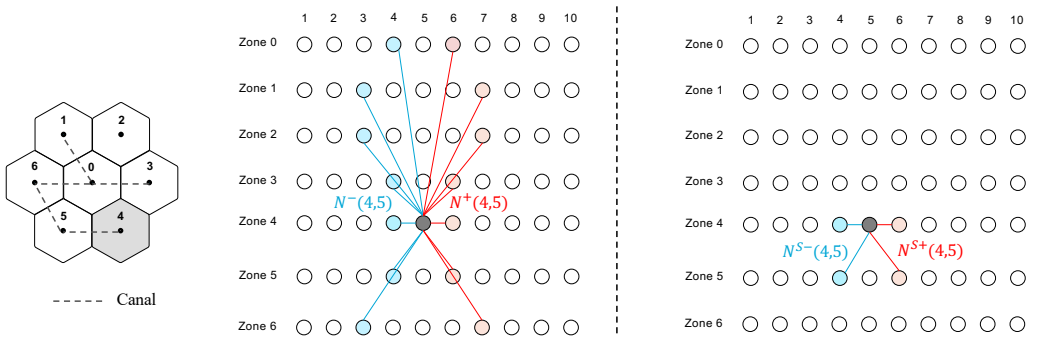

(a) Possible predecessor and successor of time-space node (4,5) for MDR movements

(a) Possible predecessor and successor of time-space node (4,5) for MH movements

Figure 4.1: An example of arcs associated with MDRs (a) and arcs associated with MHs (b) for time-space node (4,5)

The zone-period pairs are the most fundamental concept in CMFLP-MBs. We discretize the planning horizon into a set of periods $\mathcal{T} = \{1, 2, ..., |\mathcal{T}|\}$. We assume equal speed for MHs and couriers, and the time for traveling one unit distance is one period. Corresponding to the physical graph $\mathcal{G}$, we define the time-space graph $\mathcal{G}' = (\mathcal{N}, \mathcal{A})$, where $\mathcal{N} = \{(z,t)|z \in \mathcal{Z}, t \in \mathcal{T}\}$ is the set of zone-period pairs, and $\mathcal{A}$ is the set of arcs. The graph $\mathcal{G}'$ is composed of two subgraphs: $\mathcal{G}'^C = (\mathcal{N}^C, \mathcal{A}^C)$ associated with couriers, and $\mathcal{G}'^M = (\mathcal{N}^M, \mathcal{A}^M)$ for the MHs.

In $\mathcal{A}^C$ we use $(z,t)(z'',t'')$ to represent the courier movement from z to z'' starting from t and arriving in t''. In the set $\mathcal{N}^C = \mathcal{Z}^C \times \mathcal{T}$, for each node (z,t), we define its successor nodes $N^{C+}_{z,t} = \{(z'',t'')|z'' \in \mathcal{Z}, t'' = t + DIS_{zz''}\}$ and predecessor nodes $N^{C-}_{z,t} = \{(z'',t'')|z'' \in \mathcal{Z}, t'' = t - DIS_{z,z''}\}$, where $DIS_{z,z''}$ is the distance in units between z and z''. Similarly, each arc $(z,t)(z',t') \in \mathcal{A}^M$ represents the MH movement from z to z' starting in t and arriving in t'. For each node (z,t) in $\mathcal{N}^M = \mathcal{Z}^M \times \mathcal{T}$, we define $N^{M+}_{z,t} = \{(z',t')|z' \in Z^+_z, t' = t + DIS_{zz'}\}$ as the successor nodes, and $N^{M-}_{z,t} = \{(z',t')|z' \in Z^+_z, t' = t - DIS_{zz'}\}$ as predecessor nodes. Figure 4.1 gives an example of the set of arcs associated with MDRs (a) and MHs (b) for the same time-space node.

4.2. An illustrative example

In this section, we illustrate how MDR pickups and returns associated with courier service starts and ends are satisfied by five operation modes. Consider a case where a vessel operates in a service area with 7 zones over a planning horizon of 10 periods, composed of 2 intervals. The canal passes through zones 0, 6, and 5 sequentially, with one candidate DDP in each zone. Figure 4.2 depicts a potential routing and scheduling of the vessel. In the first interval, the vessel follows the canal, visiting zones 0, 6, and 5 in sequence before returning to the depot, resulting in the

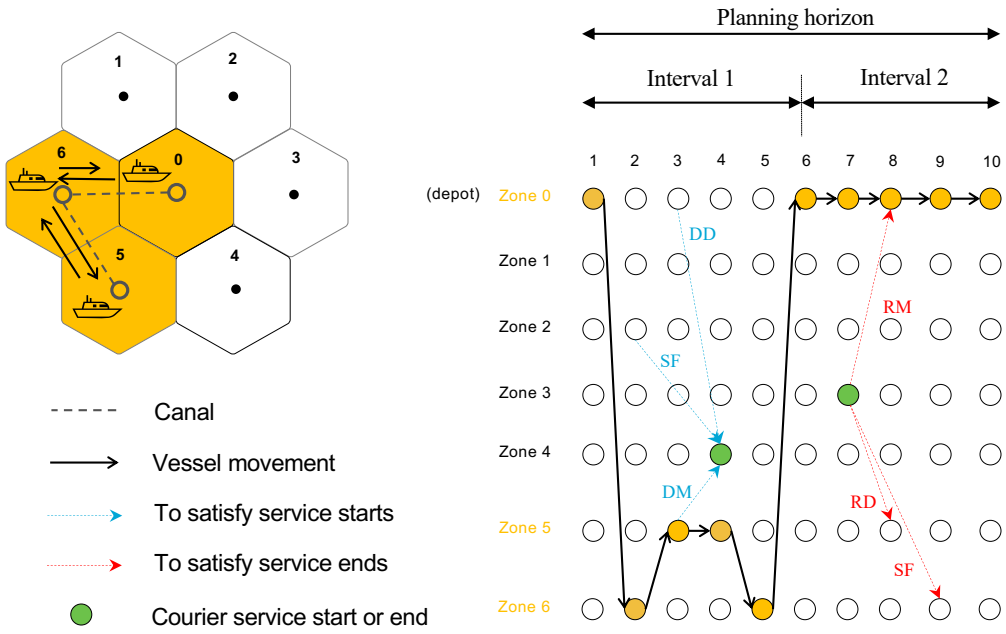

Figure 4.2: An example of courier service starts and ends satisfaction

establishment of the three DDPs. In the second interval, the vessel remains stationary.

Couriers starting service in zone 4 at period 4 can obtain an MDR through three means: Direct from Mobile-Hub (DM): Couriers wait in zone 5 at period 3 for the vessel's arrival and collect an MDR when it docks. They then spend one period traveling to zone 4 to start service. From Discretionary Docking Points (DD): Couriers reach zone 0 from their home at period 3, collect an MDR, then spend one period traveling to zone 4. Self-Fulfillment (SF): Couriers wait in zone 4 before period 4. The platform directs couriers ending their shift in other zones (e.g., zone 2 at period 2) to travel to zone 4 and hand over their MDRs to the waiting couriers.

Couriers ending service in zone 3 at period 7 can return their MDRs through three means: Return to Mobile-Hub (RM): Couriers spend one period traveling to zone 0 to return their MDRs to the docked vessel. Return to Discretionary Docking Points (RD): Couriers travel to zone 5 to return the MDRs to the DDP there. Self-Fulfillment (SF): The platform directs couriers to zones where other couriers are waiting for MDRs (in this case, zone 8).

4.3. Arc-based formulation

MH tour constraints. For each MH $v \in \mathcal{V}$, we define the binary variable $\delta^v = 1$ if MH v is deployed. Binary variable $x^v_{(z,t)(z',t')} = 1$ if MH v travels from zone z to zone z' starting in period t arriving in period t'. Constraints (4.1) check the usage of MH v. Constraints (4.2) state that a used

MH will return to the depot z_o at the closure of the planning horizon. Constraints (4.3) ensure the MH flow conservation at time-space nodes. Constraints (4.4) make sure that no more than two MHs dock at the same DDP in the same period except for at the depot. The planning horizon is divided into a set of intervals $L = \{1, 2, \ldots, l, \ldots, |L|\}$, that is $\mathcal{T} = \{T_1, T_2, \ldots, T_l, \ldots, T_{|L|}\}$, where $|L| = \frac{|\mathcal{T}|}{|T_1|}$. We define $\tilde{T} = \{|T_1|, 2|T_1|, \ldots, l|T_1|, \ldots, (|L|-1)|T_1|\}$ as the set of periods at the end of the intervals. Constraints (4.5) ensure the MHs return to depot at the end of each interval to recharge for at least one period.

$$\delta^v = \sum_{(z',t') \in N^{M+}_{z_o,1}} x^v_{(z_o,1)(z',t')}, \quad \forall v \in \mathcal{V} \tag{4.1}$$

$$\sum_{(z',t') \in N^{M+}_{z_o,1}} x^v_{(z_o,1)(z',t')} = \sum_{(z',t') \in N^{M-}_{z_o,|\mathcal{T}|}} x^v_{(z',t')(z_o,|\mathcal{T}|)}, \quad \forall v \in \mathcal{V} \tag{4.2}$$

$$\sum_{(z',t') \in N^{M+}_{z,t}} x^v_{(z,t)(z',t')} = \sum_{(z',t') \in N^{M-}_{z,t}} x^v_{(z',t')(z,t)}, \quad \forall v \in \mathcal{V}, \quad \forall z \in \mathcal{Z}^M \setminus \{z_o\}, \quad \forall t \in \mathcal{T} \tag{4.3}$$

$$\sum_{v \in \mathcal{V}} x^v_{(z,t)(z,t+1)} \leq 1, \quad \forall z \in \mathcal{Z}^M \setminus \{z_o\}, \quad \forall t \in \mathcal{T} \setminus |\mathcal{T}| \tag{4.4}$$

$$x^v_{(z_o,t)(z_o,t+1)} = 1, \quad \forall v \in \mathcal{V}, \quad \forall t \in \tilde{T} \tag{4.5}$$

$$\delta^v \in \{0,1\}, \quad \forall v \in \mathcal{V} \tag{4.6}$$

$$x^v_{(z,t)(z',t')} \in \{0,1\}, \quad \forall v \in \mathcal{V}, \quad \forall (z,t),(z',t') \in \mathcal{A}^M \tag{4.7}$$

We define the binary variable $\zeta_z = 1$ if the candidate DDP in zone z is visited. Constraints (4.8) ensure the visited candidate DDPs are established. M_1 is a constant value set as $|\mathcal{V}|(|\mathcal{T}|-1)$.

$$\zeta_z \leq \sum_{v \in \mathcal{V}} \sum_{t \in T \setminus |\mathcal{T}|} x^v_{(z,t)(z,t+1)} \leq M_1 \zeta_z, \quad \forall z \in \mathcal{Z}^M \tag{4.8}$$

$$\zeta_z \in \{0,1\}, \quad \forall z \in \mathcal{Z}^M \tag{4.9}$$

MDRs pickups and returns activation. For the MDR pickups, Recall that we have five operation MDR modes: O = {**DM**: dropped off from MHs; **RM**: returned to MHs; **DD**: dropped off from DDPs; **RD**: returned to DDPs; **SF**: self-fulfillment}. We define a non-negative integer variable for each mode: $y^{DM,v}_{(z,t)(z'',t'')}$ for the MDRs dropped off by MH v located in z in period t to fulfill the courier service starting in zone z'' in period t'; $y^{RM,v}_{(z'',t''),(z,t)}$ for the MDRs returned from z'' in t'' to MH v in z in t; $y^{DD}_{(z,t)(z'',t'')}$ for the MDRs dropped off at the DDP in z in t for the service start in z'' in t''; $y^{RD}_{(z'',t'')(z,t)}$ for the MDRs returned from z'' in t'' to the DDP in z in t; and $y^{SF}_{(z,t)(z'',t'')}$ for the self-fulfillment originating in z in t and ending in z'' in t''. d_{zt} indicates the quantity of the service start in zone z in period t, and r_{zt} is the service ending in zone z in period t. Only docked MH and established DDP can serve courier pickups and returns, constraints (4.10) and

(4.11) activate the drop-off and pick-up flows associated with MH v at (z,t). Constraints (4.12) and (4.13) activate the drop-off and pick-up flows associated with the DDP in z in t.

$$y^{DM,v}_{(z,t)(z'',t'')} \leq d_{zt} x^{v}_{(z,t)(z,t+1)}, \quad \forall v \in \mathcal{V}, \quad \forall z \in \mathcal{Z}^M, \quad \forall t \in \mathcal{T} \setminus |\mathcal{T}|, \quad \forall (z'',t'') \in N^{C+}_{z,t} \tag{4.10}$$

$$y^{RM,v}_{(z'',t''),(z,t)} \leq r_{zt} x^{v}_{(z,t),(z,t+1)}, \quad \forall v \in \mathcal{V}, \quad \forall z \in \mathcal{Z}^M, \quad \forall t \in \mathcal{T} \setminus |\mathcal{T}|, \quad \forall (z'',t'') \in N^{C-}_{z,t} \tag{4.11}$$

$$y^{DD}_{(z,t)(z'',t'')} \leq d_{zt} \zeta_z, \quad \forall z \in \mathcal{Z}^M, \quad \forall t \in \mathcal{T}, \quad \forall (z'',t'') \in N^{C+}_{z,t} \tag{4.12}$$

$$y^{RD}_{(z'',t''),(z,t)} \leq r_{zt} \zeta_z, \quad \forall z \in \mathcal{Z}^M, \quad \forall t \in \mathcal{T}, \quad \forall (z'',t'') \in N^{C-}_{z,t} \tag{4.13}$$

$$y^{DM,v}_{(z,t)(z'',t'')} \in \mathbb{Z}_{\geq 0}, \quad \forall v \in \mathcal{V}, \quad \forall z \in \mathcal{Z}^M, \quad \forall t \in \mathcal{T} \setminus |\mathcal{T}|, \quad \forall (z'',t'') \in N^{C+}_{z,t} \tag{4.14}$$

$$y^{RM,v}_{(z'',t''),(z,t)} \in \mathbb{Z}_{\geq 0}, \quad \forall v \in \mathcal{V}, \quad \forall z \in \mathcal{Z}^M, \quad \forall t \in \mathcal{T} \setminus |\mathcal{T}|, \quad \forall (z'',t'') \in N^{C-}_{z,t} \tag{4.15}$$

$$y^{DD}_{(z,t)(z'',t'')} \in \mathbb{Z}_{\geq 0}, \quad \forall z \in \mathcal{Z}^M, \quad \forall t \in \mathcal{T}, \quad \forall (z'',t'') \in N^{C+}_{z,t} \tag{4.16}$$

$$y^{RD}_{(z'',t''),(z,t)} \in \mathbb{Z}_{\geq 0}, \quad \forall z \in \mathcal{Z}^M, \quad \forall t \in \mathcal{T}, \quad \forall (z'',t'') \in N^{C-}_{z,t} \tag{4.17}$$

Demands satisfaction. Constraints (4.18) state that the all courier service starting in zone z in period t can pick up an MDR from either the MHs, DDPs or by SF. Constraints (4.19) ensure that courier ending service in zone z in period t have their MDRs return to either MHs, DDPs, or by SF.

$$\sum_{v \in \mathcal{V}} \sum_{(z'',t'') \in N^{C-}_{z,t} \cap \mathcal{N}^M} y^{DM,v}_{(z,t)(z'',t'')} + \sum_{(z'',t'') \in N^{C-}_{z,t} \cap \mathcal{N}^M} y^{DD}_{(z,t)(z'',t'')} + \sum_{(z'',t'') \in N^{C-}_{z,t}} y^{SF}_{(z'',t'')(z,t)} = d_{zt}, \quad \forall (z,t) \in \mathcal{N}^C \tag{4.18}$$

$$\sum_{v \in \mathcal{V}} \sum_{(z'',t'') \in N^{C+}_{z,t} \cap \mathcal{N}^M} y^{RM,v}_{(z'',t'')(z,t)} + \sum_{(z'',t'') \in N^{C+}_{z,t} \cap \mathcal{N}^M} y^{RD,v}_{(z'',t'')(z,t)} + \sum_{(z'',t'') \in N^{C+}_{z,t}} y^{SF}_{(z,t)(z'',t'')} = r_{zt}, \quad \forall (z,t) \in \mathcal{N}^C \tag{4.19}$$

$$y^{SF}_{(z,t)(z'',t'')} \in \mathbb{Z}_{\geq 0}, \quad \forall (z,t)(z'',t'') \in \mathcal{A}^C \tag{4.20}$$

Inventory management. We track the inventory of both the MHs and DDPs to ensure the capacity limitation is not violated. We first discuss the MH inventory, let non-negative integer I^v_{zt} be the number of MDRs stored in MH v located in zone z period t. If an arc $(z,t)(z',t')$ is on the route of MH v, the inventory at the node (z',t') equals the inventory at (z,t) adding the collected MDRs and minus the dropped ones. This is expressed by Constraints (4.21). Constraints (4.22) ensure the inventory will never exceed the fixed MH capacity Q^{MH}, and no HM inventory is considered at a time-space node when no HM is present.

$$x^v_{(z,t)(z',t')} I^v_{z't'} = x^v_{(z,t)(z',t')} \left(I^v_{zt} + \sum_{(z'',t'') \in N^{C-}_{z,t}} y^{RM,v}_{(z'',t''),(z,t)} - \sum_{(z'',t'') \in N^{C+}_{z,t}} y^{DM,v}_{(z,t)(z'',t'')} \right),$$

$$\forall v \in \mathcal{V}, \quad \forall (z,t) \in \mathcal{N}^M, \quad \forall (z',t') \in N^{M+}_{z,t} \tag{4.21}$$

$$I^v_{zt} \leq Q^{MH} \left(\sum_{(z',t') \in N^{M+}_{z,t}} x^v_{(z,t)(z',t')} + \sum_{(z',t') \in N^{M-}_{z,t}} x^v_{(z',t'),(z,t)} \right), \quad \forall v \in \mathcal{V}, \quad \forall (z,t) \in \mathcal{N}^M \tag{4.22}$$

$$I^v_{zt} \in \mathbb{Z}_{\geq 0}, \quad \forall v \in \mathcal{V}, \quad \forall (z,t) \in \mathcal{N}^M \tag{4.23}$$

For the DDP inventory, we define the non-negative integer variable I^D_{zt} as the number of bikes in the DDP in zone z in period t. Similar to the change in MH inventories between two consecutive time-space nodes, the inventory of the DDP in z in period t equals the inventory in the previous period plus the MDRs collected and minus the ones borrowed out, which is stated in Constraints (4.24). Constraints (4.25) ensure that the DDP inventory will never exceed the fixed stop capacity Q^D.

$$I^D_{z,t+1} = I^D_{zt} + \sum_{(z'',t'') \in N^{C-}_{z,t}} y^{RD}_{(z'',t''),(z,t)} - \sum_{(z'',t'') \in N^{C+}_{z,t}} y^{DD}_{(z,t)(z'',t'')}, \quad \forall z \in \mathcal{Z}^M, \quad \forall t \in \mathcal{T} \setminus |\mathcal{T}| \tag{4.24}$$

$$I^D_{zt} \leq \zeta_z Q^D, \quad \forall (z,t) \in \mathcal{N}^M \tag{4.25}$$

$$I^D_{zt} \in \mathbb{Z}_{\geq 0}, \quad \forall (z,t) \in \mathcal{N}^M \tag{4.26}$$

Objective function. The objective is to minimize the total Mobile-Hub system cost, which includes the capital investment costs (MHs leasing J_1, MDRs purchasing J_2, DDP establishment J_3) converted to a daily rate by their usage life, and the total daily operational cost for MDRs J_4 and self-fulfillment J_5. Let c^{MH} represent the daily MH leasing cost, c^{MDR} the MDR price converted to a daily rate, c^{DDP} the cost of establishing a DDP converted to a daily rate, c^{VoT} the courier value of time per period, and c^{SF} the cost per unit distance covered for self-fulfillment. The objective function is then written as:

$$MIN \quad \Phi = J_1 + J_2 + J_3 + J_4 + J_5 \tag{4.27}$$

where:

$$J_1 = c^{MH} \sum_{v \in \mathcal{V}} \delta^v \tag{4.28}$$

$$J_2 = c^{MDR}\left(\sum_{v \in \mathcal{V}} I^v_{z_o,1} + \sum_{z \in \mathcal{Z}^D} I^D_{(z,1)}\right) \tag{4.29}$$

$$J_3 = c^{DDP} \sum_{z \in \mathcal{Z}^D} \zeta_z \tag{4.30}$$

$$J_4 = c^{VoT} \sum_{(z,t) \in \mathcal{N}^M} \left(\sum_{(z'',t'') \in N^{C-}_{z,t}} \sum_{v \in \mathcal{V}} y^{RM,v}_{(z'',t'')(z,t)} DIS_{zz''} + \sum_{(z'',t'') \in N^{C+}_{z,t}} \sum_{v \in \mathcal{V}} y^{DM,v}_{(z,t)(z'',t'')} DIS_{zz''} \right.$$
$$\left. + \sum_{(z'',t'') \in N^{C-}_{z,t}} y^{RD}_{(z'',t'')(z,t)} DIS_{zz''} + \sum_{(z'',t'') \in N^{C+}_{z,t}} y^{DD}_{(z,t)(z'',t'')} DIS_{zz''} \right) \tag{4.31}$$

$$J_5 = c^{SF} \sum_{(z,t)(z'',t'') \in \mathcal{A}^C} y^{SF}_{(z,t)(z'',t'')} DIS_{zz''} \tag{4.32}$$

4.4. Route-based formulation

Route constraints. A route is a list of ordered time-space nodes that an MH is situated at in the time-space network. As mentioned in Section 4.3, the planning horizon $\mathcal{T} = \{T_1, T_2, \ldots, T_l, \ldots, T_{|L|}\}$ is divided into a set of equal-length intervals. A master MH route spans the entire planning horizon, starting in the depot z_o in the first period and ending in the depot in the period $|\mathcal{T}|$. In a master route, the MH is required to return to the depot z_o at the end of each interval. We define $\mathcal{K} = \{K_1, K_2, \ldots, K_l, \ldots, K_{|L|}\}$ as the set of MH routes, where K_l is the route set in interval l. We define the binary variable $\theta^{lk} = 1$ if route k in interval l is in the solution. In each interval, there should be at least one route, and the number of routes should not exceed the number of available MHs. This is ensured by Constraints (4.33)(4.34). A master MH route is formed by splicing together one sub-route in each interval. Constraints (4.35) ensure that the two consecutive intervals have the same number of sub-routes.

$$1 \leq \sum_{k \in K_l} \theta^{lk}, \quad \forall l \in L \tag{4.33}$$

$$\sum_{k \in K_l} \theta^{lk} \leq |\mathcal{V}|, \quad \forall l \in L \tag{4.34}$$

$$\sum_{k \in K_l} \theta^{lk} = \sum_{k' \in K_{l+1}} \theta^{l+1,k'}, \quad l \in L \setminus |L| \tag{4.35}$$

$$\theta^{lk} \in \{0,1\}, \quad \forall l \in L, \quad \forall k \in K_l \tag{4.36}$$

In case of multiple master tours, we define the binary variable $f^{l+1,k'}_{l,k} = 1$ if route k in interval l and route k' in interval $l+1$ are on the same master route in the solution. Constraints (4.37) and

(4.38) ensure a sub-tour only belongs to one master tour.

$$\theta^{lk} = \sum_{k' \in K_{l+1}} f_{l,k}^{l+1,k'}, \quad \forall l \in L \setminus \{|L|\}, \quad \forall k \in K_l \tag{4.37}$$

$$\theta^{lk} = \sum_{k' \in K_{l-1}} f_{l-1,k'}^{l,k}, \quad \forall l \in L \setminus \{1\}, \quad \forall k \in K_l \tag{4.38}$$

$$f_{l,k}^{l+1,k'} \in \{0,1\}, \quad \forall l \in L \setminus \{|L|\}, \quad \forall k \in K_l, \quad \forall k' \in K_{l+1} \tag{4.39}$$

We define the index $\alpha_z^{lk} = 1$ if sub-route k in interval l selects the candidate DDP in zone z. Constraints (4.40) check the selection of each candidate DDP z. M_2 is a constant value that is set as $|\mathcal{V}||L|$.

$$\zeta_z \leq \sum_{l \in L} \sum_{k \in K_l} \alpha_z^{lk} \theta^{lk}, \quad \forall z \in \mathcal{Z}^M \tag{4.40}$$

$$\sum_{l \in L} \sum_{k \in K_l} \alpha_z^{lk} \theta^{lk} \leq M_2 \zeta_z, \quad \forall z \in \mathcal{Z}^M \tag{4.41}$$

MH pickup and dropoff activation. MHs can not load and unload when in the move, which says that only the MHs located at the start of a holding arc can provide service to couriers. Let H^{lk} be the set of starting nodes of the holding arcs on sub-route k in interval l. We define the non-negative integer $y_{(z,t)(z'',t'')}^{DM,lk}$ indicating the number of MDRs dropped off by the MHs located at z in period t that is on sub-route k in interval l to satisfy the courier service starting in zone z'' in period t''. Similarly, $y_{(z'',t'')(z,t)}^{RM,lk}$ represents the number of MDRs returned from z'' in t'' to the MH at z in t on sub-route k in interval l. The drop-off and pick-up flows associated with MHs and DDPs are presented in Constraints (4.42) - (4.43), as well as Constraints (4.12), (4.13).

$$y_{(z,t)(z'',t'')}^{DM,lk} \leq d_{zt} \theta^{lk}, \quad \forall l \in L, \quad \forall k \in K_l, \quad \forall (z,t) \in H^{lk}, \quad \forall (z'',t'') \in N_{z,t}^{C+} \tag{4.42}$$

$$y_{(z'',t'')(z,t)}^{RM,lk} \leq r_{zt} \theta^{lk}, \quad \forall l \in L, \quad \forall k \in K_l, \quad \forall (z,t) \in H^{lk}, \quad \forall (z'',t'') \in N_{z,t}^{C-} \tag{4.43}$$

$$y_{(z,t)(z'',t'')}^{DM,lk} \in \mathbb{Z}_{\geq 0}, \quad \forall l \in L, \quad \forall k \in K_l, \quad \forall (z,t) \in H^{lk}, \quad \forall (z'',t'') \in N_{z,t}^{C+} \tag{4.44}$$

$$y_{(z'',t'')(z,t)}^{RM,lk} \in \mathbb{Z}_{\geq 0}, \quad \forall l \in L, \quad \forall k \in K_l, \quad \forall (z,t) \in H^{lk}, \quad \forall (z'',t'') \in N_{z,t}^{C-} \tag{4.45}$$

Demands satisfaction.

$$\sum_{l\in L}\sum_{k\in K_l}\sum_{(z'',t'')\in N^{C-}_{z,t}\cap H^{lk}} y^{DM,lk}_{(z'',t'')(z,t)} + \sum_{(z'',t'')\in N^{C-}_{z,t}\cap \mathcal{N}^M} y^{DD}_{(z'',t'')(z,t)} + \sum_{(z'',t'')\in N^{C-}_{z,t}} y^{SF}_{(z'',t'')(z,t)} = d_{zt}, \quad \forall (z,t)\in \mathcal{N}^C \tag{4.46}$$

$$\sum_{l\in L}\sum_{k\in K_l}\sum_{(z'',t'')\in N^{C+}_{z,t}\cap H^{lk}} y^{RM,lk}_{(z,t)(z'',t'')} + \sum_{(z'',t'')\in N^{C+}_{z,t}\cap \mathcal{N}^M} y^{RD}_{(z,t)(z'',t'')} + \sum_{(z'',t'')\in N^{C+}_{z,t}} y^{SF}_{(z,t)(z'',t'')} = r_{zt}, \quad \forall (z,t)\in \mathcal{N}^C \tag{4.47}$$

Inventory management. We define the non-negative integer variable I^{lk}_{zt} indicating the number of MDRs on the MH located in z in t on the sub-route k in interval l. The MH capacity limit is expressed in Constraints (4.48).

$$I^{lk}_{zt} \le Q^{MH}\theta^{lk}, \quad \forall l\in L, \quad \forall k\in K_l, \quad \forall (z,t)\in H^{lk} \tag{4.48}$$

$$I^{lk}_{zt} \in \mathbb{Z}_{\ge 0}, \quad \forall l\in L, \quad \forall k\in K_l, \quad \forall (z,t)\in H^{lk} \tag{4.49}$$

Let $H^{lk}(1)$ and $H^{lk}(-1)$ be the first and last nodes in the set H^{lk}. For each node (z,t) in H^{lk}, we define $\bar{H}^{lk}_{zt}$ as its next node. Constraints (4.50) track the inventory update between two consecutive nodes in H^{lk}. Constraints (4.51) state that if route k in interval l and route k' in interval $l+1$ are on the same master route, then the MH inventory at the first node in $H^{l+1,k'}$ is updated based on the inventory at the last node in H^{lk}. The DDP inventory management is presented in Constraints (4.24) and (4.25).

$$I^{lk}_{\bar{H}^{lk}_{zt}} = I^{lk}_{zt} + \sum_{(z'',t'')\in N^{C-}_{z,t}} y^{RM,lk}_{(z'',t'')(z,t)} - \sum_{(z'',t'')\in N^{C+}_{z,t}} y^{DM,lk}_{(z,t)(z'',t'')},$$
$$\forall l\in L, \quad \forall k\in K_l, \quad \forall (z,t)\in H^{lk}\setminus\{H^{lk}(-1)\} \tag{4.50}$$

$$f^{l+1,k'}_{l,k} I^{l+1,k'}_{(z't')} = f^{l+1,k'}_{l,k}\left(I^{l,k}_{(z,t)} + \sum_{(z'',t'')\in N^{C-}_{z,t}} y^{RM,lk}_{(z'',t'')(z,t)} - \sum_{(z'',t'')\in N^{C+}_{z,t}} y^{DM,lk}_{(z,t)(z'',t'')}\right),$$
$$\forall l\in L\setminus\{|L|\}, \quad \forall k\in K_l, \quad \forall k'\in K_{l+1} \quad (z't') = H^{l+1,k'}(1), \quad (z,t) = H^{lk}(-1) \tag{4.51}$$

Objective function.

$$MIN \quad \Phi = J'_1 + J'_2 + J'_3 + J'_4 + J'_5 \tag{4.52}$$

where:

$$J_1' = c^{MH} \sum_{k \in K_1} \theta^{1k} \tag{4.53}$$

$$J_2' = c^{MDR} \left(\sum_{k \in K_1} I^{1,k}_{z_o,1} + \sum_{z \in \mathcal{Z}^D} I^D_{z,1} \right) \tag{4.54}$$

$$J_3' = c^{DDP} \sum_{z \in \mathcal{Z}^D} \zeta_z \tag{4.55}$$

$$\begin{aligned} J_4' = c^{VoT} \Bigg(\sum_{l \in L} \sum_{k \in K_l} \sum_{(z,t) \in H^{lk}} \Bigg(& \sum_{(z'',t'') \in N^{C-}_{z,t}} y^{RM,lk}_{(z'',t''),(z,t)} DIS_{zz''} + \sum_{(z'',t'') \in N^{C+}_{z,t}} y^{DM,lk}_{(z,t)(z'',t'')} DIS_{zz''} \Bigg) \\ & + \sum_{(z,t) \in \mathcal{N}^M} \Bigg(\sum_{(z'',t'') \in N^{C-}_{z,t}} y^{RD}_{(z'',t'')(z,t)} DIS_{zz''} + \sum_{(z'',t'') \in N^{C+}_{z,t}} y^{DD}_{(z,t)(z'',t'')} DIS_{zz''} \Bigg) \Bigg) \end{aligned} \tag{4.56}$$

$$J_5' = c^{SF} \sum_{(z,t)(z'',t'') \in \mathcal{A}^C} y^{SB}_{(z,t)(z'',t'')} DIS_{zz''} \tag{4.57}$$

4.5. Linearization

Constraints (4.21) in the arc-based model is nonlinear, which can be linearized as follows:

$$\begin{aligned} & Q^{MH}(1 - x^v_{(z,t)(z',t')}) I^v_{z't'} \geq I^v_{zt} + \sum_{(z'',t'') \in N^{C-}_{z,t}} y^{RM,v}_{(z'',t'')(z,t)} - \sum_{(z'',t'') \in N^{C+}_{z,t}} y^{DM,v}_{(z,t)(z'',t'')}, \\ & \quad \forall v \in \mathcal{V}, \quad \forall (z,t) \in \mathcal{N}^M, \quad \forall (z',t') \in N^{M+}_{z,t} \end{aligned} \tag{4.58}$$

$$\begin{aligned} & Q^{MH}(x^v_{(z,t)(z',t')} - 1) I^v_{z't'} \leq I^v_{zt} + \sum_{(z'',t'') \in N^{C-}_{z,t}} y^{RM,v}_{(z'',t'')(z,t)} - \sum_{(z'',t'') \in N^{C+}_{z,t}} y^{DM,v}_{(z,t)(z'',t'')}, \\ & \quad \forall v \in \mathcal{V}, \quad \forall (z,t) \in \mathcal{N}^M, \quad \forall (z',t') \in N^{M+}_{z,t} \end{aligned} \tag{4.59}$$

Constraints (4.51) in the route-based model are non-linear, which can be linearized as:

$$\begin{aligned} & Q^{MH}(1 - f^{l+1,k'}_{l,k}) + I^{l+1,k'}_{(z',t')} \geq I^{lk}_{(z,t)} + \sum_{(z'',t'') \in N^{C-}_{(z,t)}} y^{RM,lk}_{(z'',t'')(z,t)} - \sum_{(z'',t'') \in N^{C+}_{(z,t)}} y^{DM,l,k}_{(z,t),(z'',t'')}, \\ & \quad \forall l \in L \setminus \{|L|\}, \quad \forall k \in K_l, \quad \forall k' \in K_{l+1}, \quad (z,t) = H^{lk}(-1), \quad (z',t') = H^{l+1,k'}(1) \end{aligned} \tag{4.60}$$

$$\begin{aligned} & Q^{MH}(f^{l+1,k'}_{l,k} - 1) + I^{l+1,k'}_{(z',t')} \leq I^{lk}_{(z,t)} + \sum_{(z'',t'') \in N^{C-}_{(z,t)}} y^{RM,lk}_{(z'',t'')(z,t)} - \sum_{(z'',t'') \in N^{C+}_{(z,t)}} y^{DM,l,k}_{(z,t),(z'',t'')}, \\ & \quad \forall l \in L \setminus \{|L|\}, \quad \forall k \in K_l, \quad \forall k' \in K_{l+1}, \quad (z,t) = H^{lk}(-1), \quad (z',t') = H^{l+1,k'}(1) \end{aligned} \tag{4.61}$$

4.6. Variable reduction

After logical analysis of the system, the upper bounds of the integer variables can be determined. When the upper bounds are 0, the corresponding variables could be removed.

- $\sum_{v\in\mathcal{V}}\sum_{(z'',t'')\in N^{C-}_{z,t}\cap\mathcal{N}^M} y^{DM,v}_{(z'',t'')(z,t)} = 0 \quad \text{if } d_{zt} = 0.$
- $\sum_{l\in L}\sum_{k\in K_l}\sum_{(z'',t'')\in N^{C-}_{z,t}\cap H^{lk}} y^{DM,lk}_{(z'',t'')(z,t)} = 0 \quad \text{if } d_{zt} = 0.$
- $\sum_{(z'',t'')\in N^{C-}_{z,t}\cap\mathcal{N}^M} y^{DD}_{(z'',t'')(z,t)} \quad \text{if } d_{zt} = 0.$
- $\sum_{v\in\mathcal{V}}\sum_{(z'',t'')\in N^{C+}_{z,t}\cap\mathcal{N}^M} y^{RM,v}_{(z,t)(z'',t'')} = 0 \quad \text{if } r_{zt} = 0.$
- $\sum_{l\in L}\sum_{k\in K_l}\sum_{(z'',t'')\in N^{C+}_{z,t}\cap H^{lk}} y^{RM,lk}_{(z,t)(z'',t'')} = 0 \quad \text{if } r_{zt} = 0.$
- $\sum_{(z'',t'')\in N^{C+}_{(z,t)}\cap\mathcal{N}^M} y^{RD}_{(z,t),(z'',t'')} = 0 \quad \text{if } r_{zt} = 0.$
- $\sum_{(z'',t'')\in N^{C-}_{z,t}} y^{SF}_{(z'',t'')(z,t)} = 0 \quad \text{if } d_{zt} = 0$
- $\sum_{(z'',t'')\in N^{C+}_{z,t}} y^{SF}_{(z,t)(z'',t'')} = 0 \quad \text{if } r_{zt} = 0$

4.7. Algorithm for route generation

We adapt the algorithm described in [3] to generate routes in each interval l. A route is a sequence of time-space nodes in a specific interval. The routes in each interval start and end at z_o. The pseudo-code of the adapted algorithm is presented in Algorithm 1. To generate all possible routes in the interval l, we begin by initializing candidate routes. In the route generation phase, we iteratively expand the candidate route set by considering the last node in each candidate route. We generate new candidate routes by adding emanating arcs from the last node of each candidate route. If a new candidate route does not end at the end period, it is added back to the candidate route set for further expansion. If a new candidate route ends at the final period and in the depot, it is registered as a valid route. The process continues until no more candidate routes are left for expansion.

Algorithm 1 Route generation algorithm for an interval

Require: interval, start zones, end zones, start period, end period

Initialization candidate routes phase:
for all emanating arcs of node (z_o,1) **do**
    create candidate routes for each emanating arc
end for
Routes generation phase:
while candidate route set is not empty **do**
    for all candidate routes **do**
        if period of last node < end period **then**
            for all emanating arcs of last node **do**
                create new candidate routes by adding the arc
                if new candidate route does not end in end period **then**
                    add the new route to candidate route set
                else if new candidate route ends in end period **then**
                    if new candidate route ends in the depot **then**
                        register new candidate route as a valid route
                    end if
                end if
            end for
        end if
        remove the candidate route from candidate route set
    end for
end while
return route set for the interval

5

Results

In this section, we experiment with the proposed CMFLP-MDs models using representative instances. In Section 5.1, we describe the input generation scheme. In Section 5.2, we test the computational performance of the arc-based and route-based models and the effect of variable reduction. In Section 5.3, we conduct various sensitivity analyses to investigate the managerial benefit of the proposed Mobile-Hub concept using generated instances. In Section 5.4 we test our model on real-world data in Amsterdam to demonstrate the added value of this new technology in current practice.

5.1. Instance generation

The on-demand delivery system operates within a predefined area discretized into hexagonal zones arranged in a circular pattern. We identify two service areas: an area of 37 hexagonal zones arranged in 4 circles (noted as Area-4), and an area of 91 hexagonal zones arranged in 6 circles (noted as Area-6). The edge of each zone is 200 meters, and one period represents 10 minutes. The innermost zone is chosen as the MH depot where the MHs start and end their shifts. For both service areas, we consider three planning horizons: {36, 48, 72} periods. We also consider a varying number of courier services: {20, 30, 40, 50, 60}. Two courier service distributions are identified to represent different geographical distributions of the courier service starting and ending locations within the service area. In the first scenario (noted as **U**), a courier has an equal probability of starting and ending their service in any of the zones. In the second scenario (noted as **C**), a courier has a 75% probability of starting in the area center and a 75% probability of ending in the outskirts. This scenario mimics the situation where restaurants are more often located in

the city center, and households are usually situated outside the city center. The area center is defined as a circle with a radius of r zones originating from the innermost zone, where $r = 2$ for Area-4 and $r = 3$ for Area-6. We assume the service start time of each courier is randomly distributed within the first half of the planning horizon, and the corresponding end time is randomly distributed within the duration between the start time and the end of the planning horizon.

For all instances, we consider two homogeneous MHs, each with a capacity Q^{MH} of 50 MDRs, and the homogeneous candidate DDPs have a capacity Q^{DDP} of 1 MDR. Four canal typologies (Figure 5.1), replicated from real city canals, are considered: Amsterdam (noted as Canal-1), Leiden (noted as Canal-2), Venice (noted as Canal-3), and Fredrikstad (noted as Canal-4). For each network type, we calculate the following indexes, which indicate the complexity of the network: α, β, and γ. The index α measures the degree of connectivity in a network by comparing the number of actual circuits (or loops) to the maximum number of circuits possible. The index β compares the number of links to the number of nodes. The index γ compares the number of actual links in the network to the maximum possible number of links between nodes. These indexes are calculated as:

$$\alpha = \frac{L - N + 1}{2N - 5}$$
$$\beta = \frac{L}{N}$$
$$\gamma = \frac{L}{3(N - 2)}$$

where L is the number of links, and N is the number of vertices.

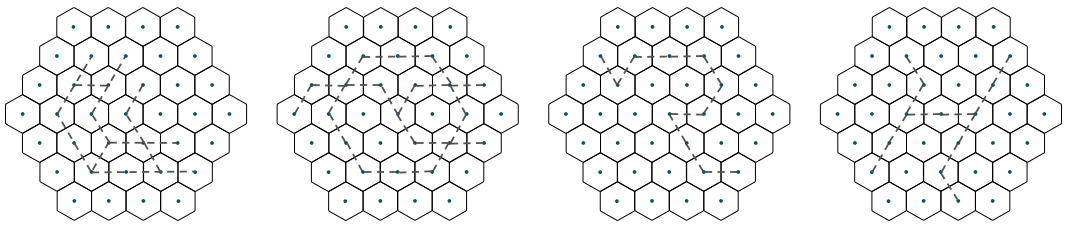

Figure 5.1: Canal typologies replicated from Amsterdam, Leiden, Venice, and Fredrikstad

In Table 5.1, we present the characteristics of the instances: (1) area size, (2) planning horizon length, (3) courier service distribution, (4) number of courier services, and (5) canal network typology. The instances are named accordingly. For example, "A4-P36-**U**-S40-N1" indicates the case of Area-4, a planning horizon of 36 periods, uniformly distributed courier services, 40

courier services, and network type 1.

We set the daily cost of an MH as 810 €, representing the fixed cost including the vessel leasing, energy, and driver salary. The average bike price in the Netherlands is 865 €. We consider the service life of a new bike to be three years, so the daily cost of one bike is set as $\frac{865}{1095} = 0.79$ €. According to the price for storing one bicycle with the Netherlands train operator NS, we set the yearly cost of a DDP as 100 euros, i.e., 0.27 euros per day. We consider the gross hourly salary of a courier to be 14.77 €, thus the opportunity cost of one period for one courier spending on pre- and post-service riding is 2.46 €.

Table 5.1: Instance characteristics

Characteristics	Types
Area size	4-circle, 6-circle
Planning horizon	36 periods, 48 periods, 72 periods
Service distribution	**U**, **C**
Courier service number	20, 30, 40, 50, 60
Network typology	Network-1, Network-2, Network-3, Network-4

5.2. Computational performance

In this section, we provide some insights of the computational performance of the models. We conduct the experiments using Python and Gurobi Optimizer version 11.0.0. All experiments are carried out on a computer with a 2.4 GHz CPU, 8 GB of RAM, and an 8-core processor. Each instance is solved with a time limit of 4 hours. In Section 5.2.1, we discuss the effect of the pre-processing. In Section 5.2.2, we compare the computational performance of the arc-based model and the route-based model. Section 5.2.3 examines the computation time sensitivity to network typology and demand scenario.

5.2.1. Effect of pre-processing

We select 12 instances to test the performance of the pre-processing on both the arc-based and route-based models. Using network Type-1, demand scenario **U**, and 40 courier services as a representative case, we vary the area size (Area-4, Area-6), planning horizon length (36 periods, 48 periods, 72 periods), and interval length (4 periods and 6 periods). Tables 5.2 and 5.3 present the characteristics of these instances with and without applying the pre-processing. We keep the automatic pre-processing of Gurobi while solving. The columns contain the integer solution

($\bar{\Phi}$), the objective value of the linear relaxation ($\bar{\Phi}_{LP}$), the percentage integrality gap ($\bar{\Phi}/\bar{\Phi}_{LP}$), the number of constraints (Cons.), the number of variables (Var.), and the number of binary variables (Bin.). The results demonstrate that applying pre-processing significantly reduces the model size in terms of the number of variables and constraints for both the arc-based and route-based formulations.

Table 5.2: Effect of pre-processing for instances under case **U**-S40-N1 (Arc-based model)

Instance	$\bar{\Phi}$	$\bar{\Phi}_{LP}$	Int. Gap	Without pre-processing			With pre-processing		
				Cons.	Vars.	Bin.	Cons.	Vars.	Bin.
A4-P36-I4	1245.66	1189.46	105%	17737	10846	9292	16241	10337	8816
A4-P36-I6	1245.66	1169.01	107%	17737	10855	9301	16358	10415	8882
A4-P48-I4	1232.57	1163.12	106%	25793	14796	12399	21494	12821	10712
A4-P48-I6	1211.39	1112.78	109%	25793	14811	12414	24202	14330	11954
A4-P72-I4	1239.95	1167.74	106%	33758	18643	15481	31577	18021	14889
A4-P72-I6	1199.57	1072.02	112%	33758	18661	15499	31684	18087	14934
A6-P36-I4	1412.24	1339.84	105%	17889	10990	9556	16350	10482	9078
A6-P36-I6	1397.96	1294.18	108%	17889	10999	9565	16464	10557	9141
A6-P48-I4	1458.80	1398.25	104%	25823	14792	12490	21434	12803	10790
A6-P48-I6	1432.70	1345.02	107%	25823	14802	12509	24033	14282	12002
A6-P72-I4	1498.16	1430.81	105%	33641	18501	15285	31355	17843	14660
A6-P72-I6	1440.56	1339.98	108%	33641	18519	15303	31446	17906	14711

Table 5.3: Effect of pre-processing for instances under case **U**-S40-N1 (Route-based model)

Instance	$\bar{\Phi}$	$\bar{\Phi}_{ZP}$	Int. Gap	Without pre-processing			With pre-processing		
				Cons.	Vars.	Bin.	Cons.	Vars.	Bin.
A4-P36-I4	1245.66	1221.17	102%	846	547	483	654	472	84
A4-P36-I6	1245.66	1225.19	101%	5495	3361	3030	5028	3204	1602
A4-P48-I4	1232.57	1208.87	102%	1172	735	623	920	643	180
A4-P48-I6	1211.39	1189.27	102%	7515	4322	3850	6791	4094	2418
A4-P72-I4	1239.95	1215.43	102%	1289	737	628	1011	673	213
A4-P72-I6	1199.57	1177.01	102%	9607	5335	4780	8603	5049	3234
A6-P36-I4	1412.24	1390.08	102%	879	591	525	686	458	87
A6-P36-I6	1397.96	1380.57	101%	5549	3417	3080	5065	3242	1602
A6-P48-I4	1458.80	1433.07	102%	1206	743	632	965	665	181
A6-P48-I6	1432.70	1407.35	102%	7546	4338	3889	6761	4082	2418
A6-P72-I4	1498.16	1471.51	102%	1303	750	633	1000	664	213
A6-P72-I6	1440.56	1416.82	102%	9533	5253	4689	8525	4954	3234

5.2.2. Comparison between two models

This section compares the computational performance of the arc-based and route-based models. We still choose network Type-1 and demand scenario **U** as a representative case. We select 18 instances by varying the area size, planning horizon, interval length and courier service number (40, 60, 80). We present in Table 5.4 the results of the instances with an interval length of 4 periods, and in Table 5.5 the results for the same instances with an interval length of 6 periods. The columns include the number of explored nodes (Nodes), the optimality gap (Gap), and runtime. The column "Imp" shows the improvement in solving time of the route-based model compared to the arc-based model.

We see that when the number of courier services is 40 and 60, both models solve the instances quickly to optimality. However, neither model converges when the number of courier services reaches 80 for instances with a planning horizon of 48 and 72 periods. Table 5.6 summarizes the results from Table 5.4 and Table 5.5. The results show that, on average, the route-based model performs better for the selected instances. Also, instances with an interval length of 6 periods take longer time to solve and have a larger gap when the time limit is reached.

5.2.3. Computation time sensitivity to network type and demand scenario

In this section we investigate the network typology and courier service distribution on the solving time. We consider the four canal network shapes and the two courier service distributions as described in Section 5.1. We use Area-4 and planning horizon of 36 periods as a representative case and consider three levels of courier services {40, 60, 80}, which are named "A4-P36-S40", "A4-P36-S60", and "A4-P36-S80". The interval length is 6 periods for all tests. Table 5.7 presents the computational results under different combinations of network typologies and service distribution. We further summarize the results in Table 5.7 in Table 5.8. The columns include the network typology, instance name, optimality gap (Gap), and time for both demand scenarios **U** and **C**. The optimality gap is calculated as $100 \times (\bar{\Phi} - LB)/\bar{\Phi}$, where $\bar{\Phi}$ is the best feasible solution and LB is the best-known lower bound.

We observe that, on average, solving instances under network Type-2 takes the longest time. This reflects the fact that Type-2 is the most complex network among the four types, with all three indexes having the highest values. In terms of demand pattern, scenario **C** is harder to solve. Specifically, solving instances with 80 courier services under scenario **C** could not prove optimality within 4 hours.

5.3. Managerial insights

This section discusses the managerial implications of the proposed Mobile-Hub strategy for on-demand delivery platforms. According to historical data from a local platform in Amsterdam,

Table 5.4: Comparison of Arc-based and Route-based model performance for instances under case "**U**-N1 (Interval of 4 periods)"

Instance	Arc-based			Route-based			Imp.
	Nodes	Gap	Run Time(s)	Nodes	Gap	Run Time(s)	
A4-P36-S40	348	0	10.63	1	0	0.28	97.37%
A4-P36-S60	1	0	8.40	1	0	0.3	96.43%
A4-P36-S80	378	0	27.01	1	0	0.73	97.30%
A4-P48-S40	4496	0	11.28	1	0	0.97	91.40%
A4-P48-S60	481	0	11.97	1	0	0.36	96.99%
A4-P48-S80	1687422	1.59%	14400.94	805144	0.28%	14402.56	-
A4-P72-S40	11179	0	27.21	1	0	0.68	97.50%
A4-P72-S60	5073	0	81.42	354	0	2.18	97.32%
A4-P72-S80	1609272	1.98%	14400.11	649713	1.35%	14401.00	-
A6-P36-S40	494	0	8.20	1	0	0.45	94.51%
A6-P36-S60	1	0	8.01	1	0	0.29	96.38%
A6-P36-S80	1145730	0.23%	14400.03	742444	0.28%	14401.00	-
A6-P48-S40	249	0	9.75	1	0	0.37	96.21%
A6-P48-S60	1	0	16.27	1	0	0.45	97.23%
A6-P48-S80	1458483	1.27%	14400.44	1002713	0.40%	14403.21	-
A6-P72-S40	5650	0	30.48	41	0	0.94	99.99%
A6-P72-S60	4151	0	27.67	1	0	0.46	98.34%
A6-P72-S80	594571	1.62%	14400.32	250476	1.58%	14407.73	-

there are approximately 180 active courier shifts on a typical operating day (9:00 - 23:00) in the whole city. In this section, we consider one vessel as an MH and use the instance "A4-P48-S40" as a representative case, assuming the vessel operates in Area-4 which is in the city center to serve 40 courier shifts during the busiest hours from 15:00 to 22:00 (a planning horizon of 48 periods). Furthermore, we assume the battery capacity of the vessel is 8 hours, which only requires the vessel to return to the depot at the closure of the planning horizon.

Section 5.3.1 explores the impact of canal network typology and courier service distributions. Section 5.3.2 studies the sensitivity of vessel battery capacity by varying the duration for which the vessel must return to the depot. Section 5.3.3 investigates the impact of the number of courier services. Section 5.3.4 tests the sensitivity of the parameter c^{SF}, which represents the cost related to courier self-fulfillment.

Table 5.5: Comparison of Arc-based and Route-based model performance for instances under case "**U**-N1 (Interval of 6 periods)"

Instance	Arc-based			Route-based			Imp.
	Nodes	Gap	Run Time(s)	Nodes	Gap	Run Time(s)	
A4-P36-S40	1727	0	25.48	1	0	2.75	89.21%
A4-P36-S60	1293	0	33.24	1	0	6.61	80.11%
A4-P36-S80	681	0	67.26	1	0	8.05	88.03%
A4-P48-S40	10205	0	42.7	115	0	10.75	74.82%
A4-P48-S60	7386	0	92.46	207	0	22.53	75.63%
A4-P48-S80	242860	1.91%	14400.69	97615	1.69%	14400.83	-
A4-P72-S40	148392	0	939.19	9993	0	95.15	89.87%
A4-P72-S60	687568	0.89%	14401.15	33942	0	1283.91	91.08%
A4-P72-S80	314445	1.97%	14402.54	272029	29.10%	14402.13	-
A6-P36-S40	2592	0	20.63	1	0	3.19	84.54%
A6-P36-S60	194	0	30.61	1	0	4.78	84.38%
A6-P36-S80	227947	0.14%	14403.80	531102	0.14%	14400.29	-
A6-P48-S40	1671	0	47.58	1	0	6.08	87.22%
A6-P48-S60	2799	0	46.53	450	0	89.29	-91.90%
A6-P48-S80	466772	1.33%	14400.36	88538	1.40%	14400.77	-
A6-P72-S40	397512	0	4181.69	5694	0	96.51	97.69%
A6-P72-S60	238913	0	3007.53	4609	0	1117.97	62.83%
A6-P72-S80	103437	26.70%	14401.34	202307	5.52%	14402.94	-

Table 5.6: The summary of results reported in Table 5.4 and Table 5.5

	Arc-based		Route-based	
	Ave. Gap	Ave. Run time(s)	Ave. Gap	Ave. Run time(s)
Interval 4	0.37%	4813.84	0.22%	4001.33
Interval 6	1.83%	5274.22	2.10%	4152.73

To study the impact of these characteristics, we define the following system performance indicators: (1) objective value indicating the total system cost (column "Obj. Val. (€)"), (2) number of required MDRs (column "MDRs"), (3) number of visited DDPs (column "DDPs"), and (4) the average non-service time a courier spends on pre- and post-service riding (column "Cour. non-service time (min)").

Table 5.7: Computation time sensitivity to network typology and service distribution

Network	Instance	**U**		**C**	
		Gap	Time(s)	Gap	Time(s)
Type-1	A4-P36-S40	0	2.67	0	8.96
	A4-P36-S60	0	3.72	0	13.62
	A4-P36-S80	0	2.7	1.54%	14400.13
Type-2	A4-P36-S40	0	24.61	0	12.15
	A4-P36-S60	0	19.52	0	20.76
	A4-P36-S80	0	29.02	0.62%	14400.44
Type-3	A4-P36-S40	0	0.82	0	1.48
	A4-P36-S60	0	6.57	0	1.7
	A4-P36-S80	0	1.78	1.44%	14400.08
Type-4	A4-P36-S40	0	2.21	0	11.08
	A4-P36-S60	0	9.79	0	11.22
	A4-P36-S80	0	14.81	1.44%	14400.10

Table 5.8: Summary of Table 5.7

Network	**U**		**C**	
	Ave. Gap	Ave. Time(s)	Ave. Gap	Ave. Time(s)
Type-1	0	3.03	0.51%	4807.47
Type-2	0	24.38	0.21%	4811.12
Type-3	0	3.06	0.48%	4801.09
Type-4	0	8.94	0.48%	4807.47

5.3.1. Impact of canal typology and courier service distribution

This analysis aims to prepare the platform for potential business expansion in different cities with distinct canal network typologies and restaurant household distributions. We consider four canal networks and two service distributions (**U** and **C**) as described in Section 5.1, resulting in eight "Network - Service distribution" combinations.

The results in Table 5.9 show that for each canal network type, the average values of the various system indicators for the two service distributions are close to each other, suggesting that the canal network shape has a negligible impact on the Mobile-Hub system infrastructure configuration and operation. When examining the influence of service distribution under the same canal type, we find that even though both distributions require the same number of MDRs, the objective value is consistently higher when courier services are geographically uniformly distributed. In

this case, the vessel needs to visit more DDPs, and couriers spend more time on non-service riding on average. This is because uniformly distributed courier services are less concentrated than the centric demand distribution, requiring the vessel to cover a wider range of the service area and spend more time en route.

Table 5.9: Sensitivity to canal network type and courier service distribution under case "A4-P48-S40"

Network	Ser. Distrb.	Obj. Val.(€)	MDRs	DDPs	Cour. non-service time (min)
1	C	1085.18	29	5	12.75
	U	1150.49	29	10	16.00
	Ave.	1117.84	29	7.5	14.375
2	C	1087.37	29	4	12.88
	U	1162.25	29	8	16.62
	Ave.	1124.81	29	6	14.75
3	C	1085.45	29	6	12.75
	U	1154.60	29	7	16.25
	Ave.	1120.03	29	6.5	14.50
4	C	1089.83	29	4	13.00
	U	1149.41	29	6	16.00
	Ave.	1119.62	29	5	14.5

5.3.2. Vessel battery capacity sensitivity

The vessel must return to the depot periodically to recharge, with the interval length depending on the vessel battery capacity. This analysis aims to inform the platform about the impact of battery capacity on the Mobile-Hub infrastructure configuration and vessel operation. We use uniformly distributed courier services, and network type-1 ("A4-P48-**U**-S40-N1") as a representative case, and vary the interval length (column "Battery life (hr)" in Table 5.10) for which duration the vessel must return to the depot: {0, 1, 2, 4, 8}. A larger battery capacity allows the vessel to cover a larger range of the service area, providing more routing and scheduling options. By changing the battery life, we impose different levels of mobility limitations on the vessel. An interval length of 0 indicates no vessel mobility, with the vessel parked at the depot throughout the planning horizon. An interval length of 1 hour only allows the vessel to cover the center area of the service area, while interval lengths over 2 hours enable the vessel to visit the outermost zones. An interval length of 8 hours represents the vessel only returning to the depot at the end of the planning horizon, having the most flexibility.

The results show that both the objective value and the average courier non-service riding time decrease with larger battery capacities. Additionally, a longer battery life allows the vessel to visit more DDPs. The results prove that a higher level of vessel mobility helps improve courier service levels. Furthermore, as the battery life of 0 hours mimics the static hub which is the current practice applied by the platform, the results demonstrate the benefit of the Mobile-Hub strategy.

Table 5.10: Sensitivity to battery life under case "A4-P48-**U**-S40-N1"

Battery life (hr)	Obj. Val. (€)	MDRs	DDPs	Courier non-service time (min)
0	1224.32	29	1	19.88
1	1185.77	29	4	17.88
2	1178.66	29	5	17.50
4	1154.33	29	6	16.25
8	1149.41	29	6	16.00

5.3.3. Courier number analysis

Changes in customer orders directly impact the size of the courier fleet. This analysis prepares the platform for situations where meal order volumes may deviate from the normal range on certain days due to special events, such as festivals. We use service distribution **U** and network Type-1 ("A4-P48-U-N1") as a representative case and vary the number of courier services as {20, 30, 40, 50, 60}, as shown in the "Cour. Nr." column in Table 5.11. The "Cost per Cour." column indicates the average cost per courier.

The results in Table 5.11 and Figure 5.2 - 5.6 show that while the objective value increases with the number of courier services, the average cost per courier decreases. The required number of MDRs is consistently maintained at a certain level (between 70% - 90%) relative to the number of courier services. This can be explained by the fact that MDR collection and drop-offs always occur concentratedly within a certain duration during the planning horizon. Sharp increases in MDR pickups always occur before and during meal peaks (16:00-18:00), which is the first half of the planning horizon in our case, while MDR returns always happen after the meal peaks. As a result, the number of required MDRs consistently increases with the quantity of courier services. On the other hand, the number of visited DDPs drops as the number of couriers to serve increases, while the courier non-service riding time is not significantly influenced by the number of courier services.

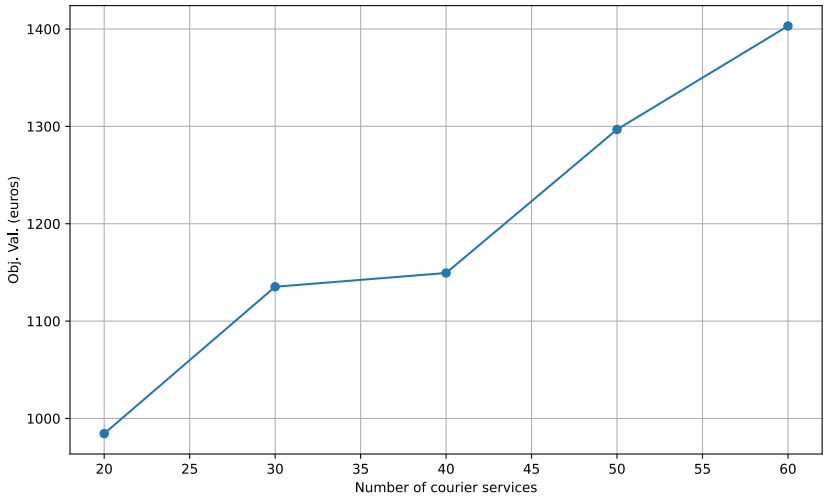

Figure 5.2: Sensitivity to courier service number on objective value (euros)

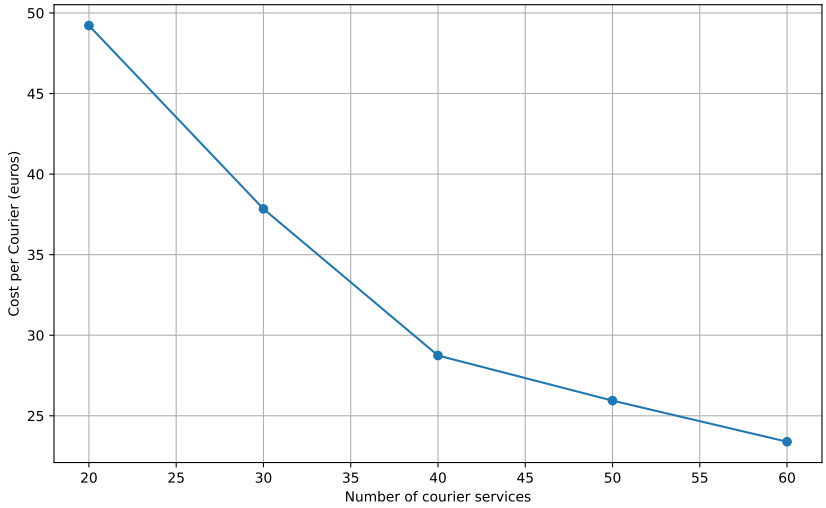

Figure 5.3: Sensitivity to courier service number on cost per courier (euros)

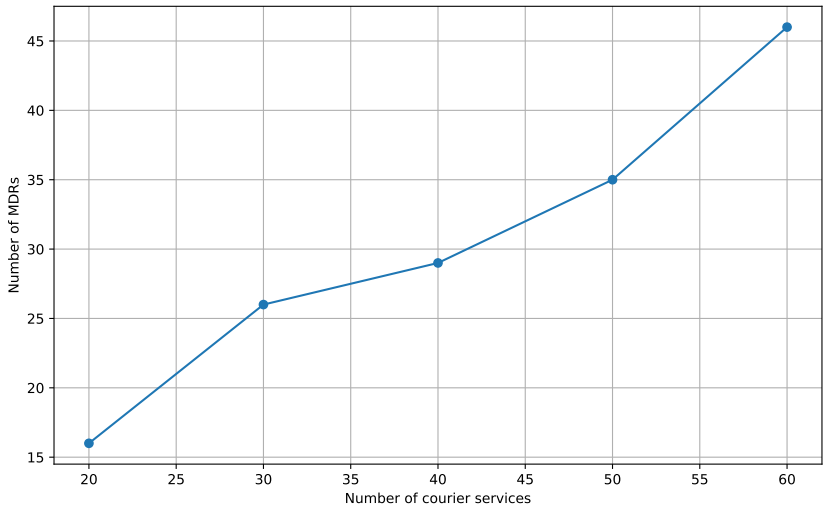

Figure 5.4: Sensitivity to courier service number on number of MDRs

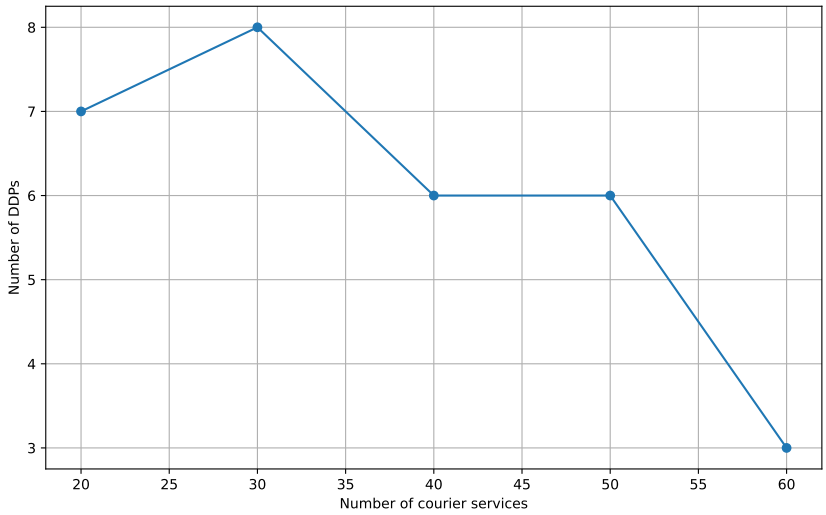

Figure 5.5: Sensitivity to courier service number on number of DDPs

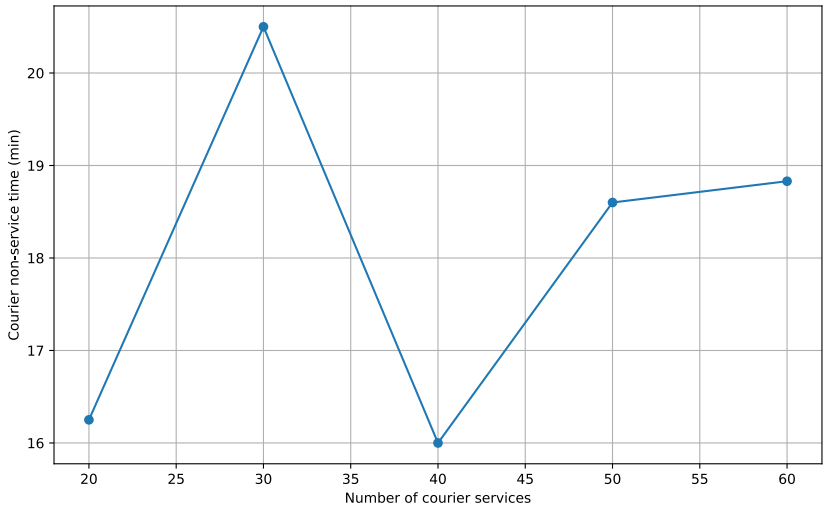

Figure 5.6: Sensitivity to courier service number on courier non-service time (min)

Table 5.11: Sensitivity to courier service number under case "A4-P48-**U**-N1"

Cour. Nr.	Obj. Val.(€)	Cost per Cour.(€)	MDRs	MDRs/Cour. Nr.	DDPs	Courier non-service time (min)
20	984.43	49.22	16	0.80	7	16.25
30	1135.28	37.84	26	0.87	8	20.5
40	1149.41	28.74	29	0.73	6	16
50	1296.83	25.94	35	0.70	6	18.6
60	1403.11	23.39	46	0.77	3	18.83

5.3.4. Self-fulfillment cost analysis

This analysis deals with the uncertainty of the unit cost associated with the courier service demand self-fulfillment. In our assumptions, courier demand self-fulfillment is realized by considering a free-floating location in each zone where two couriers can meet to hand over their bikes at no charge. However, in some cities, this may involve additional management and administration costs. In this section, we increase the ratio c^{SF}/c^{vot} between the unit cost associated with the courier demand self-fulfillment and the courier value of time as {1, 1.2, 1.4, 1.6, 1.8, 2}. In Table 5.12, the columns "By MH (%)", "By DDPs (%)", and "By self-FF. (%)" indicate the proportion of total courier service satisfied by the vessel, DDPs, and self-fulfillment, respectively. The results in Table 5.12 and Figure 5.7 - 5.9 show that the objective value slightly increases with the unit demand self-fulfillment cost. The demand satisfied by self-fulfillment decreases from 7% to 5% after c^{SF}/c^{vot} increases to 1.4. The average ride time per courier also slightly increases.

Table 5.12: Sensitivity to unit courier self-fulfillment cost under case "A4-P48-**U**-N1"

c^{SF}/c^{vot}	Obj. Val. (€)	By MH (%)	By DDP (%)	By self-FF. (%)	Courier non-service time (min)
1	1149.41	72	20	7	16.00
1.2	1151.87	75	17	7	16.00
1.4	1153.84	75	20	5	16.12
1.6	1154.82	75	20	5	16.12
1.8	1155.81	72	22	5	16.12
2	1156.79	75	20	5	16.12

5.4. Case study on Amsterdam canal area

In this section, we apply the proposed Mobile-Hub strategy to practice, testing our model on data from a local on-demand delivery platform in the Netherlands. We use courier schedules from September 13, 2021, to October 10, 2021, in the Amsterdam Canal area as our sample. We manually outline the course of the canal for the gridded service area, which contains 91 zones

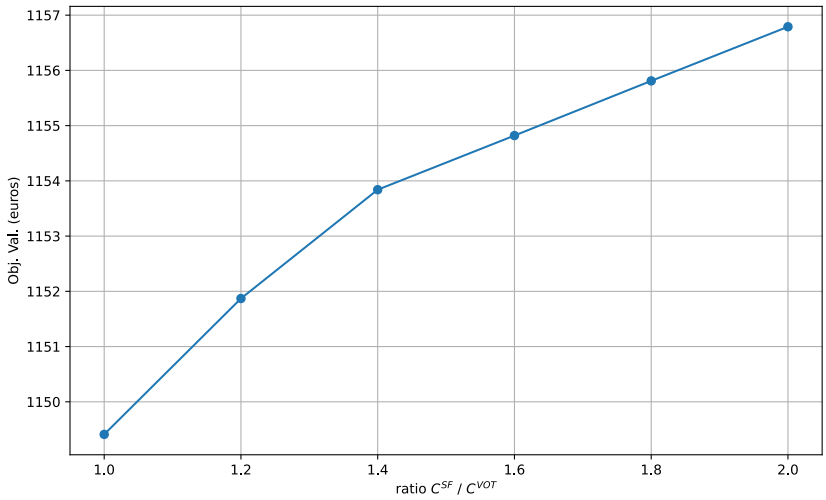

Figure 5.7: Sensitivity to unit self-fulfillment cost on objective value (euros)

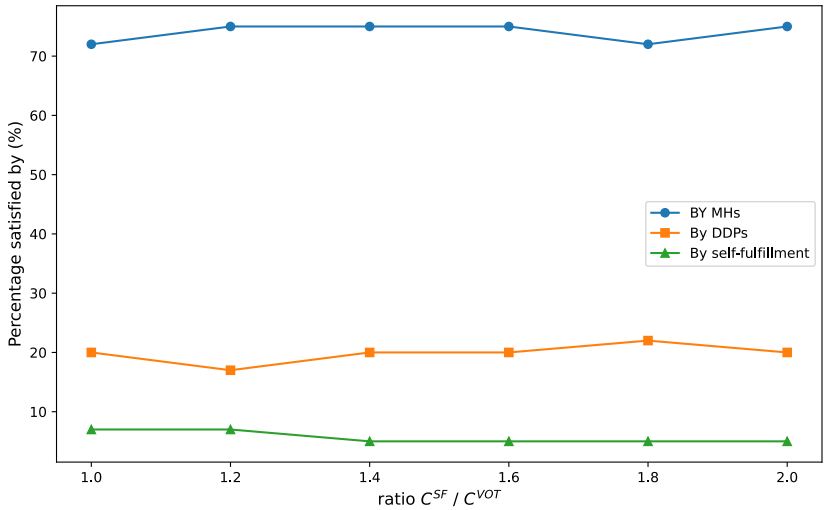

Figure 5.8: Sensitivity to unit self-fulfillment cost on the percentage of courier services satisfied by MHs, DDPs, and self-fulfillment

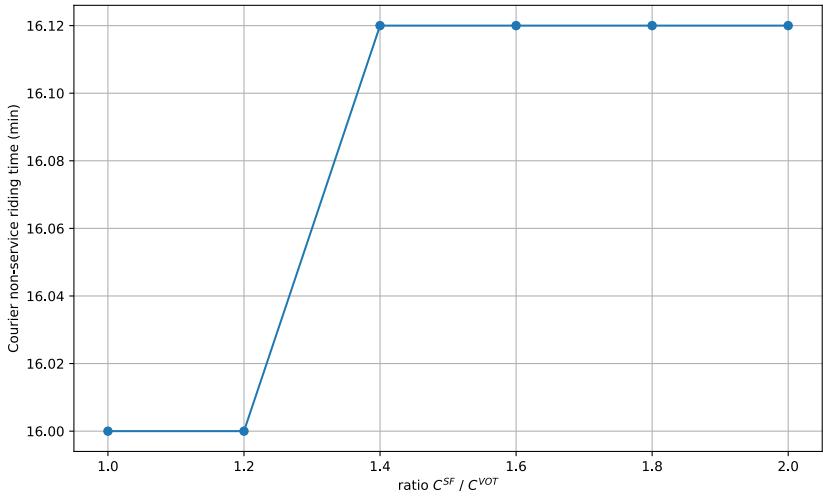

Figure 5.9: Sensitivity to unit self-fulfillment cost on courier non-service riding time (min)

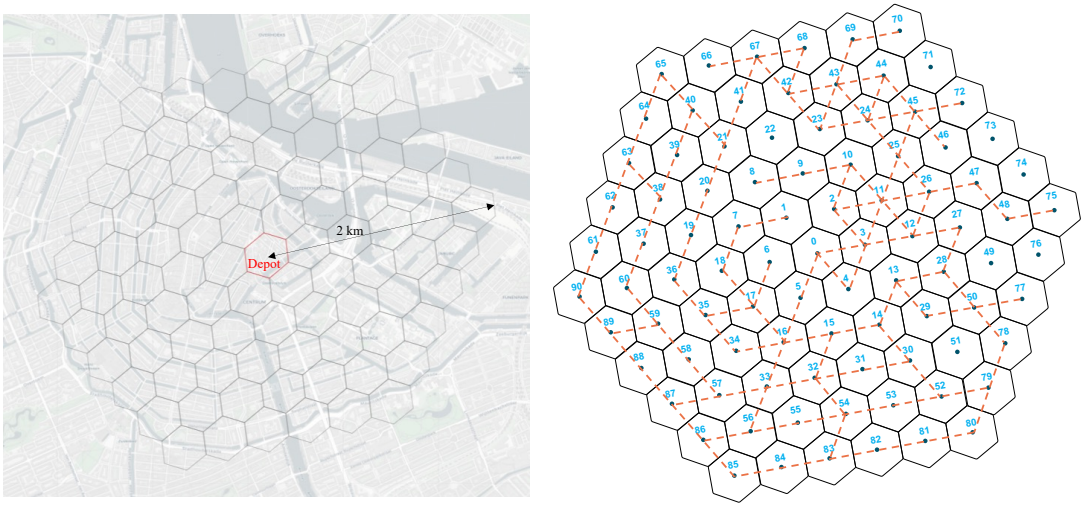

Figure 5.10: Amsterdam canal network abstraction

(Figure 5.10). Each zone has an edge length of 200 meters, and the distance between the centers of two adjacent zones is 347 meters. We consider two available homogeneous electric vessels as the MHs, each with a capacity of 50 MDRs. We assume all zones crossed by canals are capable of establishing a DDP. Given the curved canals and busy waterway transport in the Amsterdam center, we assume a vessel speed of 4 km/hour and a period length of 10 minutes. For the chosen area, we select the innermost zone as the depot for the vessels. The vessels need to return to the depot every 8 hours to recharge.

We consider the operation of a typical day from 9:00 in the morning to 24:00 at night, totaling 96 periods. The chosen area exemplifies the situation where most meal pickups and drop-offs occur in Amsterdam. After averaging the one-month courier schedules to one day and removing the

courier shifts that either start or end outside the chosen area, we obtain 46 courier shifts for the planning horizon. The launch peak of courier fleet dispatching is at 11:00, and the dinner peak is from 16:00 to 17:00. Courier service starts are uniformly distributed across all zones, and the temporal distribution of the service starts in a zone can be estimated from historical data. The parameters for capital investment and vessel operation are the same as described in Section 5.1. We construct the benchmark by forcing the vessel to remain stationary at the depot throughout the planning horizon to mimic the static hub in the current practice. To set up the benchmark, we use the optimal number of vessels in the Mobile-Hub strategy and forbid courier self-fulfillment.

The courier service dynamics feature a high level of complexity. Different temporal and spatial distributions of the courier service starts and ends may impose different pressures on the urgency of a zone requiring more bikes or having more bikes to return for certain periods. When the temporal and spatial distributions of the courier service starts are fixed, the service ends distribution pattern is determined by the transition matrix $n_{zt}^{z't'}$, where zz' is defined as the service range which is the radius centered on the start zone, and tt' is the service time length. In Sections 5.4 and 5.4, we study the impact of the average courier service range zz' and service time length on the Mobile-Hub infrastructure configurations and operations.

In addition to the basic system performance indicators mentioned in Section 5.3, we further define the following vessel-related system indicators: (1) "vessel en route time" indicating the time the vessel spends on relocation, (2) μ indicating the average MDR inventory level on the vessel throughout the planning horizon, and (3) δ indicating the standard deviation of the number of MDRs.

Sensitivity of courier service time length

In this analysis, we assume the courier service range is a circle with a radius of 10 zones and we vary the service length as {2, 3, 4, 5, 6} hours. Table 5.13 and Figure 5.11 - 5.13 presents the basic system performance indicators for both the Mobile-Hub strategy and the benchmark, as well as the percentage improvements in these indicators after adopting the Mobile-Hub strategy. The results show that longer service lengths lead to larger objective values, more required MDRs, and couriers spending more time on non-service riding. This trend applies to both the Mobile-Hub strategy and the benchmark. The comparison between the two practices shows that for all service length settings, there is always an improvement in the basic system indicators after applying our proposed strategy. On average, we see a decrease of 17% in the objective value, 7% in the required MDRs, and 35% in the average courier riding time, which demonstrates the benefits of the Mobile-Hub strategy.

In Table 5.14, we present the proportion of the courier services satisfied by the vessel, DDP, and self-fulfillment, as well as the vessel en route time and the mean value and standard deviation of the vessel inventory for both the Mobile-Hub strategy and the benchmark. The results show that the percentage of courier services satisfied by the vessel increases with the service time length, while the proportion satisfied by the DDPs drops. This is also reflected by the changes in vessel en route time which shows a decreasing trend in general. Less en route time means more stationary time during which the vessel can load and unload MDRs. On average, the vessel spends 8.5 hours out of the 16 hours of operation time en route; 64% of the couriers are satisfied by the vessel, 29% by the DDPs, and 7% by the self-FF. The mean MDR inventories and the standard deviation of the Mobile-Hub strategy is always lower than that of the benchmark, indicating that the Mobile-Hub strategy helps maintain a lower and more stable inventory level.

Table 5.13: Sensitivity to service length for basic system indicators - service range 10 zones

Ser. Len. (hrs)	Obj. Val. (€)			MDRs			Cour. non-service time (min)		
	Mobile-Hub	Bench.	Impr.	Mobile-Hub	Bench.	Impr.	Mobile-Hub	Bench.	Impr.
2	1280.75	1648.05	22%	23	27	15%	20.22	36.89	45%
3	1363.15	1646.29	17%	28	31	10%	23.78	36.67	35%
4	1373.44	1656.13	17%	31	31	0%	24.11	37.11	35%
5	1400.77	1653.67	15%	31	31	0%	25.33	37.00	32%
6	1433.32	1656.83	13%	31	35	11%	26.89	37.00	27%
Ave.	1370.29	1652.19	17%	28.8	31	7%	24.07	36.93	35%

Table 5.14: Sensitivity to service length for vessel related system indicators - service range 10 zones

Ser. Len. (hrs)	By Vessel	By DDP	By self-FF.	Vessel en route	Vessel Inventory μ		Vessel Inventory δ	
				time (hour)	Mobile-Hub	Bench.	Mobile-Hub	Bench.
2	51%	40%	9%	9.17	12.69	17.92	7.75	8.17
3	62%	36%	2%	8.83	15.15	19.12	9.28	9.20
4	69%	27%	4%	8.00	15.91	16.39	10.10	9.62
5	69%	27%	4%	8.50	13.95	13.49	9.79	10.04
6	71%	13%	16%	8.00	11.72	15.02	10.11	10.67
Ave.	64%	29%	7%	8.50	13.88	16.39	9.41	9.54

Sensitivity of courier service range

In this analysis, we choose the courier service time length to be 4 hours and vary the radius of the service range as {0, 2, 4, 6, 8, 10} zones, where a service range of 0 zones represents the case where couriers start and end in the same zone. In Tables 5.15 and Figure 5.14 - 5.15 we

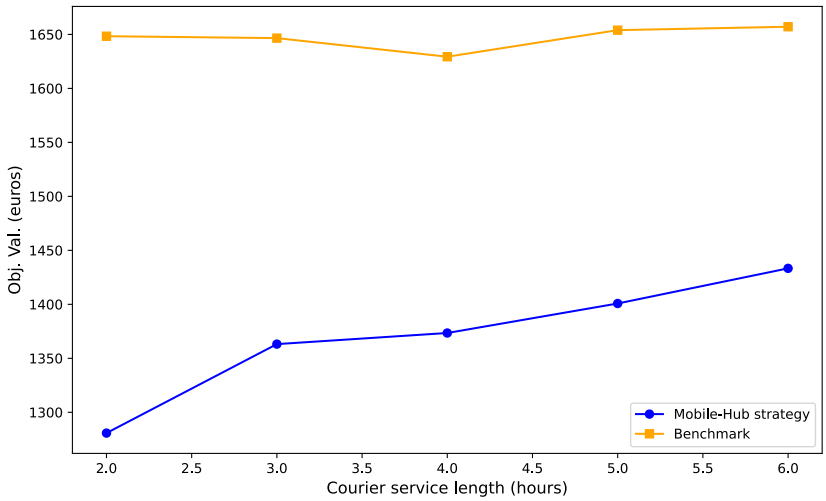

Figure 5.11: Sensitivity to courier service time length (hours) on objective values (euros)

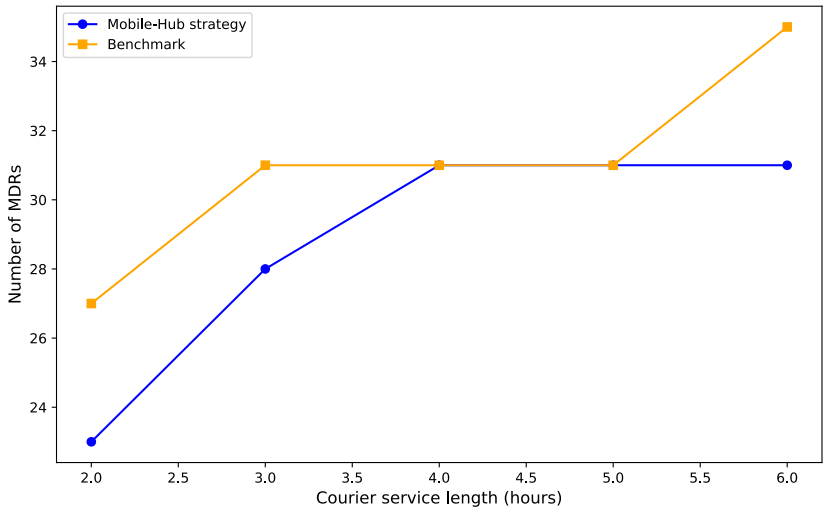

Figure 5.12: Sensitivity to courier service time length (hours) on the number of MDRs

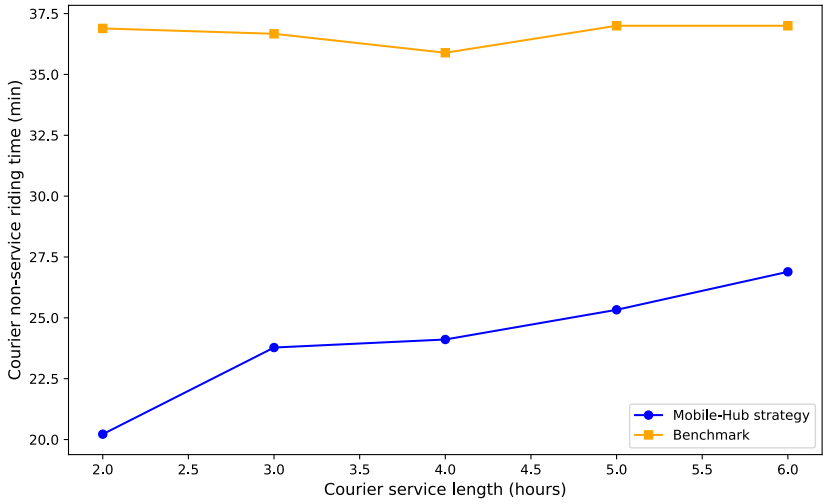

Figure 5.13: Sensitivity to courier service time length (hours) on the courier non-service riding time (min)

present the basic system performance indicators and in Table 5.14 we present vessel-related system indicators. The results show that the impact of the courier service range on the operation of the Mobile-Hub system is small. When comparing the Mobile-Hub strategy with the current practice, the number of required MDRs remains the same. On average, we observe an improvement of 15% in the objective value and 32% in the average courier non-service riding time.

Table 5.15: Sensitivity to service range for basic system indicators - service time length 4 hours

Ser. Range (zones)	Obj. Val. (€)			MDRs			Cour. non-service time (min)		
	Mobile-Hub	Bench.	Impr.	Mobile-Hub	Bench.	Impr.	Mobile-Hub	Bench.	Impr.
0	1409.80	1656.40	15%	31	31	0%	25.78	37.11	31%
2	1388.20	1646.56	16%	31	31	0%	24.78	36.67	32%
4	1389.31	1617.04	14%	31	31	0%	24.89	35.33	30%
6	1363.06	1626.88	16%	31	31	0%	23.67	35.78	34%
8	1385.47	1653.94	16%	31	31	0%	24.67	37.00	33%
10	1373.44	1656.13	17%	31	31	0%	24.11	37.11	35%
Ave.	1387.17	1640.16	15%	31	31	0%	24.76	36.38	32%

Table 5.16: Sensitivity to service range for vessel related system indicators - service time length 4 hours

Ser. Range (zones)	By Vessel	By DDP	By self-FF.	Vessel en route	Vessel Inventory μ		Vessel Inventory δ	
				time (hour)	Mobile-Hub	Bench.	Mobile-Hub	Bench.
0	69%	29%	2%	8.50	15.90	16.27	9.90	9.54
2	69%	31%	0%	7.67	15.86	16.31	9.88	9.46
4	69%	31%	0%	7.67	15.98	16.43	9.88	9.53
6	69%	29%	2%	7.67	16.12	16.40	9.74	9.37
8	69%	31%	0%	8.83	15.99	16.28	9.96	9.71
10	69%	27%	4%	8.00	15.91	16.39	10.10	9.62
Ave.	69%	30%	1%	8.06	15.96	16.35	9.91	9.54

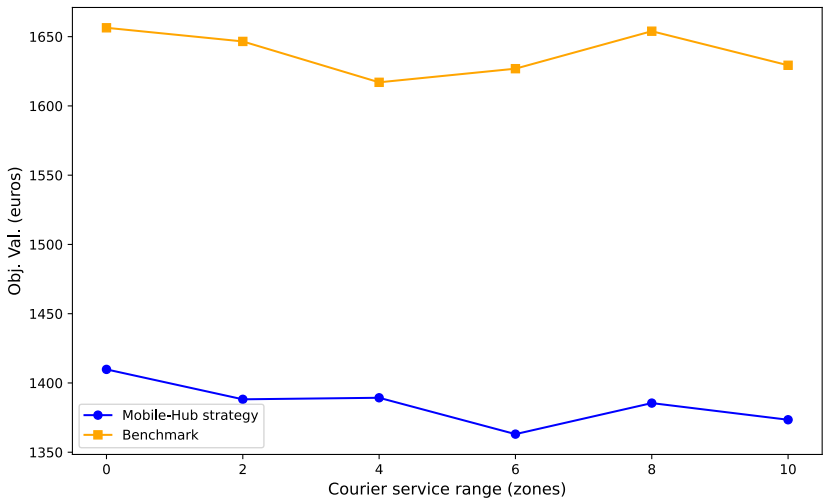

Figure 5.14: Sensitivity to courier service range (zones) on the objective value (euros)

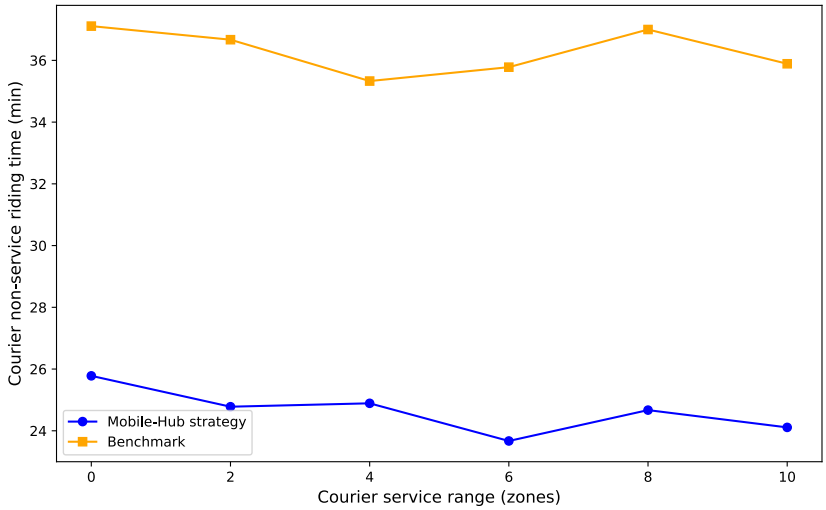

Figure 5.15: Sensitivity to courier service range (zones) on the courier non-service riding time (min)

6

Conclusion

We conclude our research in this chapter. In Section 6.1, we summarize our findings by answering the research questions developed in Chapter 1, then we discuss the limitations and future works in Section 6.2 and 6.3.

6.1. Answering research questions

We first answer the four sub-research questions and then conclude our findings by answering the main research question.

Sub-question 1:

How to consider the courier service dynamics to optimize the operation of the Mobile-Hub system while synchronizing the courier services?

Answer:

We use historical data to model courier dynamics in the highly dynamic on-demand environment. We leverage historical information about courier itineraries to identify the starting and ending locations and times of each service. We make two key observations. We assume a probability distribution for the number of services starting in each zone and period. By introducing a courier service level, we calculate the expected value (d_{zt}) of the number of couriers starting in zone z at period t. We determine the transition probability $n_{zt}^{z't'}$, indicating the likelihood of a courier starting in zone z at period t ending their service in zone z' at period t'. Using this transition probability, we calculate the expected number of services ending at a given zone z' at period t', denoted as $r_{z't'}$. By incorporating these observations into our optimization model, we effectively

consider courier service dynamics and optimize the Mobile-Hub system operation to synchronize with courier services.

Sub-question 2:
How to consider the trade-off between the infrastructure investment, and operational costs in optimizing the system?

Answer:
We model the CMFLP-MDs using integer programming in both arc-based and route-based models. Our models consider the capital investment for mobile hub leasing, DDP establishment, and MDR purchasing. We convert these costs into a daily value by specifically accounting for the usage life of resources and infrastructure. Additionally, we incorporate the opportunity cost of courier non-service riding times as operational costs. Our objective is to minimize the total Mobile-Hub system cost, which is the sum of capital investment and operational costs. The optimal solution provides the best combination of infrastructure configuration, required resources, and detailed operations for MHs and MDRs.

Sub-question 3:
What are the factors that impact the design and operation of the Mobile-Hub system?

Answer:
We conduct an extensive sensitivity analysis of various system characteristics and parameters. We identify that the following factors impact system performance: the number and geographical distribution of courier services, vessel battery life, unit self-fulfillment cost, and courier service range and length.

Sub-question 4:
How does the proposed mobile hub strategy compare to the current static hub approaches in terms of cost efficiency, resource utilization, and courier service levels?

Answer:
We compare the Mobile-Hub strategy against the current static hub approach in terms of total system cost, number of required MDRs, and average courier non-service riding time. Results from the Amsterdam canal area case study show that our proposed strategy consistently outperforms the current practice across these system performance indicators.

Lastly, we conclude our findings by answering the main research question: ***Is "waterborne vessels as mobile hubs" a viable and even better alternative for the management of shared micro-delivery***

resources (e.g. bikes, scooters) for on-demand delivery platforms? If yes, to what extent?. This study introduces a novel Mobile-Hub system using electric vessels as mobile hubs for managing shared micro-delivery resources in on-demand meal delivery platforms. Our approach addresses the limitations of the current static hub approach in urban areas with canal networks. Through the results from the mixed-integer linear programming models, we demonstrate that this strategy significantly outperforms the current static approach, achieving substantial reductions in total costs, required resources, and courier riding times. The Mobile-Hub system maintains lower and more stable inventory levels while improving courier service levels by reducing non-service riding time. These findings highlight the potential of waterborne vessels to enhance urban logistics efficiency and sustainability in canal-rich cities.

6.2. The limitations

This research considers the operation of the on-demand delivery system to be stable day-to-day and employs a deterministic model. For courier service dynamics, we use pre-processing procedures to calculate the expected values of the number of service starts and ends at each time-space node as inputs. This approach, however, does not account for unexpected situations, such as the congestion in the canal, in the delivery system. To address such uncertainties, a stochastic programming model would be necessary.

6.3. Future works

This study demonstrates the benefits of the Mobile-Hub strategy in one application, but there may be additional potential uses for waterborne vessels in urban logistics. Future research could explore extending the use of electric vessels in urban delivery processes beyond redistributing MDRs for on-demand delivery services.

References

[1] Eduardo Alarcon-Gerbier and Udo Buscher. "Minimizing movements in location problems with mobile recycling units". In: *Computational Logistics: 11th International Conference, ICCL 2020, Enschede, The Netherlands, September 28–30, 2020, Proceedings 11*. Springer. 2020, pp. 396–411.

[2] Eduardo Alarcon-Gerbier and Udo Buscher. "Modular and mobile facility location problems: A systematic review". In: *Computers & Industrial Engineering* 173 (2022), p. 108734.

[3] Jardar Andersen, Teodor Gabriel Crainic, and Marielle Christiansen. "Service network design with asset management: Formulations and comparative analyses". In: *Transportation Research Part C-emerging Technologies* 17 (2009), pp. 197–207. URL: https://api.semanticscholar.org/CorpusID:110105240.

[4] Selin Ataç, Nikola Obrenović, and Michel Bierlaire. "Vehicle sharing systems: A review and a holistic management framework". In: *EURO Journal on Transportation and Logistics* 10 (2021), p. 100033.

[5] Tristan Becker, Stefan Lier, and Brigitte Werners. "Value of modular production concepts in future chemical industry production networks". In: *European Journal of Operational Research* 276.3 (2019), pp. 957–970.

[6] Saif Benjaafar et al. "Dimensioning on-demand vehicle sharing systems". In: *Management Science* 68.2 (2022), pp. 1218–1232.

[7] Tobia Calogiuri et al. "The multi-period p-center problem with time-dependent travel times". In: *Computers & Operations Research* 136 (2021), p. 105487.

[8] Vanja Carlén, Andreas Josefsson, and Lina Olsson. "The potential role of urban waterways in sustainable urban freight transport - A case study of mass transport from the construction of Västlänken". In: 2013. URL: https://api.semanticscholar.org/CorpusID:107868222.

[9] Central Commission for the Navigation of the Rhine. *Central Commission for the Navigation of the Rhine*. https://www.ccr-zkr.org/.

[10] Erik D Demaine et al. "Minimizing movement". In: *ACM Transactions on Algorithms (TALG)* 5.3 (2009), pp. 1–30.

[11] Qiaochu Fan, J Theresia van Essen, and Gonçalo HA Correia. "Optimising fleet sizing and management of shared automated vehicle (SAV) services: A mixed-integer programming approach integrating endogenous demand, congestion effects, and accept/reject mechanism impacts". In: *Transportation Research Part C: Emerging Technologies* 157 (2023), p. 104398.

[12] Reza Zanjirani Farahani and Masoud Hekmatfar. *Facility location: concepts, models, algorithms and case studies*. 2009. URL: https://api.semanticscholar.org/CorpusID:107460537.

[13] Hüseyin Güden and Haldun Süral. "Locating mobile facilities in railway construction management". In: *Omega* 45 (2014), pp. 71–79.

[14] Zhen Guo et al. "Robust minimum fleet problem for autonomous and human-driven vehicles in on-demand ride services considering mixed operation zones". In: *Transportation Research Part C: Emerging Technologies* 132 (2021), p. 103390.

[15] Stefan Illgen and Michael Höck. "Literature review of the vehicle relocation problem in one-way car sharing networks". In: *Transportation Research Part B: Methodological* 120 (2019), pp. 193–204.

[16] Chao Lei, Wei-Hua Lin, and Lixin Miao. "A stochastic emergency vehicle redeployment model for an effective response to traffic incidents". In: *IEEE Transactions on Intelligent Transportation Systems* 16.2 (2014), pp. 898–909.

[17] Cristiano Martins Monteiro et al. "Optimization of carsharing fleet size to maximize the number of clients served". In: *Computers, Environment and Urban Systems* 87 (2021), p. 101623.

[18] Jishnu Narayan et al. "Fleet size determination for a mixed private and pooled on-demand system with elastic demand". In: *Transportmetrica A: Transport Science* 17.4 (2021), pp. 897–920.

[19] Santhanakrishnan Narayanan, Emmanouil Chaniotakis, and Constantinos Antoniou. "Shared autonomous vehicle services: A comprehensive review". In: *Transportation Research Part C: Emerging Technologies* 111 (2020), pp. 255–293.

[20] Amirreza Pashapour et al. "Capacitated Mobile Facility Location Problem with Mobile Demand: Efficient relief aid provision to en route refugees". In: *Omega* (2024), p. 103138.

[21] S Raghavan, Mustafa Sahin, and F Sibel Salman. "The capacitated mobile facility location problem". In: *European Journal of Operational Research* 277.2 (2019), pp. 507–520.

[22] Kenneth Løvold Rødseth, Kjetil Fagerholt, and Stef Proost. "Optimal Planning of an Urban Ferry Service Operated with Zero Emission Technology". In: *SSRN Electronic Journal* (2023). URL: https://api.semanticscholar.org/CorpusID:256569345.

[23] F Sibel Salman et al. "Modeling mobile health service delivery to Syrian migrant farm workers using call record data". In: *Socio-Economic Planning Sciences* 77 (2021), p. 101005.

[24] Karmel S Shehadeh. "Distributionally robust optimization approaches for a stochastic mobile facility fleet sizing, routing, and scheduling problem". In: *Transportation Science* 57.1 (2023), pp. 197–229.

[25] Carin Stillström and Mats Jackson. "The concept of mobile manufacturing". In: *Journal of Manufacturing Systems* 26.3-4 (2007), pp. 188–193.

[26] Jacek Trojanowski and Stanisław Iwan. "Analysis of Szczecin Waterways in Terms of their Use to Handle Freight Transport in Urban Areas". In: *Procedia - Social and Behavioral Sciences* 151 (2014), pp. 333–341. URL: https://api.semanticscholar.org/CorpusID:110337465.

[27] E. Tucker et al. "Employee or Independent Contractor?: Charting the Legal Significance of the Distinction in Canada". In: July 2011. URL: https://www.semanticscholar.org/paper/Employee-or-Independent-Contractor%3A-Charting-the-of-Tucker-Fudge/479a755fb21a2ef088e958efd8d541b0db748ef2 (visited on 01/09/2024).

[28] Jie Yang et al. "Fleet sizing and charging infrastructure design for electric autonomous mobility-on-demand systems with endogenous congestion and limited link space". In: *Transportation Research Part C: Emerging Technologies* 152 (2023), p. 104172.

[29] Meng Yuan et al. "A mixed integer linear programming model for optimal planning of bicycle sharing systems: A case study in Beijing". en. In: *Sustainable Cities and Society* 47 (May 2019), p. 101515. ISSN: 22106707. DOI: 10.1016/j.scs.2019.101515. URL: https://linkinghub.elsevier.com/retrieve/pii/S2210670718323825 (visited on 01/06/2024).

[30] Eda Yücel et al. "A data-driven optimization framework for routing mobile medical facilities". In: *Annals of Operations Research* 291 (2020), pp. 1077–1102.

A

Scientific paper

Strategic planning and optimization of mobile hubs for micro-delivery services

Abstract

This study addresses the challenge of managing shared micro-delivery resources (MDRs) for on-demand meal delivery platforms in urban areas with canal networks. We propose an innovative Mobile-Hub concept utilizing electric vessels as mobile hubs (MHs) for MDRs, complemented by discretionary docking points (DDPs) along city canals. We formulate this as the Capacitated Mobile Facility Location Problem with Multiple Demands (CMFLP-MDs) and develop mixed-integer linear programming models to minimize total system cost while satisfying courier demands. Our key findings demonstrate that the Mobile-Hub strategy significantly outperforms the current static central hub approach. The proposed system helps maintain lower and more stable MH inventory levels while providing superior service.

Keywords: Meal delivery problem; Mobile hub, Capacitated facility location, Urban waterway logistics

1. Introduction

As one of the most important technology innovations in the logistics sector, on-demand delivery services are rapidly reshaping urban lifestyles. These platforms provide instant delivery services by digitally and seamlessly connecting senders, couriers, and recipients (Tucker et al., 2011). In the Netherlands, a considerable proportion of couriers are directly employed by the platforms. They are paid hourly wages and use the shared micro-delivery resources (MDRs), such as scooters and bikes, provided by the platforms to conduct deliveries. Efficient management of these MDRs is crucial for the platforms to ensure timely MDR availability for couriers to start their services. Platforms often manage MDRs using a centrally located static hub within the service area.

The employed couriers operate under a shift-based business model. They begin their shifts by collecting an MDR from the hub, then travel to pick up the meal at the restaurant of the first assigned order. The time between the MDR collection and the first pickup is called the pre-service time. The courier service starts there. The service time spans from the first pickup to the last delivery. After delivering at the last household, the couriers ride back to the hub to return the MDR, with this time being called the post-service time. Thus, a typical courier shift comprises pre-service, service, and post-service periods, with the pre- and post-service periods named as non-service time.

While straightforward, the current static hub strategy has many limitations. The courier non-service riding times are paid by the platforms, so the platforms naturally seek to shorten

*Corresponding author

this time to increase courier productivity. Some platforms operate multiple hubs to distribute the MDR availability more sparsely in the service area to reduce the non-service times. This approach operates similarly to public bike-sharing systems, which require more capital investment for the hubs and additional effort to rebalance the inventories compared to the single-hub approach. Additionally, rebalancing trucks may exacerbate traffic congestion in cities with narrow streets like Amsterdam and generate heavy emissions, thus reducing the quality of life for residents.

On the other hand, electric vessels are emerging as an efficient and sustainable solution for logistics in cities with canals, helping to alleviate traffic in densely populated areas (Rødseth et al., 2023; Trojanowski and Iwan, 2014). This technology is already widely applied to various services, from parcel delivery to waste transportation (Carlén et al., 2013). The Central Commission for the Navigation of the Rhine has documented several successful or ongoing innovative projects using electric vessels in inland waterway transportation across European cities, demonstrating the technology's potential to meet diverse urban transportation needs.

In this research, we for the first time explore the use of electric vessels as a means of MDR parking and relocation for on-demand delivery services, expanding the usage portfolio of this new technology. We propose an integrated Mobile-Hub system, which features deploying electric vessels as mobile hubs (MHs) for MDRs. In our design, the operation of the MHs is complemented by discretionary docking points (DDPs) strategically positioned along the city canals. The MHs follow fixed daily routes and schedules to store, transport, and deliver MDRs to synchronize with courier services. The proposed Mobile-Hub strategy offers three key advantages: reduced land use for MDR storage, environmentally friendly operation, and minimal contribution to road traffic congestion.

The Mobile-Hub system helps satisfy two types of demand from couriers: MDR pickups and returns. We develop a model named Capacitated Mobile Facility Location Problem with Multiple Demands (CMFLP-MDs). For the Mobile-Hub system to be effective, it requires an efficient operation scheme to synchronize the courier services. The objective of the CMFLP-MDs model is to minimize the total system cost, including the capital investment for MHs, DDPs, and MDRs, as well as the opportunity cost of courier non-service times. This is achieved by simultaneously considering the following decisions: the size of the MH fleet, the number and location of DDPs, the number of required MDRs, and the operation of the MDRs.

The contributions of this research are summarized as follows: (1) an investigation into the feasibility of the Mobile-Hub strategy for managing shared courier MDRs; (2) consideration of hybrid operations involving MHs, DDPs, and courier demand self-fulfillment; and (3) the development of Mixed-Integer Programming (MIP) models, in both arc-based and route-based formulations, to study this problem.

The remainder of this paper is structured as follows: Section 2 discusses relevant literature; Section 3 formalizes the problem; Section 4 presents the mathematical formulations; Section 5 reports experimental results; and Section 6 concludes with our findings.

2. Literature Review

In this section, we discuss the literature relevant to our research. We situate our study within two streams of the literature, namely the Mobile Facility Location Problem (MFLP)

and fleet sizing for shared vehicle systems.

2.1. Mobile Facility Location Problem

The facility location problem (FLP) addresses the strategic and tactical decisions of placing facilities among several candidates to serve customers or clients through an established transportation network (Farahani and Hekmatfar, 2009). Facilities can include a variety of strategically located entities, such as transportation hubs, factories, warehouses, and fuel stations. The locations of these facilities are crucial because capital costs for infrastructure investments are often substantial, and facility locations can significantly impact the tactical and operational decisions of an organization (Yuan et al., 2019).

In recent years, advances in modularization and miniaturization have led to an increase in the use of modularized mobile facilities. Stillström and Jackson (2007) define the concept of mobility as the ability to move between geographical locations with little effort. Problems studying relocatable units are referred to as mobile facility location problems (MFLPs), introduced by Demaine et al. (2009). This problem considers the relocation of facilities and customer allocation with the aim of, for example, minimizing total transport time for both movable units and the assigned customers. Raghavan et al. (2019) further extend this problem by considering facility capacities for a more practical approach. For facilities serving as parking or storage places, like the MHs in our study, locating them close to where the goods or services are demanded helps reduce transportation distance and delivery time. This improves customer service levels and helps organizations maintain low and stable inventory levels (Becker et al., 2019).

MFLPs have been extensively studied in various applications, including healthcare, emergency services, humanitarian relief, manufacturing, and so on. Readers are referred to Alarcon-Gerbier and Buscher (2022) for a systematic review of the various topics on MFLPs. Pashapour et al. (2024) examine the relocation and scheduling of mobile humanitarian facilities to deliver aid service bundles to migrating refugees, with an objective to minimize total mobile facility costs. Shehadeh (2023) consider the stochastic MFLP and model the optimal sizing, routing, and scheduling of a fleet of mobile facilities over a planning horizon. They propose two distributionally robust optimization models to study the problem and assume random demand levels in each period with unknown probability distributions. What sets our research apart from theirs is that we consider the fleet sizing of both the MHs and shared courier vehicles in the on-demand delivery setting. Calogiuri et al. (2021) consider the problem of relocating emergency vehicles to minimize the largest service time between customers assigned to vehicles during a multi-period planning horizon. Salman et al. (2021) address the routing of mobile clinics to deliver healthcare to refugees, modeling the problem with hierarchical objectives to minimize the number of clinics and their travel distance while maximizing refugee coverage. Yücel et al. (2020) investigate the problem of stop selection and routing for mobile medical vehicles, considering partial coverage of scored customer locations to maximize the total score collected. Alarcon-Gerbier and Buscher (2020) examine the relocation of capacitated recycling units for waste collection to minimize total transport time. Lei et al. (2014) study the stochastic scheduling of emergency vehicle relocation in response to traffic accidents, considering uncertainties in both service demand and vehicle unavailability times. Güden and Süral (2014) study an MFLP in railway construction

management, synchronizing the decisions on the number, type, and schedule of capacitated mobile facilities, as well as production allocation.

2.2. Fleet Sizing for Shared Vehicle Systems

Although there is extensive literature on shared vehicle systems and fleet sizing (Illgen and Höck (2019), Narayanan et al. (2020), Ataç et al. (2021)), they only consider the static vehicle stations. Limited research considers the fleet sizing of the shared vehicles under the mobile hub situation, as in our study. However, some research is still relevant to our research. Fan et al. (2023) study the fleet sizing and management of shared autonomous vehicle service, considering optimal fleet sizing and service level decisions from a strategic perspective, as well as vehicle parking and relocation from an operational perspective. Yang et al. (2023) study an electric autonomous on-demand service and use Bayesian optimization to optimize the fleet size and charging facility locations, considering the congestion caused by the fleet. Benjaafar et al. (2022) study the dimensioning of a shared vehicle system using a closed queueing network, considering the randomness of both rental duration and vehicle availability at each location. Guo et al. (2021) model the minimum size of a hybrid fleet of autonomous and human-driven vehicles for an on-demand ride service system, considering uncertain demands. Monteiro et al. (2021) optimize the fleet size of a car-sharing system with the objective of serving as many clients as possible. They consider two service types: round-trip (pickup and dropoff locations are the same) and one-way (different locations), similar to our research, where we consider the different service ranges of couriers. Their results show that round-trip service is better for scaling up. Narayan et al. (2021) study the dimensioning of a hybrid fleet of private and pooled services, modeling the problem from the perspectives of two different stakeholders (authority and service provider). Their results show that the authority requires a larger fleet size.

Existing research offers extensive literature on the applications of MFLPs and fleet sizing for shared vehicle systems. However, to the best knowledge of the authors, no studies have explored the use of electric vessels as mobile hubs for shared courier vehicles in the on-demand delivery sector, nor the simultaneous decision-making of MHs and shared courier vehicle fleet sizes. Investigating the feasibility of the concept of Mobile-Hub for highly time-sensitive on-demand delivery services, and understanding their interaction with courier services remains a gap in the literature. This research aims to address this gap by systematically examining this strategy from an operations research perspective.

3. Problem statement

We consider an operator for an on-demand delivery platform operating in an urban area connected by canals, such as those in Amsterdam, Venice, or Bangkok. The platform utilizes two types of resources: MDRs, including bikes, scooters, and similar modes of transport that start their operations from specific zones within the system, and electric vessels that act as MHs of these MDRs.

We discretize the service area into a set of equal-sized, regular hexagon-shaped zones, classifying them into two groups: zones with a DDP where the MHs can dock temporarily

and zones without one. The itinerary of an MH includes only the zones where it can dock, and we assume these zones are connected by canals, defining the operating area of the MHs.

We assume that the on-demand delivery service operates within a company-owned business model, with MDRs owned by the company. The delivery service of a typical day operates in several courier shifts, varying in starting time, starting zone, ending time, and ending zone. Each shift begins when a courier picks up an MDR from a DDP. After picking up his/her MDR, the courier rides to collect the meal from the first restaurant, and this riding time is defined as the pre-service time. The duration between the first meal collection and the last meal delivery is defined as the service time. After delivering the last order at the last household, the courier rides to a DDP to return the bike; this duration is defined as the post-service time.

MHs initiate their routes from a central depot with charging facilities. During their operation, the MHs selectively visit a series of DDPs to load and unload MDRs. Each DDP has a small staging area with limited capacity to facilitate the synchronization of MH movements and courier activities. MHs periodically return to the central depot for recharging. The routes and schedules of the vessels must be synchronized with the shifts and operations of the couriers.

The objective is to minimize the total system cost, including capital investment and MDR operations while satisfying all courier demands for MDR pickups and returns. The objective is realized by synchronizing the following decisions: (1) the number of MHs, DDPs, and MDRs; (2) the operations of the MDRs.

3.1. Courier Dynamics

Given the highly dynamic nature of the on-demand environment, we use historical data to model courier dynamics. In this problem, we assume that the Mobile-Hub system is established in an existing operating area where the operator has historical information about the couriers. This historical data includes the couriers' itineraries, allowing us to identify courier dynamics through their service times. Specifically, we consider the starting location and time of the service, as well as the ending location and time.

Observation 1. We assume that in each zone z and each discredited period t, there is a probability distribution for the number of services starting there and when. By introducing a courier service level α, we can calculate the expected value d_{zt}, representing the number of couriers starting in zone z and period t, such that α of cases are covered. Let X_{zt} be the random variable representing the number of couriers starting in zone z and period t:

$$P(d_{zt} \geq X_{zt}) \geq \alpha$$

Furthermore, we determine the transition probability $n_{zt}^{z't'}$, which indicates the likelihood that a courier starting in zone z at period t will end their service in zone z' at period t'. Using this transition probability, we can calculate the expected number of services ending at a given zone z' at period t'. The calculated $r_{z't'}$ is a fractional number, which we round down to get the integer value. This is represented as:

$$r_{z't'} = \sum_{z} \sum_{t} n_{zt}^{z't'} d_{zt}$$

4. Mathematical formulation

In this section, we describe the proposed mathematical model based on the problem description in Section 3. In Section 4.1, we introduce the graphs and sets. In Section 4.2 and 4.3 we explain how the courier demand for MDR pickups and returns is satisfied with an example. In Section 4.4 and Section 4.5 we describe the model in its arc-based and route-based formulations.

4.1. Network representation

We define the CMFLP-MBs on a directed physical graph $\mathcal{G} = (\mathcal{Z}, \mathcal{E})$, which is composed of two subgraphs: $\mathcal{G}^C = (\mathcal{Z}^C, \mathcal{E}^C)$ associated with the couriers, and $\mathcal{G}^M = (\mathcal{Z}^M, \mathcal{E}^M)$ associated with the MHs. $\mathcal{Z} = \{1, 2, 3, \ldots, |\mathcal{Z}|\}$ is the set of zones representing the service area, each represented by its center. The set $\mathcal{Z}^C$ comprises the zones where courier services can start and end, while $\mathcal{Z}^M$ denotes the zones with candidate DDPs where the MHs can be located. Specifically, an MH located in zone $z \in \mathcal{Z}^M$ can relocate to its adjacent zones that are connected by canals, denoted by $Z^M(z)$.

Each edge in the set $\mathcal{E}^C = \{(z, z'')|z, z'' \in \mathcal{Z}\}$ represents the bike lanes between zone z and zone z''. We assume the courier travel distance is zero within the same zone. In the set $\mathcal{E}^M$ we define two types of arcs: $\mathcal{E}^D = \{\mathcal{E}^{D1}, \mathcal{E}^{D2}\}$. The arcs in $\mathcal{E}^{D1} = \{(z, z')|z \in \mathcal{Z}^M, z' \in Z^M(z)\}$ represent the relocation of MHs from z to z', while the arcs in $\mathcal{E}^{D2} = \{(z, z)|z \in \mathcal{Z}^M\}$ represent the MHs docking at the DDP in zone z to load and unload MDRs.

The zone-period pairs are the most fundamental concept in CMFLP-MBs. We discretize the planning horizon into a set of periods $\mathcal{T} = \{1, 2, ..., |\mathcal{T}|\}$. We assume equal speed for MHs and couriers, and the time for traveling one unit distance is one period. Corresponding to the physical graph $\mathcal{G}$, we define the time-space graph $\mathcal{G}' = (\mathcal{N}, \mathcal{A})$, where $\mathcal{N} = \{(z, t)|z \in \mathcal{Z}, t \in \mathcal{T}\}$ is the set of zone-period pairs, and $\mathcal{A}$ is the set of arcs. The graph $\mathcal{G}'$ is composed of two subgraphs: $\mathcal{G}'^C = (\mathcal{N}^C, \mathcal{A}^C)$ associated with couriers, and $\mathcal{G}'^M = (\mathcal{N}^M, \mathcal{A}^M)$ for the MHs.

In $\mathcal{A}^C$ we use $(z, t)(z'', t'')$ to represent the courier movement from z to z'' starting from t and arriving in t''. In the set $\mathcal{N}^C = \mathcal{Z}^C \times \mathcal{T}$, for each node (z, t), we define its successor nodes $N^{C+}_{z,t} = \{(z'', t'')|z'' \in \mathcal{Z}, t'' = t + DIS_{zz''}\}$ and predecessor nodes $N^{C-}_{z,t} = \{(z'', t'')|z'' \in \mathcal{Z}, t'' = t - DIS_{z,z''}\}$, where $DIS_{z,z''}$ is the distance in units between z and z''. Similarly, each arc $(z, t)(z', t') \in \mathcal{A}^M$ represents the MH movement from z to z' starting in t and arriving in t'. For each node (z, t) in $\mathcal{N}^M = \mathcal{Z}^M \times \mathcal{T}$, we define $N^{M+}_{z,t} = \{(z', t')|z' \in Z^+_z, t' = t + DIS_{zz'}\}$ as the successor nodes, and $N^{M-}_{z,t} = \{(z', t')|z' \in Z^+_z, t' = t - DIS_{zz'}\}$ as predecessor nodes. Figure 1 gives an example of the set of arcs associated with MDRs (a) and MHs (b) for the same time-space node.

4.2. Courier demand satisfaction

We consider three methods to fulfill courier pickup and return demands: by MHs, by established DDPs, and by courier self-fulfillment. These correspond to five MDR operation modes: $\mathcal{O} = \{$**DM**: dropped off from MHs; **RM**: returned to MHs; **DD**: dropped off from DDPs; **RD**: returned to DDPs; **SF**: self-fulfillment$\}$.

(1) "Satisfied by MHs" refers to the process where couriers pick up and return MDRs from and to docked mobile hubs. We use a set of homogeneous electric vessels $v \in \mathcal{V}$ serving as mobile hubs with a fixed capacity of Q^{MH}. An MH tour is defined as the sequence of

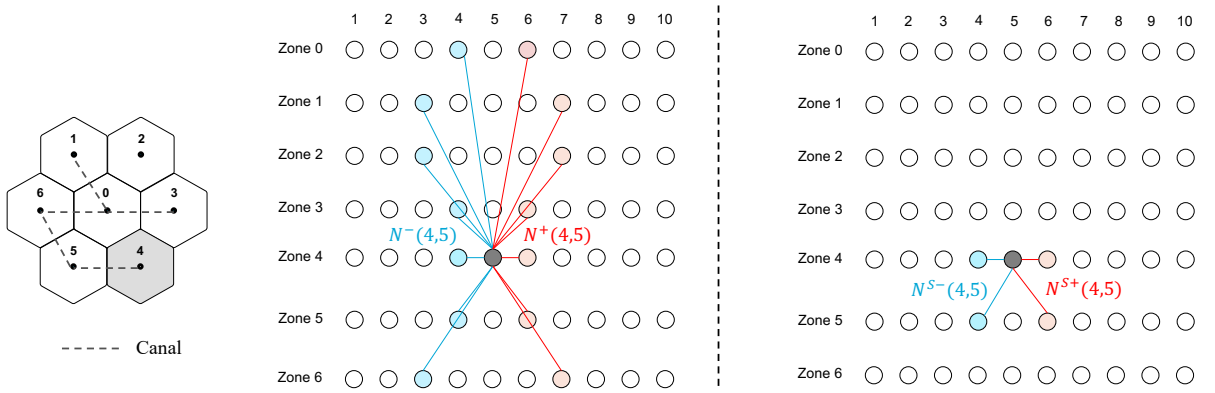

(a) Possible predecessor and successor of time-space node (4,5) for bike movements

(a) Possible predecessor and successor of time-space node (4,5) for vessel movements

Figure 1: An example of arcs associated with MDRs (a) and arcs associated with MHs (b) for time-space node (4,5)

DDP visits, including the duration of the stay at each DDP. An MH can either stay at a DDP to load and unload MDRs or bypass it without stopping. An MH tour is composed of equal-length intervals, with each interval comprising several periods. The MHs start and end the tours at a central depot z_o and must return to the depot at the end of each interval to recharge. We further consider an initial lag for which time the start of the first courier service is later than the start of the planning horizon, to ensure that the pickup demand in the outermost zones can be satisfied.

MHs operate in two modes: **DM**, indicating MDRs are dropped off from MHs, and **RM**, indicating MDRs are returned to MHs. After docking, MHs will wait for at least one period to load and unload MDRs. Couriers needing an MDR will be at a DDP before their shift starts. When the MH arrives, they board to pick up the MDR and ride to the restaurant of the first order to start the service. The monetary value of this pre-service riding is included in the operation cost. For MDR returns, after delivering their last order, couriers ride to a DDP designated by the platform, ensuring they arrive at the DDP in the same period as the MH. Their shift ends once the MDR is returned. The value of the post-service time for MDR returns is also considered, along with fixed costs associated with vessel leasing, driver salaries, and energy.

(2) "Satisfied by DDPs" is the process where couriers use established DDPs as mini static stations for MDRs, regardless of the presence of a docking vessel. The candidate locations for the homogeneous DDPs of capacity Q^{DDP} are assumed known, and the establishment of a DDP depends on whether it will be visited and docked by MHs. Operation modes **DD** and **RD** are associated with this method, namely MDRs dropped off at DDPs and returned to DDPs. The platform can assign couriers to a specific DDP for their pickup and return demands. Costs associated with this service include the capital investment for establishing DDPs and the value of couriers' riding time for pre- and post-service.

(3) We consider that in each zone there is a small free-floating location where couriers can meet to hand over MDRs at no charge. Operation mode "Self-fulfillment (SF)" refers

to the process where the platform directs courier A, who finishes the last order, to ride to the free-floating location in a zone where another courier B is asked by the platform to wait there to take over A's MDR so that B can directly start service in that zone and the MDR of A is returned. We consider the free-floating location as a hand-over location with no capacity. The riding time of couriers of type A is included in the operational cost.

4.3. Illustrative example

In this section, we illustrate how MDR pickups and returns associated with courier service starts and ends are satisfied by five operation modes. Consider a case where a vessel operates in a service area with 7 zones over a planning horizon of 10 periods, composed of 2 intervals. The canal passes through zones 0, 6, and 5 sequentially, with one candidate DDP in each zone. Figure 2 depicts a potential routing and scheduling of the vessel. In the first interval, the vessel follows the canal, visiting zones 0, 6, and 5 in sequence before returning to the depot, resulting in the establishment of the three DDPs. In the second interval, the vessel remains stationary.

Couriers starting service in zone 4 at period 4 can obtain an MDR through three means: Direct from Mobile-Hub (DM): Couriers wait in zone 5 at period 3 for the vessel's arrival and collect an MDR when it docks. They then spend one period traveling to zone 4 to start service. From Discretionary Docking Points (DD): Couriers reach zone 0 from their home at period 3, collect an MDR, then spend one period traveling to zone 4. Self-Fulfillment (SF): Couriers wait in zone 4 before period 4. The platform directs couriers ending their shift in other zones (e.g., zone 2 at period 2) to travel to zone 4 and hand over their MDRs to the waiting couriers.

Couriers ending service in zone 3 at period 7 can return their MDRs through three means: Return to Mobile-Hub (RM): Couriers spend one period traveling to zone 0 to return their MDRs to the docked vessel. Return to Discretionary Docking Points (RD): Couriers travel to zone 5 to return the MDRs to the DDP there. Self-Fulfillment (SF): The platform directs couriers to zones where other couriers are waiting for MDRs (in this case, zone 8).

4.4. Arc-based formulation

MH tour constraints. For each MH $v \in \mathcal{V}$, we define the binary variable $\delta^v = 1$ if MH v is deployed. Binary variable $x^v_{(z,t)(z',t')} = 1$ if MH v travels from zone z to zone z' starting in period t arriving in period t'. Constraints (1) check the usage of MH v. Constraints (2) state that a used MH will return to the depot z_o at the closure of the planning horizon. Constraints (3) ensure the MH flow conservation at time-space nodes. Constraints (4) make sure that no more than two MHs dock at the same DDP in the same period except for at the depot. The planning horizon is divided into a set of intervals $L = \{1, 2, \ldots, l, \ldots, |L|\}$, that is $\mathcal{T} = \{T_1, T_2, \ldots, T_l, \ldots, T_{|L|}\}$, where $|L| = \frac{|\mathcal{T}|}{|T_1|}$. We define $\tilde{T} = \{|T_1|, 2|T_1|, \ldots, l|T_1|, \ldots, (|L|-1)|T_1|\}$ as the set of periods at the end of the intervals. Constraints (5) ensure the MHs return to depot at the end of each interval to recharge for at least one period.

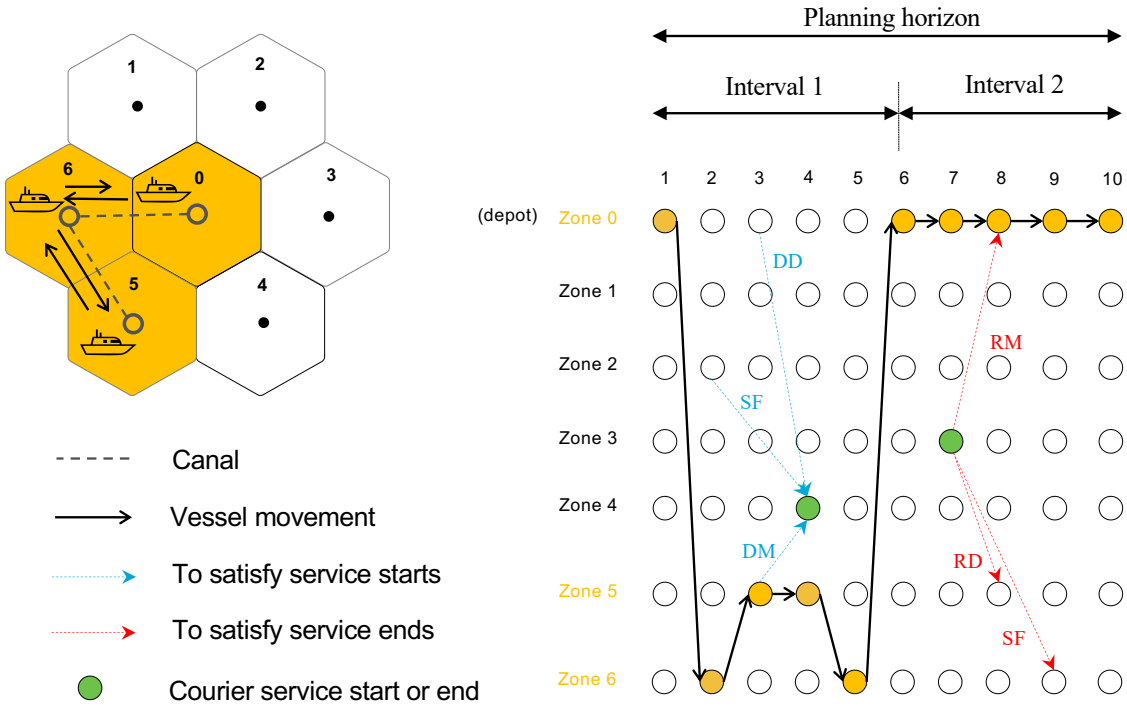

Figure 2: An example of courier service starts and ends satisfaction

$$\delta^v = \sum_{(z',t') \in N^{M+}_{z_o,1}} x^v_{(z_o,1)(z',t')}, \quad \forall v \in \mathcal{V} \tag{1}$$

$$\sum_{(z',t') \in N^{M+}_{z_o,1}} x^v_{(z_o,1)(z',t')} = \sum_{(z',t') \in N^{M-}_{z_o,|\mathcal{T}|}} x^v_{(z',t')(z_o,|\mathcal{T}|)}, \quad \forall v \in \mathcal{V} \tag{2}$$

$$\sum_{(z',t') \in N^{M+}_{z,t}} x^v_{(z,t)(z',t')} = \sum_{(z',t') \in N^{M-}_{z,t}} x^v_{(z',t')(z,t)}, \quad \forall v \in \mathcal{V}, \quad \forall z \in \mathcal{Z}^M \setminus \{z_o\}, \quad \forall t \in \mathcal{T} \tag{3}$$

$$\sum_{v \in \mathcal{V}} x^v_{(z,t)(z,t+1)} \leq 1, \quad \forall z \in \mathcal{Z}^M \setminus \{z_o\}, \quad \forall t \in \mathcal{T} \setminus |\mathcal{T}| \tag{4}$$

$$x^v_{(z_o,t)(z_o,t+1)} = 1, \quad \forall v \in \mathcal{V}, \quad \forall t \in \tilde{T} \tag{5}$$

$$\delta^v \in \{0,1\}, \quad \forall v \in \mathcal{V} \tag{6}$$

$$x^v_{(z,t)(z',t')} \in \{0,1\}, \quad \forall v \in \mathcal{V}, \quad \forall (z,t),(z',t') \in \mathcal{A}^M \tag{7}$$

We define the binary variable $\zeta_z = 1$ if the candidate DDP in zone z is visited. Constraints (8) ensure the visited candidate DDPs are established. M_1 is a constant value set as $|\mathcal{V}|(|\mathcal{T}| - 1)$.

$$\zeta_z \leq \sum_{v \in \mathcal{V}} \sum_{t \in T \setminus |\mathcal{T}|} x^v_{(z,t)(z,t+1)} \leq M_1 \zeta_z, \quad \forall z \in \mathcal{Z}^M \tag{8}$$

$$\zeta_z \in \{0,1\}, \quad \forall z \in \mathcal{Z}^M \tag{9}$$

MDRs pickups and returns activation. For the MDR pickups, Recall that we have five operation MDR modes: $\mathcal{O} = \{$**DM**: dropped off from MHs; **RM**: returned to MHs; **DD**: dropped off from DDPs; **RD**: returned to DDPs; **SF**: self-fulfillment$\}$. We define a non-negative integer variable for each mode: $y^{DM,v}_{(z,t)(z'',t'')}$ for the MDRs dropped off by MH v located in z in period t to fulfill the courier service starting in zone z'' in period t'; $y^{RM,v}_{(z'',t''),(z,t)}$ for the MDRs returned from z'' in t'' to MH v in z in t; $y^{DD}_{(z,t)(z'',t'')}$ for the MDRs dropped off at the DDP in z in t for the service start in z'' in t''; $y^{RD}_{(z'',t'')(z,t)}$ for the MDRs returned from z'' in t'' to the DDP in z in t; and $y^{SF}_{(z,t)(z'',t'')}$ for the self-fulfillment originating in z in t and ending in z'' in t''. d_{zt} indicates the quantity of the service start in zone z in period t, and r_{zt} is the service ending in zone z in period t. Only docked MH and established DDP can serve courier pickups and returns, constraints (10) and (11) activate the drop-off and pick-up flows associated with MH v at (z,t). Constraints (12) and (13) activate the drop-off and pick-up flows associated with the DDP in z in t.

$$y^{DM,v}_{(z,t)(z'',t'')} \leq d_{zt} x^{v}_{(z,t)(z,t+1)}, \quad \forall v \in \mathcal{V}, \quad \forall z \in \mathcal{Z}^M, \quad \forall t \in \mathcal{T} \setminus |\mathcal{T}|, \quad \forall (z'',t'') \in N^{C+}_{z,t} \tag{10}$$

$$y^{RM,v}_{(z'',t''),(z,t)} \leq r_{zt} x^{v}_{(z,t),(z,t+1)}, \quad \forall v \in \mathcal{V}, \quad \forall z \in \mathcal{Z}^M, \quad \forall t \in \mathcal{T} \setminus |\mathcal{T}|, \quad \forall (z'',t'') \in N^{C-}_{z,t} \tag{11}$$

$$y^{DD}_{(z,t)(z'',t'')} \leq d_{zt} \zeta_z, \quad \forall z \in \mathcal{Z}^M, \quad \forall t \in \mathcal{T}, \quad \forall (z'',t'') \in N^{C+}_{z,t} \tag{12}$$

$$y^{RD}_{(z'',t''),(z,t)} \leq r_{zt} \zeta_z, \quad \forall z \in \mathcal{Z}^M, \quad \forall t \in \mathcal{T}, \quad \forall (z'',t'') \in N^{C-}_{z,t} \tag{13}$$

$$y^{DM,v}_{(z,t)(z'',t'')} \in \mathbb{Z}_{\geq 0}, \quad \forall v \in \mathcal{V}, \quad \forall z \in \mathcal{Z}^M, \quad \forall t \in \mathcal{T} \setminus |\mathcal{T}|, \quad \forall (z'',t'') \in N^{C+}_{z,t} \tag{14}$$

$$y^{RM,v}_{(z'',t''),(z,t)} \in \mathbb{Z}_{\geq 0}, \quad \forall v \in \mathcal{V}, \quad \forall z \in \mathcal{Z}^M, \quad \forall t \in \mathcal{T} \setminus |\mathcal{T}|, \quad \forall (z'',t'') \in N^{C-}_{z,t} \tag{15}$$

$$y^{DD}_{(z,t)(z'',t'')} \in \mathbb{Z}_{\geq 0}, \quad \forall z \in \mathcal{Z}^M, \quad \forall t \in \mathcal{T}, \quad \forall (z'',t'') \in N^{C+}_{z,t} \tag{16}$$

$$y^{RD}_{(z'',t''),(z,t)} \in \mathbb{Z}_{\geq 0}, \quad \forall z \in \mathcal{Z}^M, \quad \forall t \in \mathcal{T}, \quad \forall (z'',t'') \in N^{C-}_{z,t} \tag{17}$$

Demands satisfaction. Constraints (18) state that the all courier service starting in zone z in period t can pick up an MDR from either the MHs, DDPs or by SF. Constraints (19) ensure that courier ending service in zone z in period t have their MDRs return to either MHs, DDPs, or by SF.

$$\sum_{v \in \mathcal{V}} \sum_{(z'',t'') \in N^{C-}_{z,t} \cap \mathcal{N}^M} y^{DM,v}_{(z,t)(z'',t'')} + \sum_{(z'',t'') \in N^{C-}_{z,t} \cap \mathcal{N}^M} y^{DD}_{(z,t)(z'',t'')} + \sum_{(z'',t'') \in N^{C-}_{z,t}} y^{SF}_{(z'',t'')(z,t)} = d_{zt}, \quad \forall (z,t) \in \mathcal{N}^C \tag{18}$$

$$\sum_{v \in \mathcal{V}} \sum_{(z'',t'') \in N^{C+}_{z,t} \cap \mathcal{N}^M} y^{RM,v}_{(z'',t'')(z,t)} + \sum_{(z'',t'') \in N^{C+}_{z,t} \cap \mathcal{N}^M} y^{RD,v}_{(z'',t'')(z,t)} + \sum_{(z'',t'') \in N^{C+}_{z,t}} y^{SF}_{(z,t)(z'',t'')} = r_{zt}, \quad \forall (z,t) \in \mathcal{N}^C \tag{19}$$

$$y^{SF}_{(z,t)(z'',t'')} \in \mathbb{Z}_{\geq 0}, \quad \forall (z,t)(z'',t'') \in \mathcal{A}^C \tag{20}$$

Inventory management. We track the inventory of both the MHs and DDPs to ensure the capacity limitation is not violated. We first discuss the MH inventory, let non-negative integer I^v_{zt} be the number of MDRs stored in MH v located in zone z period t. If an arc $(z,t)(z',t')$ is on the route of MH v, the inventory at the node (z',t') equals the inventory at (z,t) adding the collected MDRs and minus the dropped ones. This is expressed by Constraints (21). Constraints (22) ensure the inventory will never exceed the fixed MH capacity Q^{MH}, and no HM inventory is considered at a time-space node when no HM is present.

$$x^v_{(z,t)(z',t')} I^v_{z't'} = x^v_{(z,t)(z',t')} \left(I^v_{zt} + \sum_{(z'',t'') \in N^{C-}_{z,t}} y^{RM,v}_{(z'',t''),(z,t)} - \sum_{(z'',t'') \in N^{C+}_{z,t}} y^{DM,v}_{(z,t)(z'',t'')} \right),$$
$$\forall v \in \mathcal{V}, \quad \forall (z,t) \in \mathcal{N}^M, \quad \forall (z',t') \in N^{M+}_{z,t} \tag{21}$$

$$I^v_{zt} \leq Q^{MH} \left(\sum_{(z',t') \in N^{M+}_{z,t}} x^v_{(z,t)(z',t')} + \sum_{(z',t') \in N^{M-}_{z,t}} x^v_{(z',t'),(z,t)} \right), \quad \forall v \in \mathcal{V}, \quad \forall (z,t) \in \mathcal{N}^M \tag{22}$$

$$I^v_{zt} \in \mathbb{Z}_{\geq 0}, \quad \forall v \in \mathcal{V}, \quad \forall (z,t) \in \mathcal{N}^M \tag{23}$$

For the DDP inventory, we define the non-negative integer variable I^D_{zt} as the number of bikes in the DDP in zone z in period t. Similar to the change in MH inventories between two consecutive time-space nodes, the inventory of the DDP in z in period t equals the inventory in the previous period plus the MDRs collected and minus the ones borrowed out, which is stated in Constraints (24). Constraints (25) ensure that the DDP inventory will never exceed the fixed stop capacity Q^D.

$$I^D_{z,t+1} = I^D_{zt} + \sum_{(z'',t'') \in N^{C-}_{z,t}} y^{RD}_{(z'',t'')(z,t)} - \sum_{(z'',t'') \in N^{C+}_{z,t}} y^{DD}_{(z,t)(z'',t'')}, \quad \forall z \in \mathcal{Z}^M, \quad \forall t \in \mathcal{T} \setminus |\mathcal{T}| \tag{24}$$

$$I^D_{zt} \leq \zeta_z Q^D, \quad \forall (z,t) \in \mathcal{N}^M \tag{25}$$

$$I^D_{zt} \in \mathbb{Z}_{\geq 0}, \quad \forall (z,t) \in \mathcal{N}^M \tag{26}$$

Objective function. The objective is to minimize the total Mobile-Hub system cost, which includes the capital investment costs (MHs leasing J_1, MDRs purchasing J_2, DDP establishment J_3) converted to a daily rate by their usage life, and the total daily operational cost for MDRs J_4 and self-fulfillment J_5. Let c^{MH} represent the daily MH leasing cost, c^{MDR} the MDR price converted to a daily rate, c^{DDP} the cost of establishing a DDP converted to a daily rate, c^{VoT} the courier value of time per period, and c^{SF} the cost per unit distance covered for self-fulfillment. The objective function is then written as:

$$MIN \quad \Phi = J_1 + J_2 + J_3 + J_4 + J_5 \tag{27}$$

where:

$$J_1 = c^{MH} \sum_{v \in \mathcal{V}} \delta^v \tag{28}$$

$$J_2 = c^{MDR}(\sum_{v \in \mathcal{V}} I^v_{z_o,1} + \sum_{z \in \mathcal{Z}^D} I^D_{(z,1)}) \tag{29}$$

$$J_3 = c^{DDP} \sum_{z \in \mathcal{Z}^D} \zeta_z \tag{30}$$

$$J_4 = c^{VoT} \sum_{(z,t) \in \mathcal{N}^M} \left(\sum_{(z'',t'') \in N^{C-}_{z,t}} \sum_{v \in \mathcal{V}} y^{RM,v}_{(z'',t'')(z,t)} DIS_{zz''} + \sum_{(z'',t'') \in N^{C+}_{z,t}} \sum_{v \in \mathcal{V}} y^{DM,v}_{(z,t)(z'',t'')} DIS_{zz''} \right.$$
$$\left. + \sum_{(z'',t'') \in N^{C-}_{z,t}} y^{RD}_{(z'',t'')(z,t)} DIS_{zz''} + \sum_{(z'',t'') \in N^{C+}_{z,t}} y^{DD}_{(z,t)(z'',t'')} DIS_{zz''} \right) \tag{31}$$

$$J_5 = c^{SF} \sum_{(z,t)(z'',t'') \in \mathcal{A}^C} y^{SF}_{(z,t)(z'',t'')} DIS_{zz''} \tag{32}$$

4.5. Route-based formulation

Route constraints. A route is a list of ordered time-space nodes that an MH is situated at in the time-space network. As mentioned in Section 4.4, the planning horizon $\mathcal{T} = \{T_1, T_2, \ldots, T_l, \ldots, T_{|L|}\}$ is divided into a set of equal-length intervals. A master MH route spans the entire planning horizon, starting in the depot z_o in the first period and ending in depot in period $|\mathcal{T}|$. In a master route, the MH is required to return to the depot z_o at the end of each interval. We define $\mathcal{K} = \{K_1, K_2, \ldots, K_l, \ldots, K_{|L|}\}$ as the set of MH routes, where K_l is the route set in interval l. We define the binary variable $\theta^{lk} = 1$ if route k in interval l is in the solution. In each interval, there should be at least one route, and the number of routes should not exceed the number of available MHs. This is ensured by Constraints (33) (34). A master MH route is formed by splicing together one sub-route in each interval. Constraints (35) ensure that the two consecutive intervals have the same number of sub-routes.

$$1 \leq \sum_{k \in K_l} \theta^{lk}, \quad \forall l \in L \tag{33}$$

$$\sum_{k \in K_l} \theta^{lk} \leq |\mathcal{V}|, \quad \forall l \in L \tag{34}$$

$$\sum_{k \in K_l} \theta^{lk} = \sum_{k' \in K_{l+1}} \theta^{l+1,k'}, \quad l \in L \setminus |L| \tag{35}$$

$$\theta^{lk} \in \{0,1\}, \quad \forall l \in L, \quad \forall k \in K_l \tag{36}$$

In case of multiple master tours, we define the binary variable $f^{l+1,k'}_{l,k} = 1$ if route k in interval l and route k' in interval $l+1$ are on the same master route in the solution.

Constrains (37) and (38) ensure a sub-tour only belongs to one master tour.

$$\theta^{lk} = \sum_{k^{'} \in K_{l+1}} f_{l,k}^{l+1,k^{'}}, \quad \forall l \in L \setminus \{|L|\}, \quad \forall k \in K_l \tag{37}$$

$$\theta^{lk} = \sum_{k^{'} \in K_{l-1}} f_{l-1,k^{'}}^{l,k}, \quad \forall l \in L \setminus \{1\}, \quad \forall k \in K_l \tag{38}$$

$$f_{l,k}^{l+1,k^{'}} \in \{0,1\}, \quad \forall l \in L \setminus \{|L|\}, \quad \forall k \in K_l, \quad \forall k^{'} \in K_{l+1} \tag{39}$$

We define the index $\alpha_z^{lk} = 1$ if sub-route k in interval l select the candidate DDP in zone z. Constraints (40) check the selection of each candidate DDP z. M_2 is a constant value that is set as $|\mathcal{V}||L|$.

$$\zeta_z \leq \sum_{l \in L} \sum_{k \in K_l} \alpha_z^{lk} \theta^{lk}, \quad \forall z \in \mathcal{Z}^M \tag{40}$$

$$\sum_{l \in L} \sum_{k \in K_l} \alpha_z^{lk} \theta^{lk} \leq M_2 \zeta_z, \quad \forall z \in \mathcal{Z}^M \tag{41}$$

MH pickup and dropoff activation. MHs can not load and unload when in move, which says that only the MHs located at the start of a holding arc can provide service to couriers. Let H^{lk} be the set of starting nodes of the holding arcs on sub-route k in interval l. We define the non-negative integer $y_{(z,t)(z'',t'')}^{DM,lk}$ indicating the number of MDRs dropped off by the MHs located at z in period t that is on sub-route k in interval l to satisfy the courier service starting in zone z'' in period t''. Similarly, $y_{(z'',t'')(z,t)}^{RM,lk}$ represents the number of MDRs returned from z'' in t'' to the MH at z in t on sub-route k in interval l. The drop-off and pick-up flows associated with MHs and DDPs are presented in Constraints (42) - (43), as well as Constraints (12), (13).

$$y_{(z,t)(z'',t'')}^{DM,lk} \leq d_{zt} \theta^{lk}, \quad \forall l \in L, \quad \forall k \in K_l, \quad \forall (z,t) \in H^{lk}, \quad \forall (z'',t'') \in N_{z,t}^{C+} \tag{42}$$

$$y_{(z'',t'')(z,t)}^{RM,lk} \leq r_{zt} \theta^{lk}, \quad \forall l \in L, \quad \forall k \in K_l, \quad \forall (z,t) \in H^{lk}, \quad \forall (z'',t'') \in N_{z,t}^{C-} \tag{43}$$

$$y_{(z,t)(z'',t'')}^{DM,lk} \in \mathbb{Z}_{\geq 0}, \quad \forall l \in L, \quad \forall k \in K_l, \quad \forall (z,t) \in H^{lk}, \quad \forall (z'',t'') \in N_{z,t}^{C+} \tag{44}$$

$$y_{(z'',t'')(z,t)}^{RM,lk} \in \mathbb{Z}_{\geq 0}, \quad \forall l \in L, \quad \forall k \in K_l, \quad \forall (z,t) \in H^{lk}, \quad \forall (z'',t'') \in N_{z,t}^{C-} \tag{45}$$

Demands satisfaction.

$$\sum_{l\in L}\sum_{k\in K_l}\sum_{(z'',t'')\in N^{C-}_{z,t}\cap H^{lk}} y^{DM,lk}_{(z'',t'')(z,t)} + \sum_{(z'',t'')\in N^{C-}_{z,t}\cap\mathcal{N}^M} y^{DD}_{(z'',t'')(z,t)} + \sum_{(z'',t'')\in N^{C-}_{z,t}} y^{SF}_{(z'',t'')(z,t)} = d_{zt}, \quad \forall (z,t)\in\mathcal{N}^C \tag{46}$$

$$\sum_{l\in L}\sum_{k\in K_l}\sum_{(z'',t'')\in N^{C+}_{z,t}\cap H^{lk}} y^{RM,lk}_{(z,t)(z'',t'')} + \sum_{(z'',t'')\in N^{C+}_{z,t}\cap\mathcal{N}^M} y^{RD}_{(z,t)(z'',t'')} + \sum_{(z'',t'')\in N^{C+}_{z,t}} y^{SF}_{(z,t)(z'',t'')} = r_{zt}, \quad \forall (z,t)\in\mathcal{N}^C \tag{47}$$

Inventory management. We define the non-negative integer variable I^{lk}_{zt} indicating the number of MDRs on the MH located in z in t on the sub-route k in interval l. The MH capacity limit is expressed in Constraints (48).

$$I^{lk}_{zt} \le Q^{MH}\theta^{lk}, \quad \forall l\in L, \quad \forall k\in K_l, \quad \forall (z,t)\in H^{lk} \tag{48}$$

$$I^{lk}_{zt} \in \mathbb{Z}_{\ge 0}, \quad \forall l\in L, \quad \forall k\in K_l, \quad \forall (z,t)\in H^{lk} \tag{49}$$

Let $H^{lk}(1)$ and $H^{lk}(-1)$ be the first and last nodes in the set H^{lk}. For each node (z,t) in H^{lk}, we define $\bar{H}^{lk}_{zt}$ as its next node. Constraints (50) track the inventory update between two consecutive nodes in H^{lk}. Constraints (51) state that if route k in interval l and route k' in interval $l+1$ are on the same master route, then the MH inventory at the first node in $H^{l+1,k'}$ is updated based on the inventory at the last node in H^{lk}. The DDP inventory management is presented in Constraints (24) and (25).

$$I^{lk}_{\bar{H}^{lk}_{zt}} = I^{lk}_{zt} + \sum_{(z'',t'')\in N^{C-}_{z,t}} y^{RM,lk}_{(z'',t'')(z,t)} - \sum_{(z'',t'')\in N^{C+}_{z,t}} y^{DM,lk}_{(z,t)(z'',t'')},$$
$$\forall l\in L, \quad \forall k\in K_l, \quad \forall (z,t)\in H^{lk}\setminus\{H^{lk}(-1)\} \tag{50}$$

$$f^{l+1,k'}_{l,k} I^{l+1,k'}_{(z't')} = f^{l+1,k'}_{l,k}\left(I^{l,k}_{(z,t)} + \sum_{(z'',t'')\in N^{C-}_{z,t}} y^{RM,lk}_{(z'',t'')(z,t)} - \sum_{(z'',t'')\in N^{C+}_{z,t}} y^{DM,lk}_{(z,t)(z'',t'')}\right),$$
$$\forall l\in L\setminus\{|L|\}, \quad \forall k\in K_l, \quad \forall k'\in K_{l+1} \quad (z't') = H^{l+1,k'}(1), \quad (z,t) = H^{lk}(-1) \tag{51}$$

Objective function.

$$MIN \quad \Phi = J'_1 + J'_2 + J'_3 + J'_4 + J'_5 \tag{52}$$

where:

$$J_1' = c^{MH} \sum_{k \in K_1} \theta^{1k} \tag{53}$$

$$J_2' = c^{MDR} \left(\sum_{k \in K_1} I^{1,k}_{z_o,1} + \sum_{z \in \mathcal{Z}^D} I^D_{z,1} \right) \tag{54}$$

$$J_3' = c^{DDP} \sum_{z \in \mathcal{Z}^D} \zeta_z \tag{55}$$

$$J_4' = c^{VoT} \left(\sum_{l \in L} \sum_{k \in K_l} \sum_{(z,t) \in H^{lk}} \left(\sum_{(z'',t'') \in N^{C-}_{z,t}} y^{RM,lk}_{(z'',t''),(z,t)} DIS_{zz''} + \sum_{(z'',t'') \in N^{C+}_{z,t}} y^{DM,lk}_{(z,t)(z'',t'')} DIS_{zz''} \right) \right.$$
$$\left. + \sum_{(z,t) \in \mathcal{N}^M} \left(\sum_{(z'',t'') \in N^{C-}_{z,t}} y^{RD}_{(z'',t'')(z,t)} DIS_{zz''} + \sum_{(z',t'') \in N^{C+}_{z,t}} y^{DD}_{(z,t)(z'',t'')} DIS_{zz''} \right) \right) \tag{56}$$

$$J_5' = c^{SF} \sum_{(z,t)(z'',t'') \in \mathcal{A}^C} y^{SB}_{(z,t)(z'',t'')} DIS_{zz''} \tag{57}$$

4.6. Linearization

Constraints (21) in the arc-based model is nonlinear, which can be linearized as follows:

$$Q^{MH}(1 - x^v_{(z,t)(z',t')}) I^v_{z't'} \geq I^v_{zt} + \sum_{(z'',t'') \in N^{C-}_{z,t}} y^{RM,v}_{(z'',t'')(z,t)} - \sum_{(z'',t'') \in N^{C+}_{z,t}} y^{DM,v}_{(z,t)(z'',t'')},$$
$$\forall v \in \mathcal{V}, \quad \forall (z,t) \in \mathcal{N}^M, \quad \forall (z',t') \in N^{M+}_{z,t} \tag{58}$$

$$Q^{MH}(x^v_{(z,t)(z',t')} - 1) I^v_{z't'} \leq I^v_{zt} + \sum_{(z'',t'') \in N^{C-}_{z,t}} y^{RM,v}_{(z'',t'')(z,t)} - \sum_{(z'',t'') \in N^{C+}_{z,t}} y^{DM,v}_{(z,t)(z'',t'')},$$
$$\forall v \in \mathcal{V}, \quad \forall (z,t) \in \mathcal{N}^M, \quad \forall (z',t') \in N^{M+}_{z,t} \tag{59}$$

Constraints (51) in the route based model are non-linear, which can be linearized as:

$$Q^{MH}(1 - f^{l+1,k'}_{l,k}) + I^{l+1,k'}_{(z',t')} \geq I^{lk}_{(z,t)} + \sum_{(z'',t'') \in N^{C-}_{(z,t)}} y^{RM,lk}_{(z'',t'')(z,t)} - \sum_{(z'',t'') \in N^{C+}_{(z,t)}} y^{DM,l,k}_{(z,t),(z'',t'')},$$
$$\forall l \in L \setminus \{|L|\}, \quad \forall k \in K_l, \quad \forall k' \in K_{l+1}, \quad (z,t) = H^{lk}(-1), \quad (z',t') = H^{l+1,k'}(1) \tag{60}$$

$$Q^{MH}(f^{l+1,k'}_{l,k} - 1) + I^{l+1,k'}_{(z',t')} \leq I^{lk}_{(z,t)} + \sum_{(z'',t'') \in N^{C-}_{(z,t)}} y^{RM,lk}_{(z'',t'')(z,t)} - \sum_{(z'',t'') \in N^{C+}_{(z,t)}} y^{DM,l,k}_{(z,t),(z'',t'')},$$
$$\forall l \in L \setminus \{|L|\}, \quad \forall k \in K_l, \quad \forall k' \in K_{l+1}, \quad (z,t) = H^{lk}(-1), \quad (z',t') = H^{l+1,k'}(1) \tag{61}$$

4.7. Variable reduction

After logical analysis of the system, the upper bounds of the integer variables can be determined. When the upper bounds are 0, the corresponding variables could be removed.

- $\sum_{v\in\mathcal{V}}\sum_{(z'',t'')\in N^{C-}_{z,t}\cap\mathcal{N}^M} y^{DM,v}_{(z'',t'')(z,t)} = 0 \quad$ if $d_{zt} = 0$.
- $\sum_{l\in L}\sum_{k\in K_l}\sum_{(z'',t'')\in N^{C-}_{z,t}\cap H^{lk}} y^{DM,lk}_{(z'',t'')(z,t)} = 0 \quad$ if $d_{zt} = 0$.
- $\sum_{(z'',t'')\in N^{C-}_{z,t}\cap\mathcal{N}^M} y^{DD}_{(z'',t'')(z,t)} \quad$ if $d_{zt} = 0$.
- $\sum_{v\in\mathcal{V}}\sum_{(z'',t'')\in N^{C+}_{z,t}\cap\mathcal{N}^M} y^{RM,v}_{(z,t)(z'',t'')} = 0 \quad$ if $r_{zt} = 0$.
- $\sum_{l\in L}\sum_{k\in K_l}\sum_{(z'',t'')\in N^{C+}_{z,t}\cap H^{lk}} y^{RM,lk}_{(z,t)(z'',t'')} = 0 \quad$ if $r_{zt} = 0$.
- $\sum_{(z'',t'')\in N^{C+}_{(z,t)}\cap\mathcal{N}^M} y^{RD}_{(z,t),(z'',t'')} = 0 \quad$ if $r_{zt} = 0$.
- $\sum_{(z'',t'')\in N^{C-}_{z,t}} y^{SF}_{(z'',t'')(z,t)} = 0 \quad$ if $d_{zt} = 0$
- $\sum_{(z'',t'')\in N^{C+}_{z,t}} y^{SF}_{(z,t)(z'',t'')} = 0 \quad$ if $r_{zt} = 0$

5. Numerical results

In this section, we experiment with the proposed MFLP-MDs models using representative instances. In Section 5.1, we describe the input generation scheme. 5.2, we test the computational performance of the arc-based and route-based models and the effect of variable reduction. In Section 5.3, we investigate the managerial benefit of the proposed Mobile-Hub concept. In Section 5.4 we test the our model on real-world data to demonstrate the added value of this new technology in current practice. In Section

5.1. Instance generation

The on-demand delivery system operates within a predefined area discretized into hexagonal zones arranged in a circular pattern. We identify two service areas: an area of 37 hexagonal zones arranged in 4 circles (noted as Area-4), and an area of 91 hexagonal zones arranged in 6 circles (noted as Area-6). The edge of each zone is 200 meters, and one period represents 10 minutes. The innermost zone is chosen as the MH depot where the MHs start and end their shifts. For both service areas, we consider three planning horizons: {36, 48, 72} periods. We also consider varying number of courier services: {20, 30, 40, 50, 60}. Two courier service distributions are identified to represent different geographical distributions of the courier service starting and ending locations within the service area. In the first scenario (noted as **U**), a courier has an equal probability of starting and ending their service in any of the zones. In the second scenario (noted as **C**), a courier has a 75% probability of starting in the area center and a 75% probability of ending in the outskirts. This scenario mimics the situation where restaurants are more often located in the city center, and households are usually situated outside the city center. The area center is defined as a circle with a radius of

r zones originating from the innermost zone, where $r = 2$ for Area-4 and $r = 3$ for Area-6. We assume the service start time of each courier is randomly distributed within the first half of the planning horizon, and the corresponding end time is randomly distributed within the duration between the start time and the end of the planning horizon.

For all instances, we consider two homogeneous MHs, each with a capacity Q^{MH} of 50 MDRs, and the homogeneous candidate DDPs have a capacity Q^{DDP} of 1 MDR. Four canal typologies (Figure 3), replicated from real city canals, are considered: Amsterdam (noted as Canal-1), Leiden (noted as Canal-2), Venice (noted as Canal-3), and Fredrikstad (noted as Canal-4). For each network type, we calculate the following indexes, which indicate the complexity of the network: α, β, and γ. The index α measures the degree of connectivity in a network by comparing the number of actual circuits (or loops) to the maximum number of circuits possible. The index β compares the number of links to the number of nodes. The index γ compares the number of actual links in the network to the maximum possible number of links between nodes. These indexes are calculated as:

$$\alpha = \frac{L - N + 1}{2N - 5}$$
$$\beta = \frac{L}{N}$$
$$\gamma = \frac{L}{3(N - 2)}$$

where L is the number of links, and N is the number of vertices.

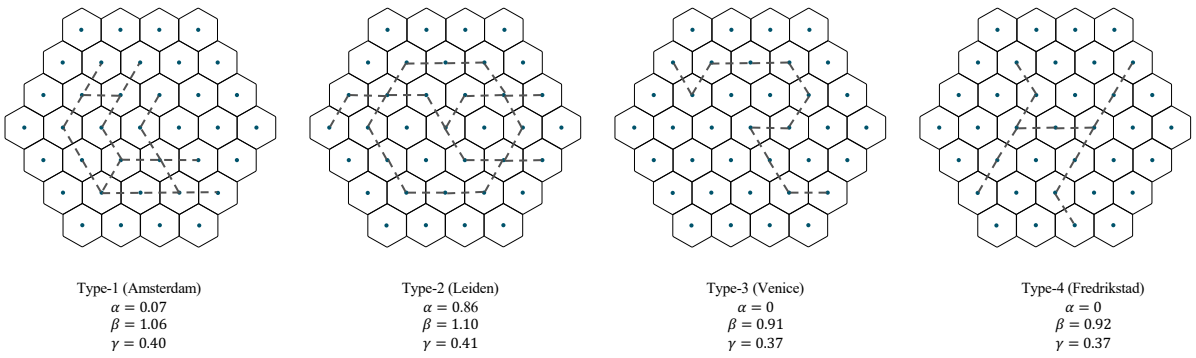

Figure 3: Canal typologies replicated from Amsterdam, Leiden, Venice, and Fredrikstad

In Table 1, we present the characteristics of the instances: (1) area size, (2) planning horizon length, (3) courier service distribution, (4) number of courier services, (5) canal network typology. The instances are named accordingly. For example, "A4-P36-**U**-S40-N1" indicates the case of Area-4, a planning horizon of 36 periods, uniformly distributed courier services, 40 courier services, and network type 1.

We set the daily cost of an MH as 810 €, representing the fixed cost including the vessel leasing, energy, and driver salary. The average bike price in the Netherlands is 865 €. We

consider the service life of a new bike to be three years, so the daily cost of one bike is set as $\frac{865}{1095} = 0.79$ €. According to the price for storing one bicycle with the Netherlands train operator NS, we set the yearly cost of a DDP as 100 euros, i.e., 0.27 euros per day. We consider the gross hourly salary of a courier to be 14.77 €, thus the opportunity cost of one period for one courier spending on pre- and post-service riding is 2.46 €.

Table 1: Instance characteristics

Characteristics	Types
Area size	4-circle, 6-circle
Planning horizon	36 periods, 48 periods, 72 periods
Service distribution	**U**, **C**
Courier service number	20, 30, 40, 50, 60
Network typology	Network-1, Network-2, Network-3, Network-4

5.2. Computational performance

In this section we provide some insights of the computational performance of the models. We conduct the experiments using Python and Gurobi Optimizer version 11.0.0. All experiments are carried out on a computer with a 2.4 GHz CPU, 8 GB of RAM, and an 8-core processor. Each instance is solved with a time limit of 4 hours. In Section 5.2.1, we discuss the effect of the pre-processing. In Section 5.2.2, we compare the computational performance of the arc-based model and the route-based model. Section 5.2.3 examines the computation time sensitivity to network typology and demand scenario.

5.2.1. Effect of pre-processing

We select 12 instances to test the performance of the pre-processing on both the arc-based and route-based models. Using network Type-1, demand scenario **U**, and 40 courier services as a representative case, we vary the area size (Area-4, Area-6), planning horizon length (36 periods, 48 periods, 72 periods), and interval length (4 periods and 6 periods). Tables 2 and 3 present the characteristics of these instances with and without applying the pre-processing. We keep the automatic pre-processing of Gurobi while solving. The columns contain the integer solution ($\bar{\Phi}$), the objective value of the linear relaxation ($\bar{\Phi}_{LP}$), the percentage integrality gap ($\bar{\Phi}/\bar{\Phi}_{LP}$), the number of constraints (Cons.), the number of variables (Var.), and the number of binary variables (Bin.). The results demonstrate that applying pre-processing significantly reduces the model size in terms of the number of variables and constraints for both the arc-based and route-based formulations.

5.2.2. Comparison between two models

This section compares the computational performance of the arc-based and route-based models. We still choose network Type-1 and demand scenario **U** as a representative case. We select 18 instances by varying the area size, planning horizon, interval length and courier service number (40, 60, 80). We present in Table 4 the results of the instances with an interval length of 4 periods, and in Table 5 the results for the same instances with an interval length of 6 periods. The columns include the number of explored nodes (Nodes), the optimality

Table 2: Effect of pre-processing for instances under case **U**-S40-N1 (Arc-based model)

Instance	$\bar{\Phi}$	$\bar{\Phi}_{LP}$	Int. Gap	Without pre-processing			With pre-processing		
				Cons.	Vars.	Bin.	Cons.	Vars.	Bin.
A4-P36-I4	1245.66	1189.46	105%	17737	10846	9292	16241	10337	8816
A4-P36-I6	1245.66	1169.01	107%	17737	10855	9301	16358	10415	8882
A4-P48-I4	1232.57	1163.12	106%	25793	14796	12399	21494	12821	10712
A4-P48-I6	1211.39	1112.78	109%	25793	14811	12414	24202	14330	11954
A4-P72-I4	1239.95	1167.74	106%	33758	18643	15481	31577	18021	14889
A4-P72-I6	1199.57	1072.02	112%	33758	18661	15499	31684	18087	14934
A6-P36-I4	1412.24	1339.84	105%	17889	10990	9556	16350	10482	9078
A6-P36-I6	1397.96	1294.18	108%	17889	10999	9565	16464	10557	9141
A6-P48-I4	1458.80	1398.25	104%	25823	14792	12490	21434	12803	10790
A6-P48-I6	1432.70	1345.02	107%	25823	14802	12509	24033	14282	12002
A6-P72-I4	1498.16	1430.81	105%	33641	18501	15285	31355	17843	14660
A6-P72-I6	1440.56	1339.98	108%	33641	18519	15303	31446	17906	14711

Table 3: Effect of pre-processing for instances under case **U**-S40-N1 (Route-based model)

Instance	$\bar{\Phi}$	$\bar{\Phi}_{ZP}$	Int. Gap	Without pre-processing			With pre-processing		
				Cons.	Vars.	Bin.	Cons.	Vars.	Bin.
A4-P36-I4	1245.66	1221.17	102%	846	547	483	654	472	84
A4-P36-I6	1245.66	1225.19	101%	5495	3361	3030	5028	3204	1602
A4-P48-I4	1232.57	1208.87	102%	1172	735	623	920	643	180
A4-P48-I6	1211.39	1189.27	102%	7515	4322	3850	6791	4094	2418
A4-P72-I4	1239.95	1215.43	102%	1289	737	628	1011	673	213
A4-P72-I6	1199.57	1177.01	102%	9607	5335	4780	8603	5049	3234
A6-P36-I4	1412.24	1390.08	102%	879	591	525	686	458	87
A6-P36-I6	1397.96	1380.57	101%	5549	3417	3080	5065	3242	1602
A6-P48-I4	1458.80	1433.07	102%	1206	743	632	965	665	181
A6-P48-I6	1432.70	1407.35	102%	7546	4338	3889	6761	4082	2418
A6-P72-I4	1498.16	1471.51	102%	1303	750	633	1000	664	213
A6-P72-I6	1440.56	1416.82	102%	9533	5253	4689	8525	4954	3234

gap (Gap), and runtime. The column "Imp" shows the improvement in solving time of the route-based model compared to the arc-based model.

We see that when the number of courier services is 40 and 60, both models solve the instances quickly to optimality. However, neither model converges when the number of courier services reaches 80 for instances with the planning horizon of 48 and 72 periods. Table 6 summarizes the results from Table 4 and Table 5. The results show that, on average, the route-based model performs better for the selected instances. Also, instances with interval length of 6 periods takes longer time to solve and have larger gap when the time limit is reached.

Table 4: Comparison of Arc-based and Route-based model performance for instances under case "**U**-N1 (Interval of 4 periods)"

Instance	Arc-based			Route-based			Imp.
	Nodes	Gap	Run Time(s)	Nodes	Gap	Run Time(s)	
A4-P36-S40	348	0	10.63	1	0	0.28	97.37%
A4-P36-S60	1	0	8.40	1	0	0.3	96.43%
A4-P36-S80	378	0	27.01	1	0	0.73	97.30%
A4-P48-S40	4496	0	11.28	1	0	0.97	91.40%
A4-P48-S60	481	0	11.97	1	0	0.36	96.99%
A4-P48-S80	1687422	1.59%	14400.94	805144	0.28%	14402.56	-
A4-P72-S40	11179	0	27.21	1	0	0.68	97.50%
A4-P72-S60	5073	0	81.42	354	0	2.18	97.32%
A4-P72-S80	1609272	1.98%	14400.11	649713	1.35%	14401.00	-
A6-P36-S40	494	0	8.20	1	0	0.45	94.51%
A6-P36-S60	1	0	8.01	1	0	0.29	96.38%
A6-P36-S80	1145730	0.23%	14400.03	742444	0.28%	14401.00	-
A6-P48-S40	249	0	9.75	1	0	0.37	96.21%
A6-P48-S60	1	0	16.27	1	0	0.45	97.23%
A6-P48-S80	1458483	1.27%	14400.44	1002713	0.40%	14403.21	-
A6-P72-S40	5650	0	30.48	41	0	0.94	99.99%
A6-P72-S60	4151	0	27.67	1	0	0.46	98.34%
A6-P72-S80	594571	1.62%	14400.32	250476	1.58%	14407.73	-

5.2.3. Computation time sensitivity to network type and demand scenario

In this section, we investigate the network typology and courier service distribution on the solving time. We consider the four canal network shapes and the two courier service distributions as described in Section 5.1. We use Area-4 and planning horizon of 36 periods as a representative case and consider three levels of courier services {40, 60, 80}, which are named "A4-P36-S40", "A4-P36-S60", and "A4-P36-S80". The interval length is 6 periods for all tests. Table 7 presents the computational results under different combinations of network typologies and service distribution. We further summarize the results in Table 7 in Table 8. The columns include the network typology, instance name, optimality gap (Gap), and time

Table 5: Comparison of Arc-based and Route-based model performance for instances under case "**U**-N1 (Interval of 6 periods)"

Instance	Arc-based			Route-based			Imp.
	Nodes	Gap	Run Time(s)	Nodes	Gap	Run Time(s)	
A4-P36-S40	1727	0	25.48	1	0	2.75	89.21%
A4-P36-S60	1293	0	33.24	1	0	6.61	80.11%
A4-P36-S80	681	0	67.26	1	0	8.05	88.03%
A4-P48-S40	10205	0	42.7	115	0	10.75	74.82%
A4-P48-S60	7386	0	92.46	207	0	22.53	75.63%
A4-P48-S80	242860	1.91%	14400.69	97615	1.69%	14400.83	-
A4-P72-S40	148392	0	939.19	9993	0	95.15	89.87%
A4-P72-S60	687568	0.89%	14401.15	33942	0	1283.91	91.08%
A4-P72-S80	314445	1.97%	14402.54	272029	29.10%	14402.13	-
A6-P36-S40	2592	0	20.63	1	0	3.19	84.54%
A6-P36-S60	194	0	30.61	1	0	4.78	84.38%
A6-P36-S80	227947	0.14%	14403.80	531102	0.14%	14400.29	-
A6-P48-S40	1671	0	47.58	1	0	6.08	87.22%
A6-P48-S60	2799	0	46.53	450	0	89.29	-91.90%
A6-P48-S80	466772	1.33%	14400.36	88538	1.40%	14400.77	-
A6-P72-S40	397512	0	4181.69	5694	0	96.51	97.69%
A6-P72-S60	238913	0	3007.53	4609	0	1117.97	62.83%
A6-P72-S80	103437	26.70%	14401.34	202307	5.52%	14402.94	-

Table 6: The summary of results reported in Table 4 and Table 5

	Arc-based		Route-based	
	Ave. Gap	Ave. Run time(s)	Ave. Gap	Ave. Run time(s)
Interval 4	0.37%	4813.84	0.22%	4001.33
Interval 6	1.83%	5274.22	2.10%	4152.73

for both demand scenarios **U** and **C**. The optimality gap is calculated as $100 \times (\bar{\Phi} - LB)/\bar{\Phi}$, where $\bar{\Phi}$ is the best feasible solution and LB is the best-known lower bound.

We observe that, on average, solving instances under network Type-2 takes the longest time. This reflects the fact that Type-2 is the most complex network among the four types, with all three indexes having the highest values. In terms of demand pattern, scenario **C** is harder to solve. Specifically, solving instances with 80 courier services under scenario **C** could not prove optimality within 4 hours.

5.3. Managerial insights

This section discusses the managerial implications of the proposed Mobile-Hub strategy for on-demand delivery platforms. According to historical data from a local platform in Amsterdam, there are approximately 180 active courier shifts on a typical operating day

Table 7: Computation time sensitivity to network typology and service distribution

Network	Instance	**U**		**C**	
		Gap	Time(s)	Gap	Time(s)
Type-1	A4-P36-S40	0	2.67	0	8.96
	A4-P36-S60	0	3.72	0	13.62
	A4-P36-S80	0	2.7	1.54%	14400.13
Type-2	A4-P36-S40	0	24.61	0	12.15
	A4-P36-S60	0	19.52	0	20.76
	A4-P36-S80	0	29.02	0.62%	14400.44
Type-3	A4-P36-S40	0	0.82	0	1.48
	A4-P36-S60	0	6.57	0	1.7
	A4-P36-S80	0	1.78	1.44%	14400.08
Type-4	A4-P36-S40	0	2.21	0	11.08
	A4-P36-S60	0	9.79	0	11.22
	A4-P36-S80	0	14.81	1.44%	14400.10

Table 8: Summary of Table 7

Network	**U**		**C**	
	Ave. Gap	Ave. Time(s)	Ave. Gap	Ave. Time(s)
Type-1	0	3.03	0.51%	4807.47
Type-2	0	24.38	0.21%	4811.12
Type-3	0	3.06	0.48%	4801.09
Type-4	0	8.94	0.48%	4807.47

(9:00 - 23:00) in the whole city. In this section, we consider one vessel as an MH and use the instance "A4-P48-S40" as a representative case, assuming the vessel operates in Area-4 which is in the city center to serve 40 courier shifts during the busiest hours from 15:00 to 22:00 (a planning horizon of 48 periods). Furthermore, we assume the battery capacity of the vessel is 8 hours, which only requires the vessel to return to the depot at the closure of the planning horizon.

Section 5.3.1 explores the impact of canal network typology and courier service distributions. Section 5.3.2 studies the sensitivity of vessel battery capacity by varying the duration for which the vessel must return to the depot. Section 5.3.3 investigates the impact of the number of courier services. Section 5.3.4 tests the sensitivity of the parameter c^{SF}, which represents the cost related to courier self-fulfillment. Finally, Section 5.4 presents a case study on the Amsterdam canal area using real-world data.

To study the impact of these characteristics, we define the following system performance indicators: (1) objective value indicating the total system cost (column "Obj. Val. (€)"), (2) number of required MDRs (column "MDRs"), (3) number of visited DDPs (column "DDPs"), and (4) the average non-service time a courier spends on pre- and post-service riding (column "Cour. non-service time (min)").

5.3.1. Impact of canal typology and courier service distribution

This analysis aims to prepare the platform for potential business expansion in different cities with distinct canal network typologies and restaurant-household distributions. We consider four canal networks and two service distributions (**U** and **C**) as described in Section 5.1, resulting in eight "Network - Service distribution" combinations.

The results in Table 9 show that for each canal network type, the average values of the various system indicators for the two service distributions are close to each other, suggesting that the canal network shape has a negligible impact on the Mobile-Hub system infrastructure configuration and operation. When examining the influence of service distribution under the same canal type, we find that even though both distributions require the same number of MDRs, the objective value is consistently higher when courier services are geographically uniformly distributed. In this case, the vessel needs to visit more DDPs, and couriers spend more time on non-service riding on average. This is because uniformly distributed courier services are less concentrated than the centric demand distribution, requiring the vessel to cover a wider range of the service area and spend more time en route.

Table 9: Sensitivity to canal network type and courier service distribution under case "A4-P48-S40"

Network	Ser. Distrb.	Obj. Val.(€)	MDRs	DDPs	Cour. non-service time (min)
1	C	1085.18	29	5	12.75
	U	1150.49	29	10	16.00
	Ave.	1117.84	29	7.5	14.375
2	C	1087.37	29	4	12.88
	U	1162.25	29	8	16.62
	Ave.	1124.81	29	6	14.75
3	C	1085.45	29	6	12.75
	U	1154.60	29	7	16.25
	Ave.	1120.03	29	6.5	14.50
4	C	1089.83	29	4	13.00
	U	1149.41	29	6	16.00
	Ave.	1119.62	29	5	14.5

5.3.2. Vessel battery capacity sensitivity

The vessel must return to the depot periodically to recharge, with the interval length depending on the vessel battery capacity. This analysis aims to inform the platform about the impact of battery capacity on the Mobile-Hub infrastructure configuration and vessel operation. We use uniformly distributed courier services, and network type-1 ("A4-P48-**U**-S40-N1") as a representative case, and vary the interval length (column "Battery life (hr)" in Table 10) for which duration the vessel must return to the depot: {0, 1, 2, 4, 8}. A larger battery capacity allows the vessel to cover a larger range of the service area, providing more routing and scheduling options. By changing the battery life, we impose different levels of mobility limitations on the vessel. An interval length of 0 indicates no vessel mobility, with

the vessel parked at the depot throughout the planning horizon. An interval length of 1 hour only allows the vessel to cover the center area of the service area, while interval lengths over 2 hours enable the vessel to visit the outermost zones. An interval length of 8 hours represents the vessel only returning to the depot at the end of the planning horizon, having the most flexibility.

The results show that both the objective value and the average courier non-service riding time decrease with larger battery capacities. Additionally, a longer battery life allows the vessel to visit more DDPs. The results prove that a higher level of vessel mobility helps improve courier service levels. Furthermore, as the battery life of 0 hours mimics the static hub which is the current practice applied by the platform, the results demonstrate the benefit of the Mobile-Hub strategy.

Table 10: Sensitivity to battery life under case "A4-P48-**U**-S40-N1"

Battery life (hr)	Obj. Val. (€)	MDRs	DDPs	Courier non-service time (min)
0	1224.32	29	1	19.88
1	1185.77	29	4	17.88
2	1178.66	29	5	17.50
4	1154.33	29	6	16.25
8	1149.41	29	6	16.00

5.3.3. Courier number analysis

Changes in customer orders directly impact the size of the courier fleet. This analysis prepares the platform for situations where meal order volumes may deviate from the normal range on certain days due to special events, such as festivals. We use service distribution **U** and network Type-1 ("A4-P48-U-N1") as a representative case and vary the number of courier services as {20, 30, 40, 50, 60}, as shown in the "Cour. Nr." column in Table 11. The "Cost per Cour." column indicates the average cost per courier.

The results show that while the objective value increases with the number of courier services, the average cost per courier decreases. The required number of MDRs is consistently maintained at a certain level (between 70% - 90%) relative to the number of courier services. This can be explained by the fact that MDR collection and drop-offs always occur concentratedly within a certain duration during the planning horizon. Sharp increases in MDR pickups always occur before and during meal peaks (16:00-18:00), which is the first half of the planning horizon in our case, while MDR returns always happen after the meal peaks. As a result, the number of required MDRs consistently increases with the quantity of courier services. On the other hand, the number of visited DDPs drops as the number of couriers to serve increases, while the courier non-service riding time is not significantly influenced by the number of courier services.

5.3.4. Self-fulfillment cost analysis

This analysis deals with the uncertainty of the unit cost associated with the courier service demand self-fulfillment. In our assumptions, courier demand self-fulfillment is realized by considering a free-floating location in each zone where two couriers can meet to hand over

Table 11: Sensitivity to courier service number under case "A4-P48-**U**-N1"

Cour. Nr.	Obj. Val.(€)	Cost per Cour.(€)	MDRs	MDRs/Cour. Nr.	DDPs	Courier non-service time (min)
20	984.43	49.22	16	0.80	7	16.25
30	1135.28	37.84	26	0.87	8	20.5
40	1149.41	28.74	29	0.73	6	16
50	1296.83	25.94	35	0.70	6	18.6
60	1403.11	23.39	46	0.77	3	18.83

their bikes at no charge. However, in some cities, this may involve additional management and administration costs. In this section, we increase the ratio c^{SF}/c^{vot} between the unit cost associated with the courier demand self-fulfillment and the courier value of time as {1, 1.2, 1.4, 1.6, 1.8, 2}. In Table 12, the columns "By MH (%)", "By DDPs (%)", and "By self-FF. (%)" indicate the proportion of total courier service satisfied by the vessel, DDPs, and self-fulfillment, respectively. The results show that the objective value slightly increases with the unit demand self-fulfillment cost. The demand satisfied by self-fulfillment decreases from 7% to 5% after c^{SF}/c^{vot} increases to 1.4. The average ride time per courier also slightly increases.

Table 12: Sensitivity to unit courier self-fulfillment cost under case "A4-P48-**U**-N1"

c^{SF}/c^{vot}	Obj. Val. (€)	By MH (%)	By DDP (%)	By self-FF. (%)	Courier non-service time (min)
1	1149.41	72	20	7	16.00
1.2	1151.87	75	17	7	16.00
1.4	1153.84	75	20	5	16.12
1.6	1154.82	75	20	5	16.12
1.8	1155.81	72	22	5	16.12
2	1156.79	75	20	5	16.12

5.4. Case study on Amsterdam canal area

In this section, we apply the proposed Mobile-Hub strategy to practice, testing our model on data from a local on-demand delivery platform in the Netherlands. We use courier schedules from September 13, 2021, to October 10, 2021, in the Amsterdam Canal area as our sample. We manually outline the course of the canal for the gridded service area, which contains 91 zones (Figure 4). Each zone has an edge length of 200 meters, and the distance between the centers of two adjacent zones is 347 meters. We consider two available homogeneous electric vessels as the MHs, each with a capacity of 50 MDRs. We assume all zones crossed by canals are capable of establishing a DDP. Given the curved canals and busy waterway transport in the Amsterdam center, we assume a vessel speed of 4 km/hour and a period length of 10 minutes. For the chosen area, we select the innermost zone as the depot for the vessels. The vessels need to return to the depot every 8 hours to recharge.

We consider the operation of a typical day from 9:00 in the morning to 24:00 at night, totaling 96 periods. The chosen area exemplifies the situation where most meal pickups and drop-offs occur in Amsterdam. After averaging the one-month courier schedules to one day

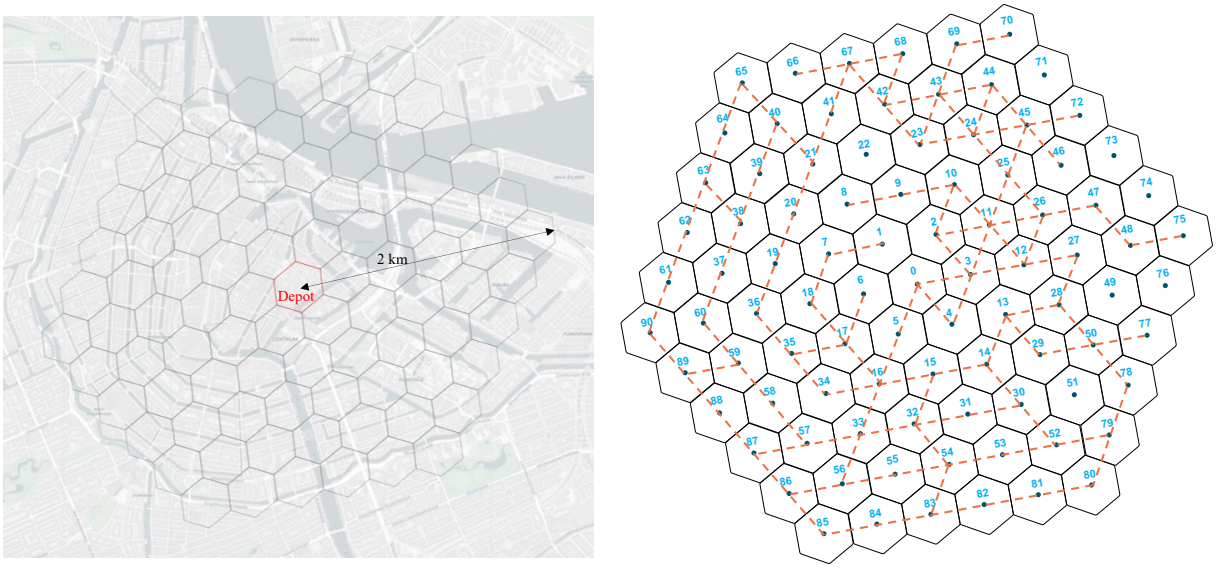

Figure 4: Amsterdam canal network abstraction

and removing the courier shifts that either start or end outside the chosen area, we obtain 46 courier shifts for the planning horizon. The launch peak of courier fleet dispatching is at 11:00, and the dinner peak is from 16:00 to 17:00. Courier service starts are uniformly distributed across all zones, and the temporal distribution of the service starts in a zone can be estimated from historical data. The parameters for capital investment and vessel operation are the same as described in Section 5.1. We construct the benchmark by forcing the vessel to remain stationary at the depot throughout the planning horizon to mimic the static hub in the current practice. To set up the benchmark, we use the optimal number of vessels in the Mobile-Hub strategy and forbid courier self-fulfillment.

The courier service dynamics feature a high level of complexity. Different temporal and spatial distributions of the courier service starts and ends may impose different pressures on the urgency of a zone requiring more bikes or having more bikes to return for certain periods. When the temporal and spatial distributions of the courier service starts are fixed, the service ends distribution pattern is determined by the transition matrix $n_{zt}^{z't'}$, where zz' is defined as the service range which is the radius centered on the start zone, and tt' is the service time length. In Sections 5.4.2 and 5.4.1, we study the impact of the average courier service range zz' and service time length on the Mobile-Hub infrastructure configurations and operations.

In addition to the basic system performance indicators mentioned in Section 5.3, we further define the following vessel-related system indicators: (1) "vessel en route time" indicating the time the vessel spends on relocation, (2) μ indicating the average MDR inventory level on the vessel throughout the planning horizon, and (3) δ indicating the standard deviation of the number of MDRs.

5.4.1. Sensitivity of courier service time length

In this analysis, we assume the courier service range is a circle with a radius of 10 zones and we vary the service length as {2, 3, 4, 5, 6} hours. Table 13 presents the basic system

performance indicators for both the Mobile-Hub strategy and the benchmark, as well as the percentage improvements in these indicators after adopting the Mobile-Hub strategy. The results show that longer service lengths lead to larger objective values, more required MDRs, and couriers spending more time on non-service riding. This trend applies to both the Mobile-Hub strategy and the benchmark. The comparison between the two practices shows that for all service length settings, there is always an improvement in the basic system indicators after applying our proposed strategy. On average, we see a decrease of 17% in the objective value, 7% in the required MDRs, and 35% in the average courier riding time, which demonstrates the benefits of the Mobile-Hub strategy.

In Table 16, we present the proportion of the courier services satisfied by the vessel, DDP, and self-fulfillment, as well as the vessel en route time and the mean value and standard deviation of the vessel inventory for both the Mobile-Hub strategy and the benchmark. The results show that the percentage of courier services satisfied by the vessel increases with the service time length, while the proportion satisfied by the DDPs drops. This is also reflected by the changes in vessel en route time which shows a decreasing trend in general. Less en route time means more stationary time during which the vessel can load and unload MDRs. On average, the vessel spends 8.5 hours out of the 16 hours of operation time en route; 64% of the couriers are satisfied by the vessel, 29% by the DDPs, and 7% by the self-FF. The mean MDR inventories and the standard deviation of the Mobile-Hub strategy is always lower than that of the benchmark, indicating that the Mobile-Hub strategy helps maintain a lower and more stable inventory level.

Table 13: Sensitivity to service length for basic system indicators - service range 10 zones

Ser. Len.	Obj. Val. (€)			MDRs			Cour. non-service time (min)		
(hrs)	Mobile-Hub	Bench.	Impr.	Mobile-Hub	Bench.	Impr.	Mobile-Hub	Bench.	Impr.
2	1280.75	1648.05	22%	23	27	15%	20.22	36.89	45%
3	1363.15	1646.29	17%	28	31	10%	23.78	36.67	35%
4	1373.44	1656.13	17%	31	31	0%	24.11	37.11	35%
5	1400.77	1653.67	15%	31	31	0%	25.33	37.00	32%
6	1433.32	1656.83	13%	31	35	11%	26.89	37.00	27%
Ave.	1370.29	1652.19	17%	28.8	31	7%	24.07	36.93	35%

Table 14: Sensitivity to service length for vessel related system indicators - service range 10 zones

Ser. Len. (hrs)	By Vessel	By DDP	By self-FF.	Vessel en route time (min)	Vessel Inventory μ		Vessel Inventory δ	
					Mobile-Hub	Bench.	Mobile-Hub	Bench.
2	51%	40%	9%	9.17	12.69	17.92	7.75	8.17
3	62%	36%	2%	8.83	15.15	19.12	9.28	9.20
4	69%	27%	4%	8.00	15.91	16.39	10.10	9.62
5	69%	27%	4%	8.50	13.95	13.49	9.79	10.04
6	71%	13%	16%	8.00	11.72	15.02	10.11	10.67
Ave.	64%	29%	7%	8.50	13.88	16.39	9.41	9.54

5.4.2. Sensitivity of courier service range

In this analysis, we choose the courier service time length to be 4 hours and vary the radius of the service range as {0, 2, 4, 6, 8, 10} zones, where a service range of 0 zones represents the case where couriers start and end in the same zone. In Tables 15 and **??**, we present the basic and vessel-related system indicators. The results show that the impact of the courier service range on the operation of the Mobile-Hub system is small. When comparing the Mobile-Hub strategy with the current practice, the number of required MDRs remains the same. On average, we observe an improvement of 15% in the objective value and 32% in the average courier non-service riding time.

Table 15: Sensitivity to service range for basic system indicators - service time length 4 hours

Ser. Range	Obj. Val. (€)			MDRs			Cour. non-service time (min)		
(zones)	Mobile-Hub	Bench.	Impr.	Mobile-Hub	Bench.	Impr.	Mobile-Hub	Bench.	Impr.
0	1409.80	1656.40	15%	31	31	0%	25.78	37.11	31%
2	1388.20	1646.56	16%	31	31	0%	24.78	36.67	32%
4	1389.31	1617.04	14%	31	31	0%	24.89	35.33	30%
6	1363.06	1626.88	16%	31	31	0%	23.67	35.78	34%
8	1385.47	1653.94	16%	31	31	0%	24.67	37.00	33%
10	1373.44	1656.13	17%	31	31	0%	24.11	37.11	35%
Ave.	1387.17	1640.16	15%	31	31	0%	24.76	36.38	32%

Table 16: Sensitivity to service range for vessel related system indicators - service time length 4 hours

Ser. Range (zones)	By Vessel	By DDP	By self-FF.	Vessel en route time (min)	Vessel Inventory μ		Vessel Inventory δ	
					Mobile-Hub	Bench.	Mobile-Hub	Bench.
0	69%	29%	2%	8.50	15.90	16.27	9.90	9.54
2	69%	31%	0%	7.67	15.86	16.31	9.88	9.46
4	69%	31%	0%	7.67	15.98	16.43	9.88	9.53
6	69%	29%	2%	7.67	16.12	16.40	9.74	9.37
8	69%	31%	0%	8.83	15.99	16.28	9.96	9.71
10	69%	27%	4%	8.00	15.91	16.39	10.10	9.62
Ave.	69%	30%	1%	8.06	15.96	16.35	9.91	9.54

6. Conclusion

This study introduces a novel Mobile-Hub system utilizing electric vessels as mobile hubs for managing shared micro-delivery resources in on-demand meal delivery platforms. Our proposed approach addresses the limitations of static central hubs in urban areas with canal networks. Through mixed-integer linear programming models, we demonstrate that this strategy significantly outperforms traditional methods, achieving substantial reductions in total costs, required resources, and courier riding times. The Mobile-Hub system maintains lower and more stable inventory levels while improving service quality. These findings highlight

the potential of waterborne vessels to enhance urban logistics efficiency and sustainability in canal-rich cities. Our research contributes to the growing field of sustainable urban logistics and explores a new application for leveraging urban waterways in last-mile delivery operations.

References

Alarcon-Gerbier, E., Buscher, U., 2020. Minimizing movements in location problems with mobile recycling units, in: Computational Logistics: 11th International Conference, ICCL 2020, Enschede, The Netherlands, September 28–30, 2020, Proceedings 11, Springer. pp. 396–411.

Alarcon-Gerbier, E., Buscher, U., 2022. Modular and mobile facility location problems: A systematic review. Computers & Industrial Engineering 173, 108734.

Ataç, S., Obrenović, N., Bierlaire, M., 2021. Vehicle sharing systems: A review and a holistic management framework. EURO Journal on Transportation and Logistics 10, 100033.

Becker, T., Lier, S., Werners, B., 2019. Value of modular production concepts in future chemical industry production networks. European Journal of Operational Research 276, 957–970.

Benjaafar, S., Wu, S., Liu, H., Gunnarsson, E.B., 2022. Dimensioning on-demand vehicle sharing systems. Management Science 68, 1218–1232.

Calogiuri, T., Ghiani, G., Guerriero, E., Manni, E., 2021. The multi-period p-center problem with time-dependent travel times. Computers & Operations Research 136, 105487.

Carlén, V., Josefsson, A., Olsson, L., 2013. The potential role of urban waterways in sustainable urban freight transport - a case study of mass transport from the construction of västlänken. URL: https://api.semanticscholar.org/CorpusID:107868222.

Central Commission for the Navigation of the Rhine, . Central commission for the navigation of the rhine. https://www.ccr-zkr.org/. Accessed: YYYY-MM-DD.

Demaine, E.D., Hajiaghayi, M., Mahini, H., Sayedi-Roshkhar, A.S., Oveisgharan, S., Zadimoghaddam, M., 2009. Minimizing movement. ACM Transactions on Algorithms (TALG) 5, 1–30.

Fan, Q., van Essen, J.T., Correia, G.H., 2023. Optimising fleet sizing and management of shared automated vehicle (sav) services: A mixed-integer programming approach integrating endogenous demand, congestion effects, and accept/reject mechanism impacts. Transportation Research Part C: Emerging Technologies 157, 104398.

Farahani, R.Z., Hekmatfar, M., 2009. Facility location: concepts, models, algorithms and case studies. URL: https://api.semanticscholar.org/CorpusID:107460537.

Güden, H., Süral, H., 2014. Locating mobile facilities in railway construction management. Omega 45, 71–79.

Guo, Z., Hao, M., Yu, B., Yao, B., 2021. Robust minimum fleet problem for autonomous and human-driven vehicles in on-demand ride services considering mixed operation zones. Transportation Research Part C: Emerging Technologies 132, 103390.

Illgen, S., Höck, M., 2019. Literature review of the vehicle relocation problem in one-way car sharing networks. Transportation Research Part B: Methodological 120, 193–204.

Lei, C., Lin, W.H., Miao, L., 2014. A stochastic emergency vehicle redeployment model for an effective response to traffic incidents. IEEE Transactions on Intelligent Transportation Systems 16, 898–909.

Monteiro, C.M., Machado, C.A.S., de Oliveira Lage, M., Berssaneti, F.T., Davis Jr, C.A., Quintanilha, J.A., 2021. Optimization of carsharing fleet size to maximize the number of clients served. Computers, Environment and Urban Systems 87, 101623.

Narayan, J., Cats, O., van Oort, N., Hoogendoorn, S.P., 2021. Fleet size determination for a mixed private and pooled on-demand system with elastic demand. Transportmetrica A: Transport Science 17, 897–920.

Narayanan, S., Chaniotakis, E., Antoniou, C., 2020. Shared autonomous vehicle services: A comprehensive review. Transportation Research Part C: Emerging Technologies 111, 255–293.

Pashapour, A., Günneç, D., Salman, F.S., Yücel, E., 2024. Capacitated mobile facility location problem with mobile demand: Efficient relief aid provision to en route refugees. Omega , 103138.

Raghavan, S., Sahin, M., Salman, F.S., 2019. The capacitated mobile facility location problem. European Journal of Operational Research 277, 507–520.

Rødseth, K.L., Fagerholt, K., Proost, S., 2023. Optimal planning of an urban ferry service operated with zero emission technology. SSRN Electronic Journal URL: https://api.semanticscholar.org/CorpusID:256569345.

Salman, F.S., Yücel, E., Kayı, İ., Turper-Alışık, S., Coşkun, A., 2021. Modeling mobile health service delivery to syrian migrant farm workers using call record data. Socio-Economic Planning Sciences 77, 101005.

Shehadeh, K.S., 2023. Distributionally robust optimization approaches for a stochastic mobile facility fleet sizing, routing, and scheduling problem. Transportation Science 57, 197–229.

Stillström, C., Jackson, M., 2007. The concept of mobile manufacturing. Journal of Manufacturing Systems 26, 188–193.

Trojanowski, J., Iwan, S., 2014. Analysis of szczecin waterways in terms of their use to handle freight transport in urban areas. Procedia - Social and Behavioral Sciences 151, 333–341. URL: https://api.semanticscholar.org/CorpusID:110337465.

Tucker, E., Fudge, J., Fudge, J., Vosko, L., 2011. Employee or Independent Contractor?: Charting the Legal Significance of the Distinction in Canada. URL: https://www.semanticscholar.org/paper/Employee-or-Independent-Contractor%3A-Charting-the-of-Tucker-Fudge/479a755fb21a2ef088e958efd8d541b0db748ef2.

Yang, J., Levin, M.W., Hu, L., Li, H., Jiang, Y., 2023. Fleet sizing and charging infrastructure design for electric autonomous mobility-on-demand systems with endogenous congestion and limited link space. Transportation Research Part C: Emerging Technologies 152, 104172.

Yuan, M., Zhang, Q., Wang, B., Liang, Y., Zhang, H., 2019. A mixed integer linear programming model for optimal planning of bicycle sharing systems: A case study in Beijing. Sustainable Cities and Society 47, 101515. URL: https://linkinghub.elsevier.com/retrieve/pii/S2210670718323825, doi:doi:10.1016/j.scs.2019.101515.

Yücel, E., Salman, F.S., Bozkaya, B., Gökalp, C., 2020. A data-driven optimization framework for routing mobile medical facilities. Annals of Operations Research 291, 1077–1102.